REPORT NUMBER 163

NOVEMBER 1965

PRELIMINARY FLUTTER ANALYSIS

VOLUME III CONTROL SURFACES

XV-5A

LIFT FAN FLIGHT RESEARCH AIRCRAFT PROGRAM

CONTRACT NUMBER DA44-177-TC-715

GENERAL ⊛ ELECTRIC

NASA Scientific and Technical Information Facility'

operated for the National Aeronautics and Space Administration by Documentation Incorporated

FACILITY CONTROL NO. 33905

DATE 5/24/66

ATTACHED IS A DOCUMENT ON LOAN

FROM: NASA Scientific and Technical Information Facility

TO: Defense Documentation Center
          Attn: DDC-IRC (Control Branch)
          Cameron Station
          Alexandria, Va. 22314

In accordance with the NASA-DOD Cooperative AD Number Assignment Agreement it is requested that an AD number be assigned to the attached report.

☑ As this is our only available copy the return of the document (with AD number and any applicable distribution limitations) to the address below is essential.

☐ This document may be retained by DDC. If retained, please indicate AD number and any applicable distribution limitations on the reproduced copy of the title page and return to the address below.

Return Address: NASA Scientific and Technical Information Facility
                Attention: INPUT BRANCH
                P. O. Box 33
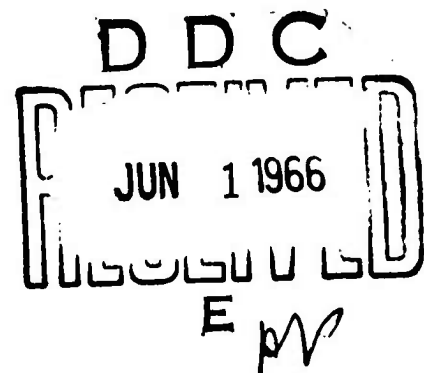   College Park, Maryland 20740

FFNo 244 Revised Aug 65

Report Number 163

PRELIMINARY FLUTTER ANALYSIS
VOLUME III - CONTROL SURFACES

XV-5A Lift Fan
Flight Research Aircraft
Contract DA 44-177-TC-715

December 1965

ADVANCED ENGINE & TECHNOLOGY DEPARTMENT
GENERAL ELECTRIC COMPANY
CINCINNATI, OHIO 45215

CONTENTS

(Continued)

LIST OF FIGURES

BLANK PAGE

LIST OF FIGURES (Continued)

TABLES

1.0 SUMMARY

The overall preliminary theoretical flutter analysis of the Ryan
XV-5A Lift Fan Aircraft is presented in three volumes, each under
separate cover. This is Volume III which reports the investigation
of the flutter characteristics of the control surfaces. Volumes
I and II detail the analysis of the wing and empennage, respectively.

Equations of motion and stability equations are formulated using
lumped spring-mass idealization and incompressible strip theory
aerodynamics; control system elasticity and inertia are taken into
account. One altitude only, sea level, is investigated. Solutions
of the stability equations are obtained, giving flutter frequencies
and complex damping coefficients required to maintain flutter as
functions of flutter velocities for various values of stiffness
parameter, both with and without aerodynamic balancing (centering)
of the control surface.

Both a symmetric and an antisymmetric analysis of the aileron-
aileron flight tab - aileron control system are made. An analysis of
the rudder - rudder trim tab - rudder control system is included
and a symmetric analysis of the horizontal stabilizer - elevator -
elevator control system is also made.

On the basis of preliminary input information used in the analyses
herein, increased stiffness of the aileron flight tab restraint is
required (the symmetric aileron condition is critical), and the
stiffness of the rudder trim tab actuator should be such that the
uncoupled rigid body tab rotation frequency is at least 50 cps,
in order to insure a flutter-free airplane within the established
flight envelope. The antisymmetric aileron condition and elevator
are flutter-free.

2.0 INTRODUCTION

This report presents a portion of the preliminary flutter analysis of the U.S. Army XV-5A Lift Fan Research Aircraft. Volumes I and II of the preliminary flutter analysis are concerned with the wing and with the empennage, respectively. The report herein is Volume III.

The XV-5A is a V/STOL aircraft designed for research flight testing of the General Electric X353-5 lift fan propulsion system. A three-view drawing and a cutaway drawing of the aircraft are presented in Volume I. The XV-5A also features high subsonic conventional flight operation. It has a basic design gross weight of 9200 pounds, a limit dive speed of 500 KEAS (q = 850 psf) and corresponding 0.90 maximum Mach number. Thus, only one altitude, sea level, is investigated herein.

The analysis is based on incompressible strip theory aerodynamics with a lumped spring-mass system idealization, taking into account control system elasticity and inertia.

The purpose of the analysis is to calculate flutter velocities where they exist, for various values of stiffness parameters that reflect design unknowns, both with and without aerodynamic balancing (centering) of the control surfaces. Comparison of results with limit dive speed requirements then affords a basis for design changes to ensure a flutter-free aircraft, or for assurance that current design is flutter safe.

The report is subdivided into two main parts, Sections 3.0 and 4.0. Section 3.0 presents a general approach to the analysis method, developed for a control surface - flight tab system, both symmetric and antisymmetric, and also developed for a symmetric parent surface - control surface system. Equations of motion and of stability are formulated in general form, the aerodynamics are explained, as are mass terms, stiffness terms, coordinates, and basic assumptions, and the general characteristics of the solutions are discussed.

Section 4.0 shows the application of the method of approach to the specific cases at hand:

1.   The aileron and aileron flight tab system (Both symmetric and antisymmetric aileron analyses are made.)

2.   The rudder and rudder tab system

BLANK PAGE

3.   The horizontal stabilizer and elevator system (Only a symmetric analysis is made, since antisymmetric elevator flutter is clearly not critical; this conclusion is discussed in Section 4.0.)

In Section 4.0, for each of the three cases above, schematics of the control system, of the aerodynamic balancing arrangement, and of the idealization are given, and plan views of the surfaces are shown. Values of the numerous input parameters are given, and results are presented both tabularly and graphically. The results are interpreted, and conclusions are drawn.

3.0 METHOD OF APPROACH

The equations of motion for a flutter investigation of a control surface and flight tab system, which applies to the lateral control system (CTOL mode) of the XV-5A aircraft, are developed for both a symmetric and antisymmetric analysis. In general, the procedure follows the development of the governing equations, as presented in Reference 1. The same equations of motion also apply to the directional control system (CTOL mode) of the XV-5A aircraft, since the rudder trim tab is one of zero gearing and thus may be treated as a flight tab with nonexistent connections between it and the pedal.

A similar development, for the symmetric case only but with different components, (a parent surface and a control surface) is the case of the longitudinal system (CTOL mode) of the XV-5A aircraft, and is presented separately.

Specific details applicable to each individual analysis are discussed in Section 4.0

3.1 CONTROL SURFACE - FLIGHT TAB SYSTEM, SYMMETRIC AND ANTISYMMETRIC

The degrees of freedom considered are:

β = Control surface rotation

δ = Control surface flight tab rotation, relative to the control surface

γ = Control stick or pedal rotation

Lagrange's equations of motion for the system governed by the above degrees of freedom are:

$$\frac{d}{dt}\left(\frac{\partial T}{\partial \dot{\beta}}\right) + \frac{\partial U}{\partial \beta} = Q_\beta \tag{1}$$

$$\frac{d}{dt}\left(\frac{\partial T}{\partial \dot{\delta}}\right) + \frac{\partial U}{\partial \delta} = Q_\delta \tag{2}$$

$$\frac{d}{dt}\left(\frac{\partial T}{\partial \dot{\gamma}}\right) + \frac{\partial U}{\partial \gamma} = 0 \tag{3}$$

where

T is the kinetic energy of the system

U is the potential energy (internal strain energy) of the system

Q_β, Q_δ are the generalized aerodynamic forces applied to the system

The kinetic energy of the system is

$$T = \frac{1}{2}\left(I_\beta \dot{\beta}^2 + 2\dot{\beta}\dot{\delta} \ P_{\beta\delta} + I_\delta \dot{\delta}^2\right) + \frac{1}{2}\left(J\dot{\gamma}^2\right) \tag{4}$$

where

I_β = Mass moment of inertia of control surface including tab, about control surface hinge line

I_δ = Mass moment of inertia of flight tab about its hinge line

$P_{\beta\delta}$ = Mass product of inertia of flight tab about control surface hinge line and tab hinge line

$$= I_\delta + S_\delta \ell_t$$

where:

S_δ = Static unbalance of flight tab about its hinge line

ℓ_t = Distance between control surface and tab hinge lines, measured perpendicular to control surface hinge line

J = Mass moment of inertia of control stick or pedal, including linkages, about control stick or pedal axis of rotation

The potential energy of the system is derived from the displacements of concentrated springs within the control surface - flight tab systems. A symmetric or antisymmetric analysis is determined by the springs that participate in the motion of the control surface and flight tab. For present purposes, the potential energy is, in general terms,

$$U = \frac{1}{2} \sum_{i=1}^{3} \sum_{j=1}^{3} S_{ij} q_i q_j \tag{5}$$

where

q_i, q_j = The degrees of freedom considered: β, δ, γ

S_{ij} = Constants generated through the rates of the concentrated springs and linkage arms through which they act. These constants are the elements of a stiffness matrix.

The virtual work done by the air forces is

$$\delta W_i = Q_i \, \delta q_i \tag{6}$$

where

δW_i = The virtual work for the ith degree of freedom

Q_i = The total generalized aerodynamic force in the ith degree of freedom

δq_i = The virtual displacement of the ith degree of freedom

The symbol δ means "a variation of".

Consider the following displacements:

d_1 = Angle of rotation of control surface about its hinge line (plus trailing edge down)

d_2 = Angle of rotation of flight tab about the tab hinge line, relative to the control surface (plus trailing edge down)

and let

$$\left| d \right| = [\varphi] \left| q \right| \tag{7}$$

where

$$[\varphi] = \begin{bmatrix} 1.0 & 0 \\ 0 & 1.0 \end{bmatrix} \tag{8}$$

The displacements expressed by Equation (7) represent rigid body displacements about the hinge lines of the control surface and flight tab. These displacements normally are about swept axes, and we require rotations about axes perpendicular to the free stream. Therefore,

$$\begin{Bmatrix} \beta' \\ \delta' \end{Bmatrix} = \begin{bmatrix} \cos \psi_{\mathbb{E}_c} & 0 \\ 0 & \cos \psi_{\mathbb{E}_t} \end{bmatrix} \begin{Bmatrix} d_1 \\ d_2 \end{Bmatrix} \tag{9}$$

where:

β' = Angle of rotation of control surface about an axis perpendicular to the free stream

δ' = Angle of rotation of flight tab about an axis perpendicular to the free stream

$\psi_{\mathbb{E}_c}$ = Sweepback angle of control surface hinge line

$\psi_{\pounds_t}$ = Sweepback angle of flight tab hinge line

Combining Equations (7), (8) and (9),

$$\begin{Bmatrix} \beta' \\ \delta' \end{Bmatrix} = \begin{bmatrix} \cos \psi_{\pounds_c} & 0 \\ 0 & \cos \psi_{\pounds_t} \end{bmatrix} \begin{bmatrix} 1.0 & \\ & 1.0 \end{bmatrix} \begin{Bmatrix} \beta \\ \delta \end{Bmatrix} = \begin{bmatrix} \cos \psi_{\pounds_c} & 0 \\ 0 & \cos \psi_{\pounds_t} \end{bmatrix} \begin{Bmatrix} \beta \\ \delta \end{Bmatrix} \quad (10)$$

Using two-dimensional oscillatory aerodynamic coefficients and in the rotation of References 2 and 3 (Section 6.0), the aerodynamic moments acting on the control surface and flight tab, per unit span are

$$\begin{Bmatrix} T' \\ Q' \end{Bmatrix} = \pi\rho\omega^2 b^4 \cos \psi_{c/4} \begin{bmatrix} T_\beta & T_\delta \\ Q_\beta & Q_\delta \end{bmatrix} \begin{Bmatrix} \beta' \\ \delta' \end{Bmatrix} \quad (11)$$

where

ρ = Mass density of air at altitudes under consideration

ω = Circular frequency of oscillation

b   = Half-chord length

$\psi_{c/4}$ = Sweepback angle of quarter-chord line of parent surface

T_β, T_δ, Q_β, Q_δ = Oscillatory aerodynamic coefficients (nondimensional) in the rotation of References 2 and 3, in general, complex numbers. They contain no terms to account for the effects of aerodynamic balance; i.e., nose sections are assumed simply rounded. Corrections to account for the internal balancing system for the control surfaces used in the XV-5A aircraft are discussed on Page 11.

From the principle of virtual work, the work done by the moments of Equation (11) in undergoing a virtual displacement is

$$\delta W = \int_0^S (T' \delta\beta' + Q' \delta\delta') \, dy \quad (12)$$

where S is the semispan parallel to the y-axis which is perpendicular to the free stream. Primes indicate "in the stream direction".

In matrix notation

$$\delta W = \int_0^S \lfloor \delta\beta' \ \delta\delta' \rfloor \begin{Bmatrix} T' \\ Q' \end{Bmatrix} dy \tag{13}$$

Since, from Equation (10) we have

$$\begin{Bmatrix} \beta' \\ \delta' \end{Bmatrix} = \begin{bmatrix} \cos \psi_{\mathcal{L}_c} & 0 \\ 0 & \cos \psi_{\mathcal{L}_t} \end{bmatrix} \begin{Bmatrix} \beta \\ \delta \end{Bmatrix}$$

and therefore

$$\begin{Bmatrix} \delta\beta' \\ \delta\delta' \end{Bmatrix} = \begin{bmatrix} \cos \psi_{\mathcal{L}_c} & 0 \\ 0 & \cos \psi_{\mathcal{L}_t} \end{bmatrix} \begin{Bmatrix} \delta\beta \\ \delta\delta \end{Bmatrix}$$

or, transposing,

$$\lfloor \delta\beta' \ \delta\delta' \rfloor = \lfloor \delta\beta \ \delta\delta \rfloor \begin{bmatrix} \cos \psi_{\mathcal{L}_c} & 0 \\ 0 & \cos \psi_{\mathcal{L}_t} \end{bmatrix} \tag{14}$$

Combining Equations (11), (13) and (14), and noting that β, δ and their variations are not functions of y, the virtual work is

$$\delta W = \lfloor \delta\beta \ \delta\delta \rfloor \left[\pi\rho\omega^2 \cos \psi_{c/4} \int_0^S b^4 \begin{bmatrix} \cos \psi_{\mathcal{L}_c} & 0 \\ 0 & \cos \psi_{\mathcal{L}_t} \end{bmatrix} \right.$$

$$\left. \begin{bmatrix} T_\beta & T_\delta \\ Q_\beta & Q_\delta \end{bmatrix} \begin{bmatrix} \cos \psi_{\mathcal{L}_c} & 0 \\ 0 & \cos \psi_{\mathcal{L}_t} \end{bmatrix} dy \right] \begin{Bmatrix} \beta \\ \delta \end{Bmatrix} \tag{15}$$

therefore, since $\delta W = \displaystyle\sum_{i=1}^{3} \delta W_i = \sum_{i=1}^{3} Q_i \delta q_i = Q_\beta \delta\beta + Q_\delta \delta\delta + 0\cdot\delta\gamma$

$$= \lfloor \delta\beta \;\; \delta\delta \rfloor \begin{Bmatrix} Q_\beta \\ Q_\delta \end{Bmatrix}$$

the column of two-dimensional, generalized aerodynamic forces is

$$\begin{Bmatrix} Q_\beta \\ Q_\delta \end{Bmatrix} = \frac{\pi \rho \omega^2 \cos \psi_{c/4}}{} \int_0^S \begin{bmatrix} \cos \psi_{\bigstar_c} & 0 \\ 0 & \cos \psi_{\bigstar_t} \end{bmatrix} \begin{bmatrix} T_\beta & T_\delta \\ Q_\beta & Q_\delta \end{bmatrix}$$

$$\begin{bmatrix} \cos \psi_{\bigstar_c} & 0 \\ 0 & \cos \psi_{\bigstar_t} \end{bmatrix} dy \begin{Bmatrix} \beta \\ \delta \end{Bmatrix} \tag{16}$$

These generalized forces are the right-hand sides of the Lagrange's equations of motion, Equations (1) and (2).

We next treat the required correction to the generalized force Q_β as a result of internal aerodynamic balance of the control surface, maintaining zero aerodynamic balance for the flight tab. Using References 1 and 4, the incremental two-dimensional aerodynamic moment acting on the control surface, per unit span is

$$\Delta T' = -\pi \rho \omega^2 b^4 \cos \psi_{c/4} \lfloor \bar{A} \quad \bar{B} \rfloor \begin{Bmatrix} \beta' \\ \delta' \end{Bmatrix} \tag{17}$$

where

$$\bar{A} = F_{BB} \, K \frac{\left(\Delta C_{H_{c_\delta}} \right)_{c/\text{Exp}}}{\left(\Delta C_{H_{c_\delta}} \right)_{c/3}} C(c,\, g,\, k)$$

$$\bar{B} = F_{BB}\, K\, \frac{\left(\Delta C_{H_{c_{\delta_t}}}\right)_{Exp}}{\left(\Delta C_{H_{c_{\delta_t}}}\right)_3}\, D(c,\, d,\, k)$$

and

F_{BB} is an auxiliary function defining the internal aerodynamic balance geometry and is equal to $\left| c(e' - e'') - \dfrac{(e' - e'')\,(e' + e'')}{2} \right|$. (See Figure 3.)

K is a pressure recovery factor to account for leakage across the internal balance arrangement. $\left(\Delta C_{H_{c_{\delta_c}}}\right)_{Exp.}$, $\left(\Delta C_{H_{c_{\delta_c}}}\right)_3$ are control surface, steady-state hinge moment derivatives, experimental and theoretical, respectively (aerodynamic balance contribution through control surface deflection).

$\left(\Delta C_{H_{c_{\delta_t}}}\right)_{Exp.}$, $\left(\Delta C_{H_{c_{\delta_t}}}\right)_3$ are control surface, steady-state hinge moment derivatives, experimental and theoretical, respectively (aerodynamic balance contribution through flight tab deflection).

C(c, g, k) is a dimensionless coefficient similar to T_β (Equation (11)) and is a function only of airfoil and control surface geometry.

D(c, d, k) is a dimensionless coefficient similar to T_δ (Equation (11)) and is a function only of airfoil, control surface and flight tab geometry.

The elements of the row matrix in Equation (17) are, in general, complex numbers. Now, again using the principle of virtual work, the work done by the internal balance forces in undergoing a virtual displacement is

$$\delta W_\beta = \int_0^\ell \Delta T'\, \delta\beta'\, dy \qquad (18)$$

where ℓ is the semispan of the internal aerodynamic balance arrangement (i.e., simple nose overhang) parallel to the y axis, which axis is perpendicular to the free stream.

Combining Equations (10), (14), (17) and (18), the virtual work of internal balance forces is written:

$$\delta W_\beta = -\delta\beta \left[\pi\rho\omega^2 \cos\psi_{c/4} \cos\psi_{\textrm{HL}_c} \int_0^\ell b^4 \lfloor \bar{A} \quad \bar{B} \rfloor \right.$$

$$\left. \begin{bmatrix} \cos\psi_{\textrm{HL}_c} & 0 \\ 0 & \cos\psi_{\textrm{HL}_t} \end{bmatrix} dy \right] \begin{Bmatrix} \beta \\ \delta \end{Bmatrix} \qquad (19)$$

Since $\delta W_\beta = \Delta Q_\beta \, \delta\beta$ in this case of correction for control surface internal aerodynamic balance, the incremental two-dimensional generalized aerodynamic force to be added to Q_β in Equation (16) is

$$\Delta Q_\beta = -\pi\rho\omega^2 \cos\psi_{c/4} \cos\psi_{\textrm{HL}_c} \int_0^\ell b^4 \lfloor \bar{A} \quad \bar{B} \rfloor$$

$$\begin{bmatrix} \cos\psi_{\textrm{HL}_c} & 0 \\ 0 & \cos\psi_{\textrm{HL}_t} \end{bmatrix} dy \begin{Bmatrix} \beta \\ \delta \end{Bmatrix} \qquad (20)$$

Addition of the increment ΔQ_β from Equation (20) to Q_β in Equation (16) gives the case of the XV-5A aileron and rudder systems, namely, internal aerodynamic balance for the control surface and no aerodynamic balance for the tab.

The generalized aerodynamic forces are expressed simply in 3x1 matrix form as

$$\begin{Bmatrix} Q_\beta \\ Q_\delta \\ 0 \end{Bmatrix} = \omega^2 \begin{bmatrix} I'_{11} & I'_{12} & 0 \\ I'_{21} & I'_{22} & 0 \\ 0 & 0 & 0 \end{bmatrix} \begin{Bmatrix} \beta \\ \delta \\ \gamma \end{Bmatrix} \qquad (21)$$

where the I'_{ij} elements, in general complex numbers contain both the contributions of the basic surface (control aft of the hinge line) and of the internal aerodynamic balance (given by ΔQ_β). Q_β and Q_δ are now corrected values.

13

For convenience of calculations, the I' matrix of Equation (21) is decomposed into the sum of two matrices, the first containing the terms due to the basic surfaces (control surface and unbalanced flight tab), and the second containing the terms due to the internal aerodynamic balancing arrangement of the control surface.

Thus, Equation (21) becomes

$$
\begin{Bmatrix} Q_\beta \\ Q_\delta \\ 0 \end{Bmatrix} = \omega^2 \left[\begin{bmatrix} A_{11} & A_{12} & 0 \\ A_{21} & A_{22} & 0 \\ 0 & 0 & 0 \end{bmatrix} - \begin{bmatrix} B_{11} & B_{12} & 0 \\ 0 & 0 & 0 \\ 0 & 0 & 0 \end{bmatrix} \right] \begin{Bmatrix} \beta \\ \delta \\ \gamma \end{Bmatrix}
\tag{22}
$$

where

$$
A_{11} = \pi \rho \cos \psi_{c/4} \int_{\substack{\text{Control} \\ \text{Surface}}} b^4 \cos^2 \psi_{\text{\AE}_c} \frac{\left(C_{H_{c_\delta}} \right)_c}{\left(C_{H_{c_\delta}} \right)_3} \text{Exp. } T_\beta \, dy
$$

$$
A_{12} = \pi \rho \cos \psi_{c/4} \int_{\text{Tab}} b^4 \cos \psi_{\text{\AE}_c} \cos \psi_{\text{\AE}_t} \frac{\left(C_{H_{c_\delta}} \right)_t}{\left(C_{H_{c_\delta}} \right)_3} \text{Exp. } T_\delta \, dy
$$

$$
A_{21} = \pi \rho \cos \psi_{c/4} \int_{\text{Tab}} b^4 \cos \psi_{\text{\AE}_c} \cos \psi_{\text{\AE}_t} \frac{\left(C_{H_{t_\delta}} \right)_c}{\left(C_{H_{t_\delta}} \right)_3} \text{Exp. } Q_\beta \, dy
$$

$$
A_{22} = \pi \rho \cos \psi_{c/4} \int_{\text{Tab}} b^4 \cos^2 \psi_{\text{\AE}_t} \frac{\left(C_{H_{t_\delta}} \right)_t}{\left(C_{H_{t_\delta}} \right)_3} \text{Exp. } Q_\delta \, dy
$$

$$B_{11} = \pi \rho \cos \psi_{c}/4 \int_{\substack{\text{Aero.}\\\text{Bal.}}} b^4 \cos^2 \psi_{\text{\textcentoldstyle}_c} F_{BB} K \frac{\left(\dfrac{\Delta C_{H_{c_{\delta_c}}}}{\Delta C_{H_{c_{\delta_c}}}}\right)_{3}}{} \text{Exp.} C(c,g,k)dy$$

$$B_{12} = \pi \rho \cos \psi_{c}/4 \int_{\substack{\text{Aero.}\\\text{Bal.}}} b^4 \cos \psi_{\text{\textcentoldstyle}_c} \cos \psi_{\text{\textcentoldstyle}_t} F_{BB} K \frac{\left(\dfrac{\Delta C_{H_{c_{\delta_t}}}}{\Delta C_{H_{c_{\delta_t}}}}\right)_{3}}{} \text{Exp.} D(c,d,k)dy$$

Note that the basic surface expressions A_{11}, A_{12}, A_{21} and A_{22} have been modified by hinge moment correction factors $\left(C_{H_{c_{\delta_c}}}\right)_{\text{Exp.}} / \left(C_{H_{c_{\delta_c}}}\right)_{3}$,
etc. in order that these terms be consistent with the expressions for the internal aerodynamic balance arrangement.

In order to evaluate the elements of [A] and [B] given above, the control surface, flight tab and internal balance are divided into equal spanwise segments appropriate to the system under investigation, and all integration is performed numerically using the trapezoidal rule.

The equations of motion for a control surface-flight tab flutter analysis are written in the familiar $F = ma$ form by substituting Equations (4), (5) and (21) into Lagrange's Equations (1), (2), and (3).

Expressing the results in matrix form,

$$\begin{bmatrix} I_\beta & P_{\beta\delta} & 0 \\ P_{\beta\delta} & I_\delta & 0 \\ 0 & 0 & J \end{bmatrix} \begin{Bmatrix} \ddot{\beta} \\ \ddot{\delta} \\ \ddot{\gamma} \end{Bmatrix} + \begin{bmatrix} S_{11} & S_{12} & S_{13} \\ S_{21} & S_{22} & S_{23} \\ S_{31} & S_{32} & S_{33} \end{bmatrix} \begin{Bmatrix} \beta \\ \delta \\ \gamma \end{Bmatrix} - \omega^2 \begin{bmatrix} I'_{11} & I'_{12} & 0 \\ I'_{21} & I'_{22} & 0 \\ 0 & 0 & 0 \end{bmatrix} \begin{Bmatrix} \beta \\ \delta \\ \gamma \end{Bmatrix} = \begin{Bmatrix} 0 \\ 0 \\ 0 \end{Bmatrix}$$

(23)

We assume harmonic motion $q_i = q_{i_0} e^{i\omega t}$ and introduce a reference

spring rate $\overline{K}$, which is merely a scaling factor for computing convenience. Further, we formulate the variable Ω, which is the basic unknown,

$$\Omega = \frac{\overline{K}}{\omega^2} \ (1 + ig) \tag{24}$$

Note that Ω introduces a damping force that is proportional to displacement and in phase with the velocity, with g being a measure of this damping force, and is the so-called complex damping coefficient.

Substitution of $q_i = q_{i_0} e^{i\omega t}$ and Equation (24) into Equation (23) gives

$$\left[\begin{bmatrix} I_\beta & P_{\beta\delta} & 0 \\ P_{\beta\delta} & I_\delta & 0 \\ 0 & 0 & J \end{bmatrix} - \Omega \begin{bmatrix} S_{11} & S_{12} & S_{13} \\ S_{21} & S_{22} & S_{23} \\ S_{31} & S_{32} & S_{33} \end{bmatrix} + \begin{bmatrix} I'_{11} & I'_{12} & 0 \\ I'_{21} & I'_{22} & 0 \\ 0 & 0 & 0 \end{bmatrix} \right] \begin{Bmatrix} \beta \\ \delta \\ \gamma \end{Bmatrix} = \begin{Bmatrix} 0 \\ 0 \\ 0 \end{Bmatrix} \tag{25}$$

where it is now understood that the S_{ij} elements of the matrix derived from the potential energy expression are divided by the scaling factor $\overline{K}$.

Upon expansion of the characteristic determinant, the determinant of the summed 3 x 3 matrix in Equation (25), there results a stability equation of the form:

$$A\Omega^3 + B\Omega^2 + C\Omega + D = 0 \tag{26}$$

where A is real and B, C and D are, in general, complex.

The degree of the above equation depends implicitly on the type of analysis, i.e. symmetric or antisymmetric, being performed.

The solution of Equation (26) gives, in general, the complex roots Ω from which g and ω are obtained. Negative g is the stable state, and positive g is the unstable (flutter) state. ω is the circular flutter frequency. [I'] in Equation (25) is chosen for several prescribed values of the dimensionless parameter $V/_{b_0\omega}$, the reduced velocity. (b_0 is some reference half chord). Thus, solutions of Equation (26) give plots of g vs. ω, and, by substitution of ω into corresponding $V/_{b_0\omega}$ values, plots of

g vs V are obtained. These are the basic stability relationships. The smallest nonzero value of V at g = 0 is the flutter velocity, V_f. Also, cross-plots of ω vs V are useful, showing modal coalescence to the unstable state. Because of the three (at most) complex roots Ω from Equation (26), for each analysis, there are no more than three branches to the g - V and ω - V plots.

Setting $[I'] = [0]$ and g = 0 in Equation (25), the uncoupled natural frequency $f_\beta = \omega_\beta/2\pi$, control surface rotation, may be calculated, for interpretive purposes, from

$$I_\beta - \frac{\overline{K}}{\omega_\beta^2} \; S_{11} = 0 \tag{27}$$

The uncoupled natural frequency $f_\delta = \omega_\delta/2\pi$, flight tab rotation, may be calculated from

$$I_\delta - \frac{\overline{K}}{\omega_\delta^2} \; S_{22} = 0 \tag{28}$$

and the uncoupled natural frequency $f_\gamma = \omega_\gamma/2\pi$, control stick or pedal rotation, from

$$J - \frac{\overline{K}}{\omega_\gamma^2} \; S_{33} = 0 \tag{29}$$

3.2 PARENT SURFACE-CONTROL SURFACE SYSTEM, SYMMETRIC

The degrees of freedom considered are

α = Parent surface rotation

β = Control surface rotation relative to parent surface

γ = Control stick rotation

The general analysis herein is applied in Paragraph 4.3 to the horizontal stabilizer-elevator system of the XV-5A aircraft. All of the general analysis made in Paragraph 3.1 applies for the system under consideration here, with some important differences:

1. The generalized coordinates β and δ in Paragraph 3.1 are replaced by the generalized coordinates α and β, respectively, α referring to the generalized coordinate "parent surface rotation". The generalized coordinate "tab rotation" does not apply to the present case, since there is no tab.

2. The kinetic energy, T, of the system is given by an equation of form similar to Equation (4) in Paragraph 3.1, but the definitions of terms are slightly modified and the symbol J is replaced by J_0 with a different definition:

$$T = \frac{1}{2}(I_\alpha \dot{\alpha}^2 + 2\dot{\alpha}\dot{\beta}\,P_{\alpha\beta} + I_\beta \dot{\beta}^2) + \frac{1}{2}(J_0 \dot{\gamma}^2) \tag{30}$$

where

I_α = Mass moment of inertia of half the parent surface, including the half of entire control surface, about the pivot axis of the parent surface

I_β = Mass moment of inertia of one control surface about its hinge line. It is assumed that the complete system contains two control surfaces, a right-hand and a left-hand one

$P_{\alpha\beta}$ = Mass product of inertia of one control surface about parent surface pivot axis and control surface hinge line

$= I_\beta + S_\beta \ell$

where:

S_β = Static unbalance of <u>one</u> control surface about its hinge line

ℓ = Streamwise distance between parent surface pivot axis and control surface hinge line

J_0 = Effective mass moment of inertia of <u>half</u> the control circuit and control stick, about control stick axis of rotation

3.   The generalized forces and, in particular, the aerodynamic matrix $[I']$ in Equation (23) are reformulated to take into account normal-to-plane motion of the parent surface.

The virtual work done by the air forces is as before:

$$\delta \omega_i = Q_i \, \delta q_i \qquad i = 1, \, 2, \, 3$$

Consider the following displacements at a representative station:

d_1 = Deflection of the elastic axis of the parent surface in the z (normal-to-plane) direction (plus down)

d_2 = Angle of rotation of parent surface about its elastic axis (plus leading edge up)

d_3 = Angle of rotation about an axis perpendicular to the elastic axis of the parent surface (plus when tip of surface is depressed); d_3 is a bending displacement

d_4 = Angle of rotation of control surface about its hinge line, relative to the parent surface (plus trailing edge down)

And let

$$\{d\} = [\varphi] \{q\} \qquad \text{as before} \tag{31}$$

where

$$\{q\} = \left\{ \begin{matrix} \alpha \\ \beta \end{matrix} \right\} \qquad \text{here}$$

and

$$[\varphi] = \begin{bmatrix} \phi_{11} & 0 \\ \phi_{21} & 0 \\ \phi_{31} & 0 \\ 0 & \varphi_{41} \end{bmatrix}$$

(32)

Note that there are no generalized aerodynamic force components due to γ.

From the geometry and definition of the displacements d_i,

$$\phi_{11} = (1.0) \, g$$

$$\phi_{21} = (1.0) \cos \psi_{e.a.}$$

$$\phi_{31} = (1.0) \sin \psi_{e.a.}$$

$$\phi_{41} = 1.0$$

where

g = Distance from parent surface pivot axis to its elastic axis in the stream direction (plus aft of pivot axis); this dimensional variable is not the same as expressed in Equation (22)

$\psi_{e.a.}$ = Sweepback angle of parent surface elastic axis

Substituting element values into Equation (32),

$$[\varphi] = \begin{bmatrix} g & 0 \\ \cos \psi_{e.a.} & 0 \\ \sin \psi_{e.a.} & 0 \\ 0 & 1.0 \end{bmatrix}$$

(33)

Since the deflections d_i, at this point, are deflections relative to the elastic axis (except for d_4, which is relative to the control surface hinge line) we transform the four displacements to axes parallel and perpendicular to the free stream at the representative station.

Let

d'_1 = Vertical displacement of the parent surface at its elastic axis

d'_2 = Angle of rotation of parent surface about an axis perpendicular to the free stream, through the elastic axis of the parent surface (pitch angle of parent surface)

d'_3 = Angle of rotation of parent surface about an axis parallel to the free stream, through the elastic axis of the parent surface (roll angle of parent surface)

d'_4 = Angle of rotation of control surface about an axis perpendicular to the free stream, through the control surface hinge line; the rotation being relative to d'_2 (pitch angle of control surface rotation relative to parent surface)

From the geometry and definitions of the displacements d'_1,

$$
\begin{Bmatrix} d'_1 \\ d'_2 \\ d'_3 \\ d'_4 \end{Bmatrix} = \begin{bmatrix} 1.0 & 0 & 0 & 0 \\ 0 & \cos\psi_{e.a.} & \sin\psi_{e.a.} & 0 \\ 0 & -\sin\psi_{e.a.} & \cos\psi_{e.a.} & 0 \\ 0 & 0 & 0 & \cos\psi_{H_c} \end{bmatrix} \begin{Bmatrix} d_1 \\ d_2 \\ d_3 \\ d_4 \end{Bmatrix} \tag{34}
$$

where ψ_{H_c} = sweepback angle of the control surface hinge line. Since the air forces are written for displacements of the quarter chord, maintaining rotations relative to free stream axes, we transform the vertical displacement at the elastic axis to that at the quarter-chord line, still at the same representative station.

Let

h = Vertical displacement of parent surface at the quarter-chord line. h is a linear combination of d'_1 and d'_2.

α' = Angle of rotation of parent surface about axis perpendicular to free stream direction, axis passing through the quarter chord point (pitch angle of parent surface); thus $\alpha' = d'_2$

$\beta' = $ Angle of rotation of control surface about axis perpendicular to free stream direction, relative to parent surface; axis passing through the hinge line (pitch angle of control surface relative to parent surface); thus $\beta' = d'_4$

Note that neither h, α' nor β' is a function of d'_3.

The required transformation is

$$\left\{ \begin{array}{c} h \\ \alpha' \\ \beta' \end{array} \right\} = \begin{bmatrix} 1.0 & -a & 0 & 0 \\ 0 & 1.0 & 0 & 0 \\ 0 & 0 & 0 & 1.0 \end{bmatrix} \left\{ \begin{array}{c} d'_1 \\ d'_2 \\ d'_3 \\ d'_4 \end{array} \right\} \tag{35}$$

where a = streamwise distance from quarter-chord line to elastic axis at representative station. Combining Equations (31), (32), (33), (34) and (35), and multiplying out gives

$$\left\{ \begin{array}{c} h \\ \alpha' \\ \beta' \end{array} \right\} = \begin{bmatrix} g-a & 0 \\ 1.0 & 0 \\ 0 & \cos \psi_{H_c} \end{bmatrix} \left\{ \begin{array}{c} \alpha \\ \beta \end{array} \right\} \tag{36}$$

Equation (36) could have been written out directly from considerations of the rigid body degrees of freedom involved; the preceding was developed from the XV-5A empennage flutter analysis and used herein for continuity.

Using two-dimensional aerodynamic oscillatory coefficients in the notation of References 2 and 3 and assuming, at this point, zero aerodynamic balance for the control surface, the aerodynamic forces acting per unit span are

$$\left\{ \begin{array}{c} L'b \\ M' \\ T' \end{array} \right\} = \pi \rho \omega^2 b^4 \cos \psi_{c/4} \begin{bmatrix} L_h & L_\alpha & L_\beta \\ M_h & M_\alpha & M_\beta \\ T_h & T_\alpha & T_\beta \end{bmatrix} \left\{ \begin{array}{c} h/b \\ \alpha' \\ \beta' \end{array} \right\} \tag{37}$$

From the principle of virtual work,

$$\delta W = \int_0^S \left[(L'\,b)\,\delta\left(\frac{h}{b}\right) + M'\,\delta\,\alpha' + T'\,\delta\beta' \right] dy \tag{38}$$

22

where S is again the semispan parallel to the y-axis, which is perpendicular to the free stream. Primes indicate "in the stream direction".

In matrix notation:

$$\delta W = \int_0^S \left\lfloor \delta\left(\frac{h}{b}\right) \; \delta\alpha' \; \delta\beta' \right\rfloor \begin{Bmatrix} L'b \\ M' \\ T' \end{Bmatrix} dy \tag{39}$$

Nondimensionalizing the h deflection and applying a variation in the variables of Equation (36), we have

$$\begin{Bmatrix} \delta\left(\frac{h}{b}\right) \\ \delta\alpha' \\ \delta\beta' \end{Bmatrix} = \begin{bmatrix} \dfrac{g-a}{b} & 0 \\ 1.0 & 0 \\ 0 & \cos\psi_{\frac{1}{4}c} \end{bmatrix} \begin{Bmatrix} \delta\alpha \\ \delta\beta \end{Bmatrix}$$

or, transposing,

$$\left\lfloor \delta\left(\frac{h}{b}\right) \; \delta\alpha' \; \delta\beta' \right\rfloor = \left\lfloor \delta\alpha \; \delta\beta \right\rfloor \begin{bmatrix} \dfrac{g-a}{b} & 1.0 & 0 \\ 0 & 0 & \cos\psi_{\frac{1}{4}c} \end{bmatrix} \tag{40}$$

Combining Equations (36), (37), (39) and (40) and noting that α and β and their variations are not functions of y, the virtual work is

$$\delta W = \left\lfloor \delta\alpha \; \delta\beta \right\rfloor \left[\pi\rho\omega^2 \cos\psi_{c/4} \int_0^S b^4 \begin{bmatrix} \dfrac{g-a}{b} & 1.0 & 0 \\ 0 & 0 & \cos\psi_{\frac{1}{4}c} \end{bmatrix} \right. $$
$$\left. \begin{bmatrix} L_h & L_\alpha & L_\beta \\ M_h & M_\alpha & M_\beta \\ T_h & T_\alpha & T_\beta \end{bmatrix} \begin{bmatrix} \dfrac{g-a}{b} & 0 \\ 1.0 & 0 \\ 0 & \cos\psi_{\frac{1}{4}c} \end{bmatrix} dy \right] \begin{Bmatrix} \alpha \\ \beta \end{Bmatrix} \tag{41}$$

Since $\delta W = \left\lfloor \delta\alpha \; \delta\beta \right\rfloor \begin{Bmatrix} Q_\alpha \\ Q_\beta \end{Bmatrix}$, from the basic definition of virtual work, the

column of two-dimensional, generalized aerodynamic forces is

$$\left\{\begin{array}{c} Q_\alpha \\ \\ Q_\beta \end{array}\right\} = \pi\rho\omega^2 \cos \psi_{c/4} \int_0^S b^4 \begin{bmatrix} \dfrac{g-a}{b} & 1.0 & 0 \\ \\ 0 & 0 & \cos \psi_{c/4} \end{bmatrix}$$

$$\begin{bmatrix} L_h & L_\alpha & L_\beta \\ M_h & M_\alpha & M_\beta \\ T_h & T_\alpha & T_\beta \end{bmatrix} \begin{bmatrix} \dfrac{g-a}{b} & 0 \\ 1.0 & 0 \\ 0 & \cos \psi_{c/4} \end{bmatrix} dy \left\{\begin{array}{c} \alpha \\ \beta \end{array}\right\} \tag{42}$$

These generalized forces are the right-hand sides of Lagrange's equations of motion for the system at hand.

These equations are:

$$\frac{d}{dt}\left(\frac{\partial T}{\partial \dot{\alpha}}\right) + \frac{\partial U}{\partial \alpha} = Q_\alpha \tag{43}$$

$$\frac{d}{dt}\left(\frac{\partial T}{\partial \dot{\beta}}\right) + \frac{\partial U}{\partial \beta} = Q_\beta \tag{44}$$

$$\frac{d}{dt}\left(\frac{\partial T}{\partial \dot{\gamma}}\right) + \frac{\partial U}{\partial \gamma} = 0 \tag{45}$$

where γ is the degree of freedom "control stick rotation". We next treat the correction to the generalized force Q_β as a result of the internal aerodynamic balance arrangement of the control surface. The XV-5A elevator system is of this type, since it uses a simple nose overhang with a curtain seal.

Again using References 1 and 4, the incremental, two-dimensional aerodynamic moment acting on the control surface, per unit span, is

$$\Delta T' = -\pi\rho\omega^2 b^4 \cos \psi_{c/4} \lfloor \bar{A} \quad \bar{B} \quad \bar{C} \rfloor \left\{\begin{array}{c} h/b \\ \alpha' \\ \beta' \end{array}\right\} \tag{46}$$

where

$$\overline{A} = F_{BB} \; K \; \frac{\left(\Delta C_{H_{c_\alpha}} \right)_{Exp.}}{\left(\Delta C_{H_{c_\alpha}} \right)_3} \quad A(c, \; k)$$

$$\overline{B} = F_{BB} \; K \; \frac{\left(\Delta C_{H_{c_\alpha}} \right)_{Exp.}}{\left(\Delta C_{H_{c_\alpha}} \right)_3} \quad B(c, \; a, \; k)$$

$$\overline{C} = F_{BB} \; K \; \frac{\left(\Delta C_{H_{c_{\delta_c}}} \right)_{Exp.}}{\left(\Delta C_{H_{c_{\delta_c}}} \right)_3} \quad C(c, \; g, \; k)$$

and

F_{BB} and K are the same as defined in Paragraph 3.1

$\left(\Delta C_{H_{c_\alpha}} \right)_{Exp.}$, $\left(\Delta C_{H_{c_\alpha}} \right)_3$ are control surface steady-state hinge moment derivatives, experimental and theoretical, respectively (aerodynamic balance contribution through angle of attack)

$\left(\Delta C_{H_{c_{\delta_c}}} \right)_{Exp.}$, $\left(\Delta C_{H_{c_{\delta_c}}} \right)_3$ are the same as defined in Paragraph 3.1

A(c, k) is a dimensionless coefficient similar to T_h (Equation (37)) and is a function only of airfoil and control surface geometry. B(c, a, k) is a dimensionless coefficient similar to T_α (Equation (37)) and is a function only of airfoil and control surface geometry (the parameter "a" being equal to -0.5 for this analysis, different from that expressed in Equation (36))

C(c, g, k) is the same as defined in Paragraph 3.1

The elements of the row matrix in Equation (46) are, in general, complex numbers. Using again the principle of virtual work, the work done by the internal balance forces in undergoing a virtual displacement is

$$\delta W_\beta = \int_0^\ell (\Delta T')(\delta \beta')\ dy$$

where ℓ is the semispan of the internal aerodynamic balance arrangement (i.e., simple nose overhang), as before.

The work may be written in the equivalent form:

$$\delta W = \int_0^\ell \left\lfloor \delta\left(\frac{h}{b}\right)\ \delta\alpha'\ \delta\beta' \right\rfloor \left\{ \begin{array}{c} 0 \\ 0 \\ \Delta T' \end{array} \right\} dy \tag{47}$$

Combining Equations (36), (40), (46) and (47), the virtual work of internal balance forces is

$$\delta W = - \left\lfloor \delta\alpha\ \ \delta\beta \right\rfloor \left[\pi\rho\omega^2 \cos\psi_{c/4} \int_0^\ell b^4 \begin{bmatrix} \dfrac{g-a}{b} & 1.0 & 0 \\ 0 & 0 & \cos\psi_{\Phi_c} \end{bmatrix} \right.$$

$$\left. \begin{bmatrix} 0 & 0 & 0 \\ 0 & 0 & 0 \\ \overline{A} & \overline{B} & \overline{C} \end{bmatrix} \begin{bmatrix} \dfrac{g-a}{b} & 0 \\ 1.0 & 0 \\ 0 & \cos\psi_{\Phi_c} \end{bmatrix} dy \right] \left\{ \begin{array}{c} \alpha \\ \beta \end{array} \right\} \tag{48}$$

Since $\delta W = \Delta Q_\beta\ \delta\beta$, in this case of correction for the control surface internal aerodynamic balance, the incremental, two-dimensional, generalized aerodynamic force to be added to Q_β in Equation (42) is

$$\Delta Q_\beta = -\pi\rho\omega^2 \cos\psi_{c/4} \int_0^\ell b^4 \begin{bmatrix} \dfrac{g-a}{b} & 1.0 & 0 \\ 0 & 0 & \cos\psi_{\Phi_c} \end{bmatrix} \begin{bmatrix} 0 & 0 & 0 \\ 0 & 0 & 0 \\ \overline{A} & \overline{B} & \overline{C} \end{bmatrix}$$

$$\begin{bmatrix} \dfrac{g-a}{b} & 0 \\ 1.0 & 0 \\ 0 & \cos\psi_{\Phi_c} \end{bmatrix} dy \left\{ \begin{array}{c} \alpha \\ \beta \end{array} \right\} \tag{49}$$

From Equations (42) and (49) we write the generalized aerodynamic forces, in 3x1 matrix form, as follows:

$$
\begin{Bmatrix} Q_\alpha \\ Q_\beta \\ 0 \end{Bmatrix} = \omega^2 \begin{bmatrix} A_{11} & A_{12} & 0 \\ A_{21} & A_{22} & 0 \\ 0 & 0 & 0 \end{bmatrix} \begin{Bmatrix} \alpha \\ \beta \\ \gamma \end{Bmatrix}
\qquad
\begin{array}{l}\text{(generalized aerodynamic}\\ \text{force, no aerodynamic}\\ \text{balance)}\end{array}
\qquad (50)
$$

$$
\begin{Bmatrix} 0 \\ \Delta Q_\beta \\ 0 \end{Bmatrix} = -\omega^2 \begin{bmatrix} 0 & 0 & 0 \\ B_{21} & B_{22} & 0 \\ 0 & 0 & 0 \end{bmatrix} \begin{Bmatrix} \alpha \\ \beta \\ \gamma \end{Bmatrix}
\qquad
\begin{array}{l}\text{(generalized aerodynamic}\\ \text{force, aerodynamic}\\ \text{balance increment)}\end{array}
\qquad (51)
$$

where, by expanding out Equations (42) and (49)

$$
A_{11} = \pi \rho \cos \psi_{c/4} \int_{\substack{\text{Parent}\\\text{Surface}}} b^4 \left[L_h \left(\frac{g-a}{b} \right)^2 + (L_\alpha + M_h)\left(\frac{g-a}{b} \right) + M_\alpha \right] dy
$$

$$
A_{12} = \pi \rho \cos \psi_{c/4} \int_{\substack{\text{Control}\\\text{Surface}}} b^4 \cos \psi_{\text{ÆL}_c} \left[L_\beta \left(\frac{g-a}{b} \right) + M_\beta \right] dy
$$

$$
A_{21} = \pi \rho \cos \psi_{c/4} \int_{\substack{\text{Control}\\\text{Surface}}} b^4 \cos \psi_{\text{ÆL}_c} \frac{\left(C_{H_{c_\alpha}} \right)}{\left(C_{H_{c_\alpha}} \right)_3} \text{Exp.} \left[T_h \left(\frac{g-a}{b} \right) + T_\alpha \right] dy
$$

$$
A_{22} = \pi \rho \cos \psi_{c/4} \int_{\substack{\text{Control}\\\text{Surface}}} b^4 \cos^2 \psi_{\text{ÆL}_c} \frac{\left(C_{H_{c_{\delta_c}}} \right)}{\left(C_{H_{c_{\delta_c}}} \right)_3} \text{Exp.} \ T_\beta \ dy
$$

$$B_{21} = \pi\rho \cos \psi_{c/4} \int_{\substack{\text{Aero.}\\\text{Bal.}}} b^4 \cos \psi_{\text{\textcent}_c} \, F_{BB} \, K \, \frac{\left(\dfrac{\Delta C_{H_{c_\alpha}}}{}\right)}{\left(\dfrac{\Delta C_{H_{c_\alpha}}}{}\right)_3} \text{Exp.} \left[A(c,k)\left(\frac{g-a}{b}\right) \right.$$

$$\left. + B(c,a,k) \right] dy$$

$$B_{22} = \pi\rho \cos \psi_{c/4} \int_{\substack{\text{Aero.}\\\text{Bal.}}} b^4 \cos^2 \psi_{\text{\textcent}_c} \, F_{BB} \, K \, \frac{\left(\dfrac{\Delta C_{H_{c_\delta}}}{}\right)_c}{\left(\dfrac{\Delta C_{H_{c_\delta}}}{}\right)_3} \text{Exp.} \; C(c,g,h) \, dy$$

Note that the basic surface expressions A_{21} and A_{22} have been modified by hinge moment correction factors $\left(C_{H_{c_\alpha}} \right)_{\text{Exp.}} \Big/ \left(C_{H_{c_\alpha}} \right)_3$, etc. in order that these terms be consistent with the expressions for the internal aerodynamic balance arrangement.

The remaining portions of the analysis parallel the procedure treated in Paragraph 3.1, with changes in generalized coordinates as discussed in this paragraph. Note also that $[I'] = [A] - [B]$.

4.0 DISCUSSION AND RESULTS

4.1   AILERON AND AILERON FLIGHT TAB

A schematic of the aileron and aileron flight tab system is shown in
Figure 1. A plan view of the wing, outer panel, aileron, and flight tab,
showing the geometry of the analysis, is given in Figure 2, and the aero-
dynamic balancing arrangement is shown in Figure 3.

Parameters

Table 1 lists the aerodynamic parameters required to evaluate the oscil-
latory forces as defined in References 2, 3 and 4 and in Equation (22).

The inertia parameters are:

$$I_\beta = 4.80598 \text{ lb.-in.-sec.}^2$$

$$I_\delta = 0.03108 \text{ lb.-in.-sec.}^2$$

$$S_\delta = -0.00086 \text{ lb.-sec.}^2 \text{ (nose heavy)}$$

$$\ell_t = 14.974 \text{ in.}$$

$$\Delta I_\delta = 0.10834 \text{ lb.-in.-sec.}^2 \text{ (see page 34 for definition)}$$

$$J = 1.50690 \text{ lb.-in.-sec.}^2$$

The uncoupled aileron rotation natural frequencies, a ... ic parameter
for this preliminary analysis, are: $f_\beta = 15, 20, \text{ and } 30$ cps.

Symmetric Analysis

For the purpose of a symmetric flutter analysis, the system is idealized
as shown i. Figure 4.

Since symmetric motion of the ailerons is contrary to the normal opera-
tion of the system, the control stick is assumed locked; hence the stick
rotation freedom is not imposed in the symmetric analysis. It is further
assumed that there is no mechanical gearing between flight tab and
aileron. Note that the restraint of the power boost for the control system
is represented herein by a simple spring.

AILERON TAB

Trim Actuator

AILERON

Power Boost Actuator

WING

Point A

& sym.
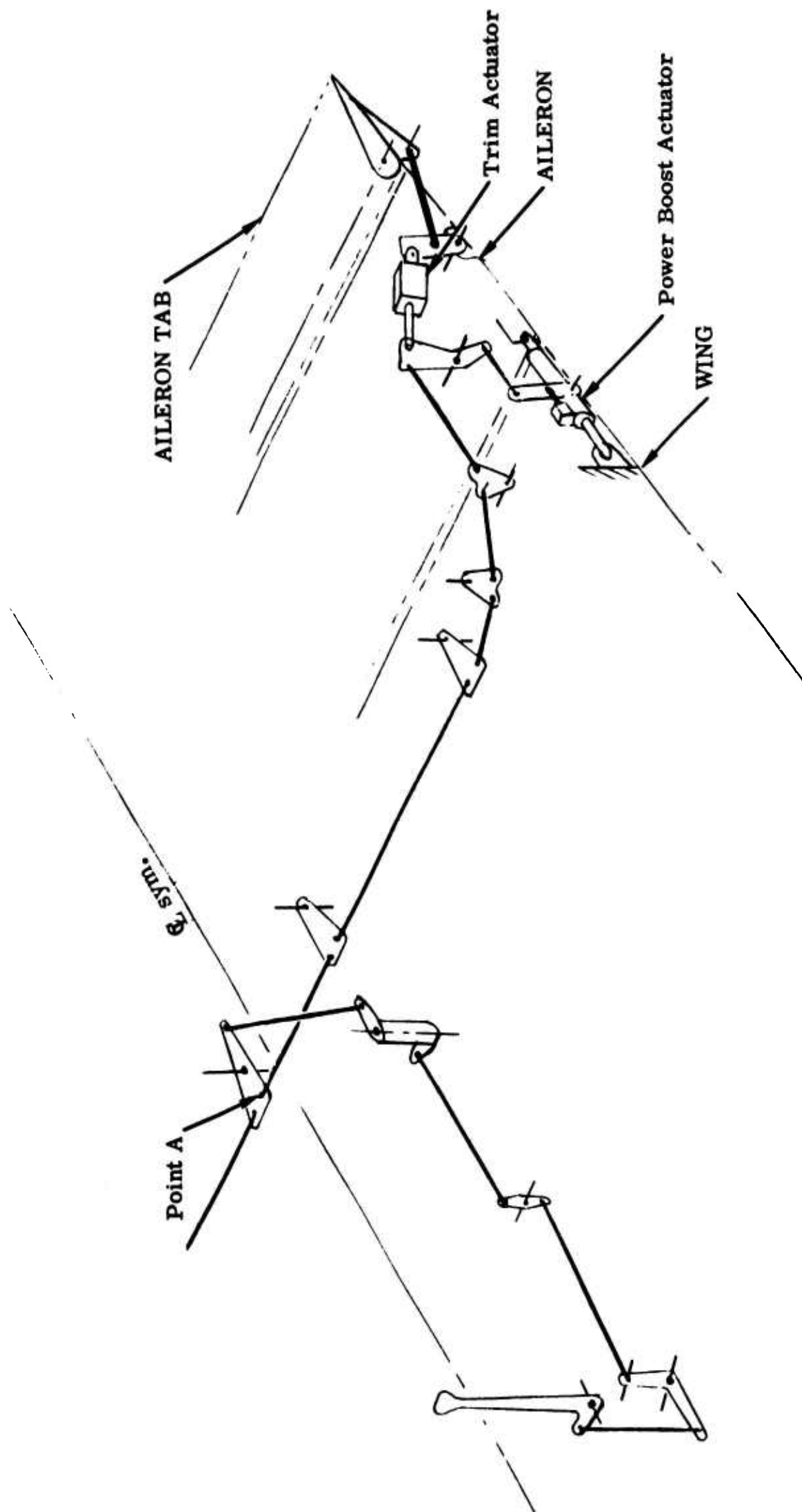
Figure 1 Schematic of Aileron System

30
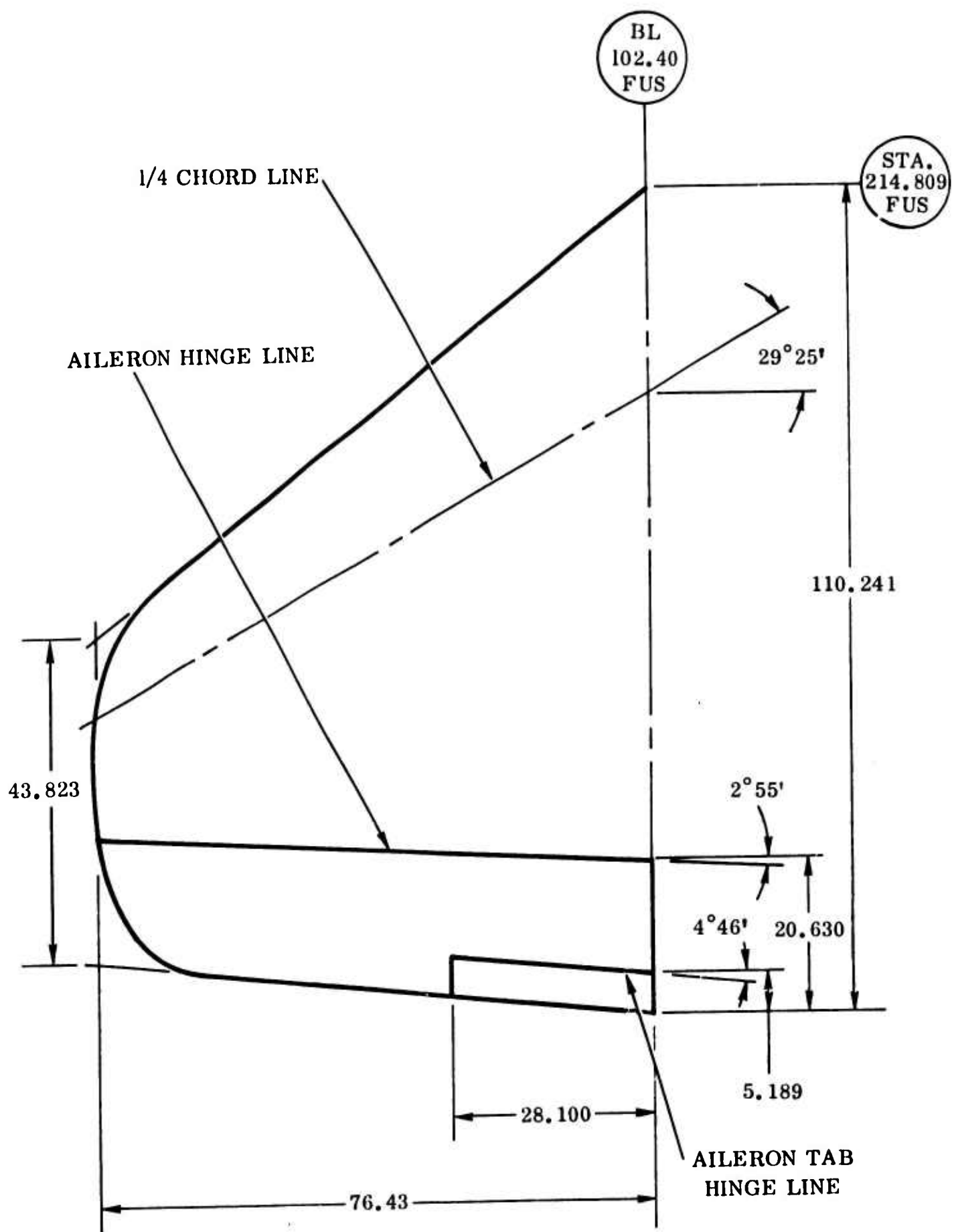
Figure 2 Wing Outer Panel – Plan View
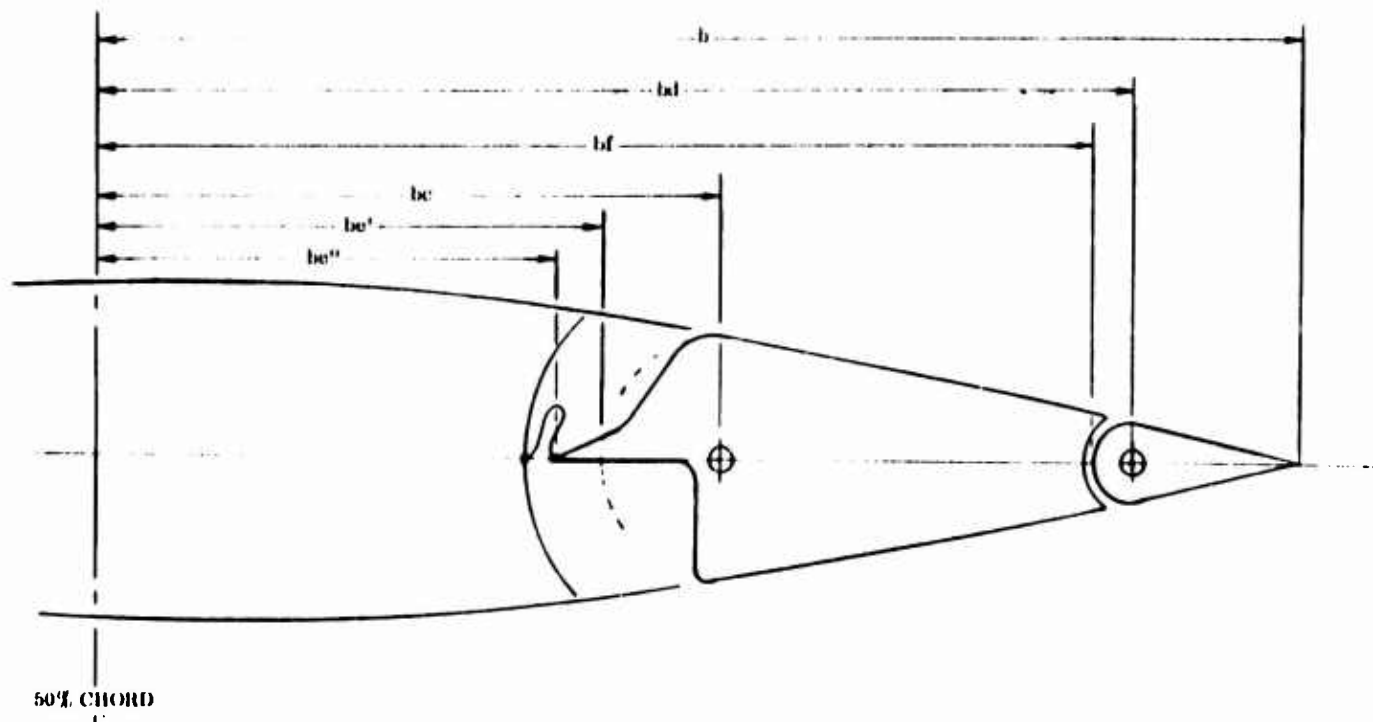
Figure 3   Aileron Aerodynamic Balancing Arrangement
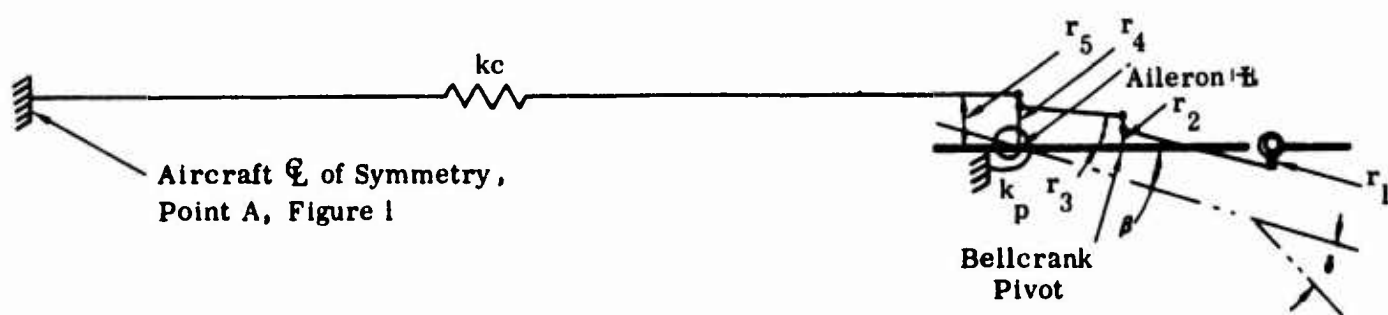
Figure 4   Idealization of Symmetric Aileron System

The degrees of freedom considered are

β = Aileron rotation

δ = Aileron flight tab rotation, relative to the aileron

The potential energy of the system is

$$U = \frac{1}{2} k_c (r_5 \beta - \frac{r_1}{r_2} \frac{r_3}{r_4} r_5 \delta)^2 + \frac{1}{2} K_p \beta^2 \qquad (52)$$

where

k_c = Linear spring restraint offered by control circuit, i.e., effective spring of half the control circuit from Point A to floating link at aileron hinge line

K_p = Rotational spring restraint offered by power actuator

r_1, r_2, r_3, r_4, r_5 = Linkage arm lengths

(See Figure 4 for a schematic representation of k_c, K_P and the r's.)

Calculating the potential energy terms that are part of Lagrange's equations of motion (Equations (1) and (2)) by taking partial derivatives of Equation (52).

$$\frac{\partial U}{\partial \beta} = k_c (b_1 \beta - b_4 \delta) + K_p \beta$$

and

$$\frac{\partial U}{\partial \delta} = k_c (-b_4 \beta + b_2 \delta)$$

where

$$b_1 = r_5^2$$

$$b_2 = \left(\frac{r_1}{r_2} \frac{r_3}{r_4} r_5 \right)^2$$

$$b_4 = \frac{r_1}{r_2} \frac{r_3}{r_4} r_5^2$$

In matrix notation, the potential energy (spring) terms are,

$$
\begin{bmatrix} b_1 k_c + K_p & - b_4 k_c \\ -b_4 k_c & b_2 k_c \end{bmatrix} \begin{vmatrix} \beta \\ \delta \end{vmatrix} = [s] \ \{q\}
$$

and Equation (25), then, is

$$
\left[\begin{bmatrix} I_\beta & P_{\beta\delta} \\ P_{\delta\beta} & I_\delta \end{bmatrix} \frac{-\Omega}{\bar{K}} \begin{bmatrix} b_1 k_c + K_p & - b_4 k_c \\ -b_4 k_c & b_2 k_c \end{bmatrix} + \begin{bmatrix} I'_{11} & I'_{12} \\ I'_{21} & I'_{22} \end{bmatrix} \right] \begin{bmatrix} \beta \\ \delta \end{bmatrix} = \begin{bmatrix} 0 \\ 0 \end{bmatrix}
$$

(53)

For the symmetric case, $\bar{I}_\delta$ is the mass moment of the inertia of the tab about its hinge line I_δ plus the effective mass moments of inertia ΔI_δ of half the control circuit (from Point A to tab) about the tab hinge line. The circuit members are assumed to move with the tab, not with the aileron nor independently, in this condition.

Upon expansion of the characteristic determinant of Equation (53), the following stability equation is obtained:

$$
A\Omega^2 + B\Omega + C = 0
$$

(54)

where A is real, and B and C are complex.

Parameters for the Symmetric Analysis

The linkage parameters are

$$r_1 = 2.50 \text{ in.}$$

$$r_2 = 2.26 \text{ in.}$$

$$r_3 = 3.40 \text{ in.}$$

$$r_4 = 2.50 \text{ in.}$$

$$r_5 = 2.50 \text{ in.}$$

The spring constants are

$$k_c = 5373 \text{ lb.}/\text{in.}$$

$$K_P = 9109;\ 42,312;\ \text{and } 137,178 \text{ lb.-in.}/\text{rad.},\ \text{corresponding to}$$
$$f_\beta = 15,\ 20 \text{ and } 30 \text{ cps, respectively.}$$

$$\bar{K} = 10,000 \text{ lb.-in.}/\text{rad.}$$

The value for k_c was calculated from design values for the aileron flight control tab system. The values for K_P were determined in using Equation 27, for the various values of the uncoupled aileron frequency f_β. The scaling constant $\bar{K}$ was assigned its value arbitrarily, for computing convenience.

Results

Tables 2 through 7 and Figures 5 through 10 show the effects of varying the aileron uncoupled frequency f_β and aerodynamic balance. Figure 11 shows a cross-plot of sea-level flutter velocity V_f versus f_β for the symmetric aileron condition.

Conclusions

In order to clear the flight envelope to 500 knots +15% (575 knots) at sea level, as required, examination of the tables and curves shows that the uncoupled tab frequency f_δ must be made greater than indicated (51.9 cps) either with or without aerodynamic balancing for the aileron. Since f_δ is not a parameter of the analysis, quantitative requirements for f_δ are not available. The coupled, predominantly aileron mode (the lower-frequency branch) is stable for all f_β values investigated. The symmetric flutter condition occurs in the coupled, predominantly tab mode (the higher-frequency branch). f_δ, particularly the value of k_c, would strongly affect the flutter mode.

The uncoupled aileron frequency f_β has little effect on the flutter frequency, but the flutter velocity decreases with increasing f_β. This effect is understandable in that the predominantly aileron mode coalesces to the predominantly tab mode with increasing f_β, thereby increasing the coupling between the two modes. Increased coupling means a lower flutter velocity. Stating the above conclusions in another way, the (coupled) frequencies of the two branches should be separated more. Since the flutter mode consists predominantly of tab motion, the best way to secure increased separation is to increase f_δ, which in turn is best increased

by an increased value of k_c, the circuit stiffness. Further analysis should be made on calculated refinements to the circuit stiffness as the design develops and on the basis of tested values of uncoupled aileron and tab natural frequencies.

Aerodynamic balance of the aileron has little effect on the flutter <u>frequency</u>; however, the cases with balanced aileron (B≠0) yield slightly higher flutter <u>velocities</u>, by about 30 knots, than the cases with unbalanced aileron (B=0) for the same f_β value.

TABLE 1

AILERON - AILERON FLIGHT TAB AERODYNAMIC PARAMETERS

Aileron - Aileron Flight Tab Geometry:

Sta. No.	B.L. in.	b in.	c	e'	e''	g*	F_{BB}	d	f	
1	102.40	55.120	0.626	0.559	0.498	0.708	0.00590	0.906	0.906	⎫ Aileron
2	111.77	50.742	0.602	0.533	0.473	0.682	0.00590	0.901	0.901	⎬ &
3	121.13	46.364	0.574	0.502	0.443	0.654	0.00589	0.894	0.894	⎪ Tab
4_I	130.50	41.986	0.539	0.464	0.407	0.619	0.00587	0.887	0.887	⎭
4_0	130.50	41.986	0.539	0.464	0.407	0.619	0.00587	-	-	⎫
5	140.17	37.919	0.501	0.422	0.368	0.581	0.00579	-	-	⎪
6	149.83	33.852	0.454	0.370	0.318	0.534	0.00566	-	-	⎬ Aileron
7	159.50	29.785	0.393	0.303	0.255	0.473	0.00548	-	-	⎪
8	169.16	25.718	0.314	0.216	0.172	0.394	0.00519	-	-	⎪
9	178.83	21.652	0.204	0.130	0.130	0.284	0.0	-	-	⎭

Function C (c, g, k) evaluated for c = 0.467 (Avg.) and g = 0.547
Function D (c, d, k) evaluated for c = 0.467 (Avg.) and d = 0.897 (Avg.)
* For g - c = 0.08

Aerodynamic Balance Arrangement:

       Aileron, internal - simple nose overhang (curtain seal)
       Flight Tab, none - radius nose

Hinge Moment Corrections:

$$\frac{\left(C_{H_{c_{\delta_c}}}\right)_{Exp.}}{\left(C_{H_{c_{\delta_c}}}\right)_3} = 1.0 \quad ; \quad \frac{\left(C_{H_{c_{\delta_t}}}\right)_{Exp.}}{\left(C_{H_{c_{\delta_t}}}\right)_3} = 1.0$$

TABLE 1 (Continued)

$$\frac{\left(C_{H_{t_{\delta_c}}}\right)_{Exp.}}{\left(C_{H_{t_{\delta_c}}}\right)_3} = 1.0 \quad ; \quad \frac{\left(C_{H_{t_{\delta_t}}}\right)_{Exp.}}{\left(C_{H_{t_{\delta_t}}}\right)_3} = 1.0$$

$$\frac{\left(\Delta C_{H_{c_{\delta_c}}}\right)_{Exp.}}{\left(\Delta C_{H_{c_{\delta_c}}}\right)_3} = 1.0 \quad ; \quad \frac{\left(\Delta C_{H_{c_{\delta_t}}}\right)_{Exp.}}{\left(\Delta C_{H_{c_{\delta_t}}}\right)_3} = 1.0$$

Pressure Recovery Factor:

$$K = 1.0$$

General:

Reference half-chord (b_0) = 55.120 in.

$$\cos \psi_{c/4} = 0.87114$$

$$\cos \psi_{\textit{£}_c} = 0.99871$$

$$\cos \psi_{\textit{£}_t} = 0.99657$$

Altitude - Sea Level ($\rho = 0.114626 \times 10^{-6}$ lb.-sec^2 - in.$^{-4}$)

TABLE 2

SOLUTIONS OF STABILITY EQUATIONS

(Symmetric Analysis)

Plot: Figure 5

Uncoupled Natural Frequency, Aileron Rotation: $f_\beta = 15$ cps

Spring Constants:

$$k_c = 5373 \text{ lb./in.}$$

$$K_p = 9109 \text{ lb.-in./rad.}$$

Aerodynamics: Basic Surface with Aerodynamic Balance $(B \neq 0)$

$\dfrac{1}{k_o}$	f_1 cps	V_1 Knots	g_1	f_2 cps	V_2 Knots	g_2
.00	6.7	0.0	.000	53.9	0.0	.000
.05	6.5	5.6	-.032	53.8	46.0	-.004
.10	6.5	11.2	-.064	53.8	92.0	-.008
.15	6.6	16.9	-.097	53.8	138.0	-.011
.20	6.7	22.8	-.131	53.8	184.0	-.014
.50	7.7	65.7	-.433	53.5	457.7	-.002
.75	10.9	139.3	-1.280	54.2	695.5	.146
1.00	-	-	-	68.7	1174.1	.434

$V_f = 463$ knots

Uncoupled Natural Frequency, Tab Rotation: $f_\delta = 51.9$ cps

TABLE 3

SOLUTIONS OF STABILITY EQUATIONS

(Symmetric Analysis)

Plot: Figure 6

Uncoupled Natural Frequency, Aileron Rotation: $f_\beta = 20$ cps

Spring Constants:

$$k_c = 5373 \text{ lb./in.}$$
$$K_p = 42,312 \text{ lb.-in./rad.}$$

Aerodynamics: Basic Surface with Aerodynamic Balance (B $\neq$ 0)

$\dfrac{1}{k_o}$	f_1 cps	V_1 Knots	g_1	f_2 cps	V_2 Knots	g_2
.00	14.3	0.0	.000	54.1	0.0	.000
.05	14.0	12.0	-.032	53.9	46.1	-.004
.10	14.1	24.1	-.064	53.9	92.2	-.008
.15	14.2	36.4	-.097	53.9	138.3	-.011
.20	14.3	49.0	-.132	53.9	184.3	-.014
.50	16.6	142.2	-.443	53.4	456.7	.007
.75	23.9	306.5	-1.381	54.6	700.3	.184
1.00	-	-	-	70.1	1198.3	.442

$V_f = 432$ knots

Uncoupled Natural Frequency, Tab Rotation: $f_\delta = 51.9$ cps

TABLE 4

SOLUTIONS OF STABILITY EQUATIONS

(Symmetric Analysis)

Plot: Figure 7

Uncoupled Natural Frequency, Aileron Rotation: f_β = 30 cps

Spring Constants:

$$k_c = 5373 \text{ lb./in.}$$

$$K_p = 137,178 \text{ lb.-in./rad.}$$

Aerodynamics: Basic Surface with Aerodynamic Balance (B ≠ 0)

$\dfrac{1}{k_0}$	f_1 cps	V_1 Knots	g_1	f_2 cps	V_2 Knots	g_2
.00	25.6	0.0	.000	54.5	0.0	.000
.05	25.0	21.4	-.032	54.4	46.5	-.004
.10	25.1	43.0	-.064	54.3	92.9	-.007
.15	25.4	65.0	-.098	54.3	139.2	-.010
.20	25.6	87.7	-.134	54.2	185.3	-.012
.50	30.3	259.4	-.485	53.2	454.7	.042
.75	44.7	572.7	-1.677	56.9	729.7	.278
1.00	-	-	-	73.4	1255.3	.446

V_f = 356 knots

Uncoupled Natural Frequency, Tab Rotation: f_δ = 51.9 cps

TABLE 5

SOLUTIONS OF STABILITY EQUATIONS

(Symmetric Analysis)

Plot: Figure 8

Uncoupled Natural Frequency, Aileron Rotation: $f_\beta = 15$ cps

Spring Constants:

$$k_c = 5373 \text{ lb./in.}$$

$$K_p = 9109 \text{ lb.-in./rad.}$$

Aerodynamics: Basic Surface without Aerodynamic Balance ($B = 0$)

$\dfrac{1}{k_o}$	f_1 cps	V_1 Knots	g_1	f_2 cps	V_2 Knots	g_2
.00	6.7	0.0	.000	53.9	0.0	.000
.05	6.5	5.6	-.033	53.8	46.0	-.004
.10	6.5	11.2	-.067	53.8	92.0	-.008
.15	6.6	16.9	-.102	53.8	138.0	-.011
.20	6.7	22.8	-.139	53.8	184.0	-.014
.50	7.8	66.9	-.475	53.4	456.6	.005
.75	11.9	153.1	-1.634	54.7	701.2	.196
1.00	-	-	-	73.1	1250.4	.483

$$V_f = 434 \text{ knots}$$

Uncoupled Natural Frequency, Tab Rotation: $f_\delta = 51.9$ cps

TABLE 6

SOLUTIONS OF STABILITY EQUATIONS

(Symmetric Analysis)

Plot: Figure 9

Uncoupled Natural Frequency, Aileron Rotation: f_β = 20 cps

Spring Constants:

$$k_c = 5373 \text{ lb./in.}$$

$$K_p = 42,312 \text{ lb.-in./rad.}$$

Aerodynamics: Basic Surface without Aerodynamic Balance (B = 0)

$\dfrac{1}{k_o}$	f_1 cps	V_1 Knots	g_1	f_2 cps	V_2 Knots	g_2
.00	14.3	0.0	.000	54.1	0.0	.000
.05	14.0	12.0	-.033	53.9	46.1	-.004
.10	14.1	24.0	-.067	53.9	92.2	-.008
.15	14.2	36.4	-.103	53.9	138.3	-.011
.20	14.3	49.0	-.140	53.9	184.2	-.014
.50	16.9	144.9	-.487	53.3	455.7	.015
.75	26.3	377.4	-1.773	55.3	709.8	.234
1.00	-	-	-	74.3	1269.9	.479

V_f = 404 knots

Uncoupled Natural Frequency, Tab Rotation: f_δ = 51.9 cps

TABLE 7

SOLUTIONS OF STABILITY EQUATIONS

(Symmetric Analysis)

Plot: Figure 10

Uncoupled Natural Frequency, Aileron Rotation: $f_\beta = 30$ cps

Spring Constants:

$k_c = 5373$ lb./in.

$K_p = 137,178$ lb.-in./rad.

Aerodynamics: Basic Surface without Aerodynamic Balance (B = 0)

$\dfrac{1}{k_o}$	f_1 cps	V_1 Knots	g_1	f_2 cps	V_2 Knots	g_2
.00	25.6	0.0	.000	54.5	0.0	.000
.05	25.0	21.4	-.034	54.4	46.5	-.004
.10	25.1	43.0	-.068	54.3	92.9	-.007
.15	25.4	65.0	-.104	54.3	139.2	-.010
.20	25.7	87.8	-.142	54.2	185.3	-.012
.50	30.9	264.4	-.535	53.1	454.4	.053
.75	48.9	627.7	-2.127	58.1	745.7	.313
1.00	-	-	-	76.9	1315.5	.461

$V_f = 320$ knots

Uncoupled Natural Frequency, Tab Rotation: $f_\delta = 51.9$ cps

Figure 5   g-V and f-V Plots, Symmetric Aileron, $f_{\beta} = 15$ cps, B $\neq$ 0

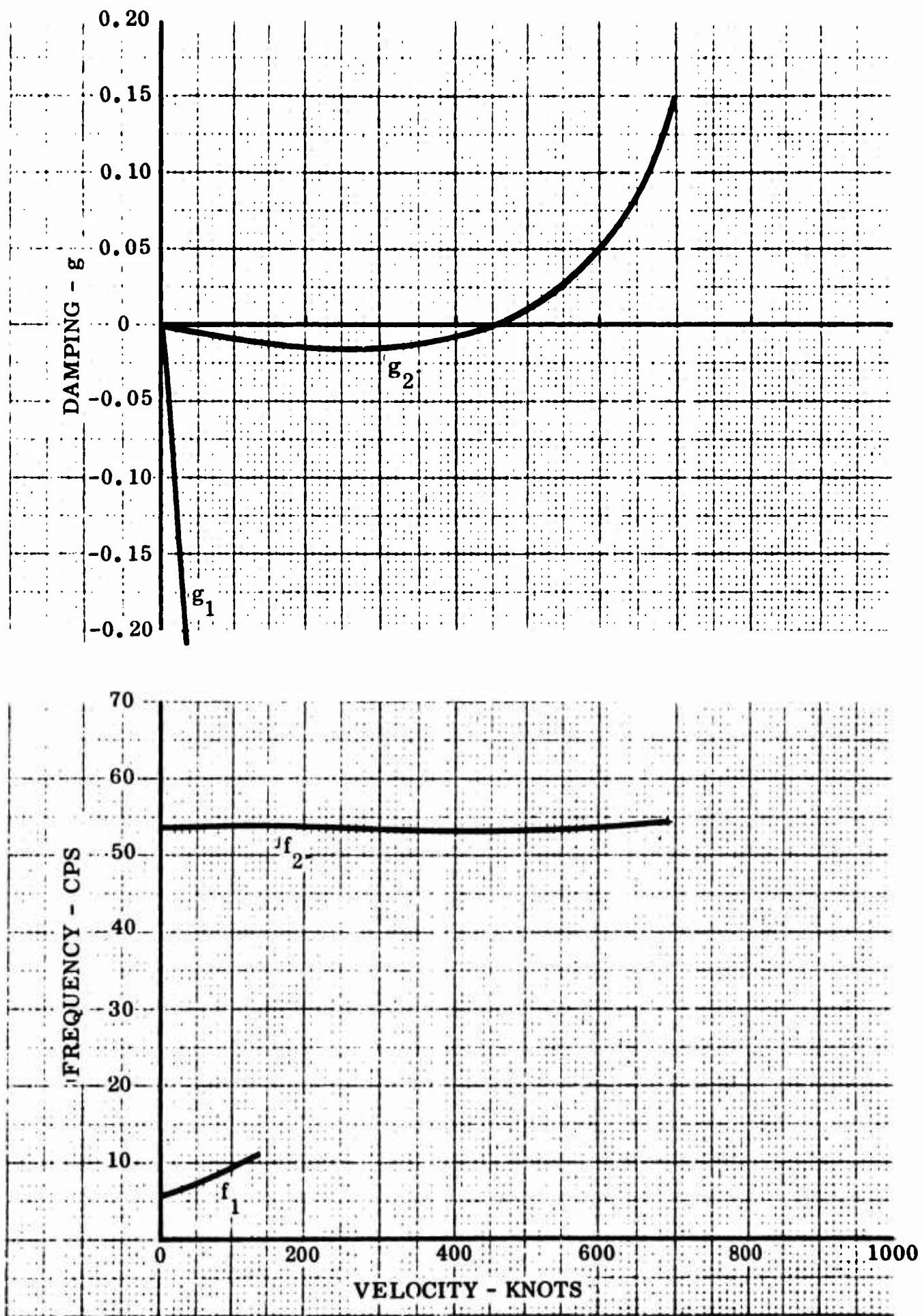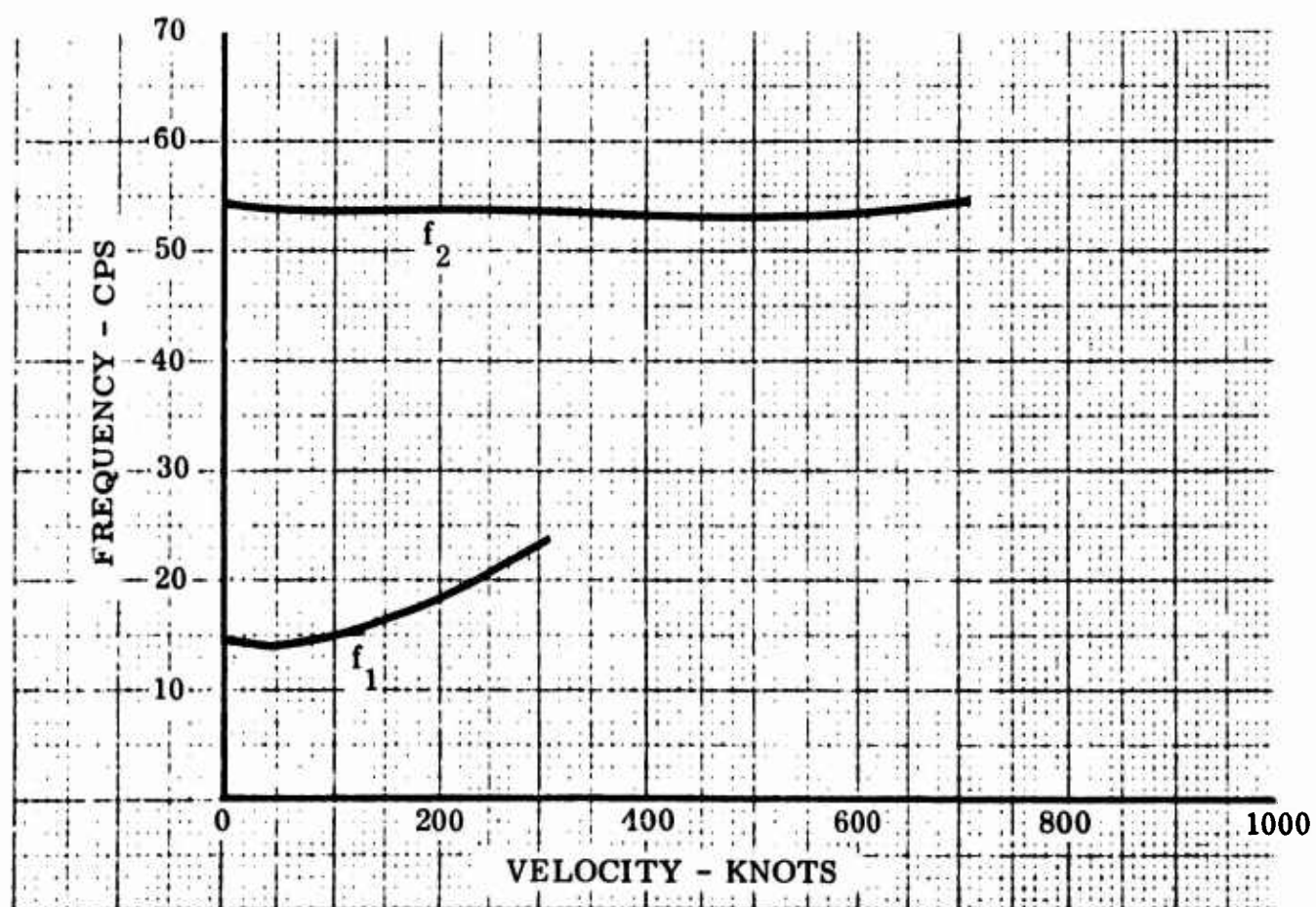Figure 6   g-V and f-V Plots, Symmetric Aileron, f_β = 20 cps, B $\neq$ 0

Figure 7   g-V and f-V Plots, Symmetric Aileron, $f_\beta = 30$ cps, $B \neq 0$

Figure 8   g-V and f-V Plots, Symmetric Aileron, f_β = 15 cps, B = 0
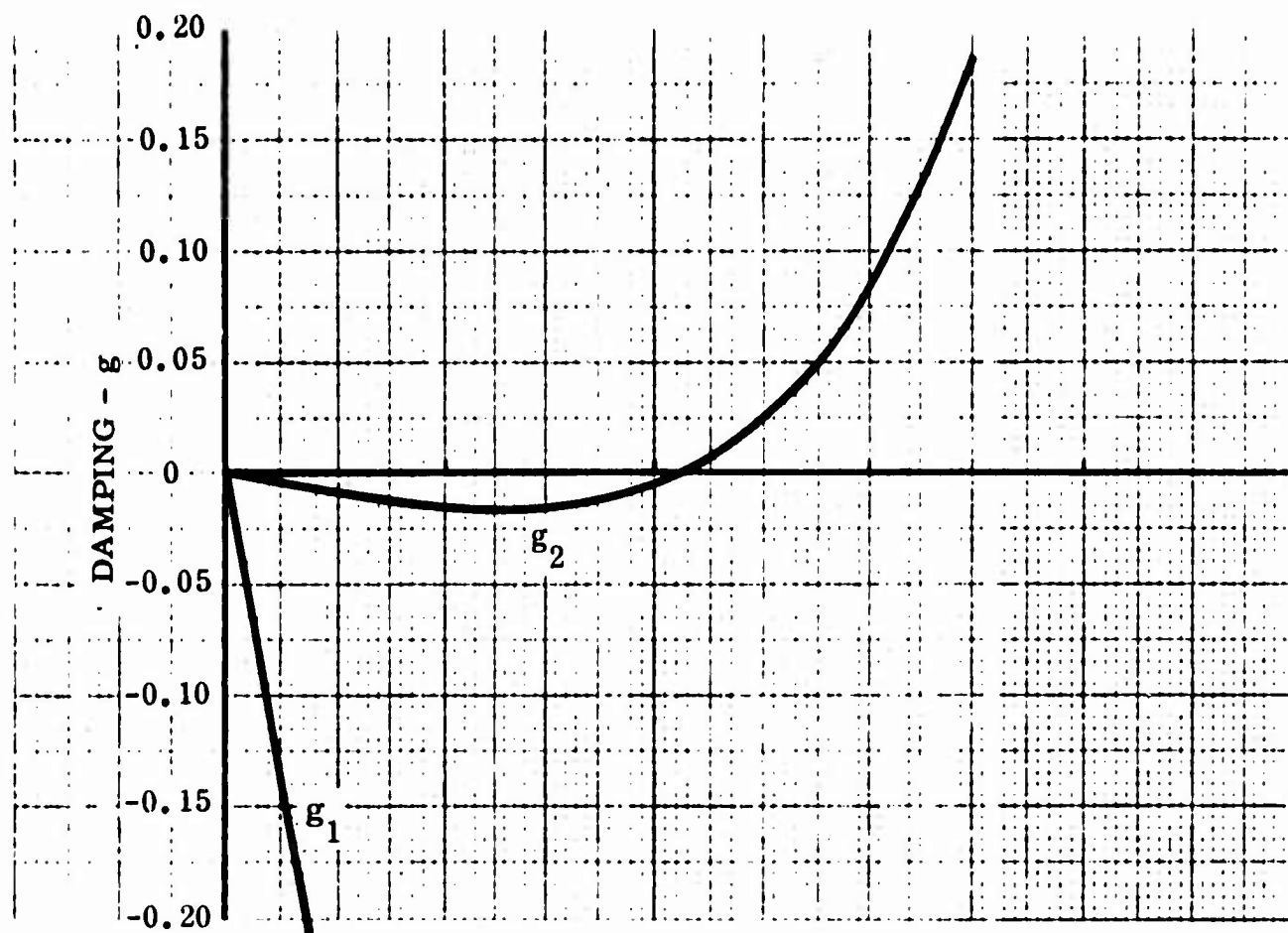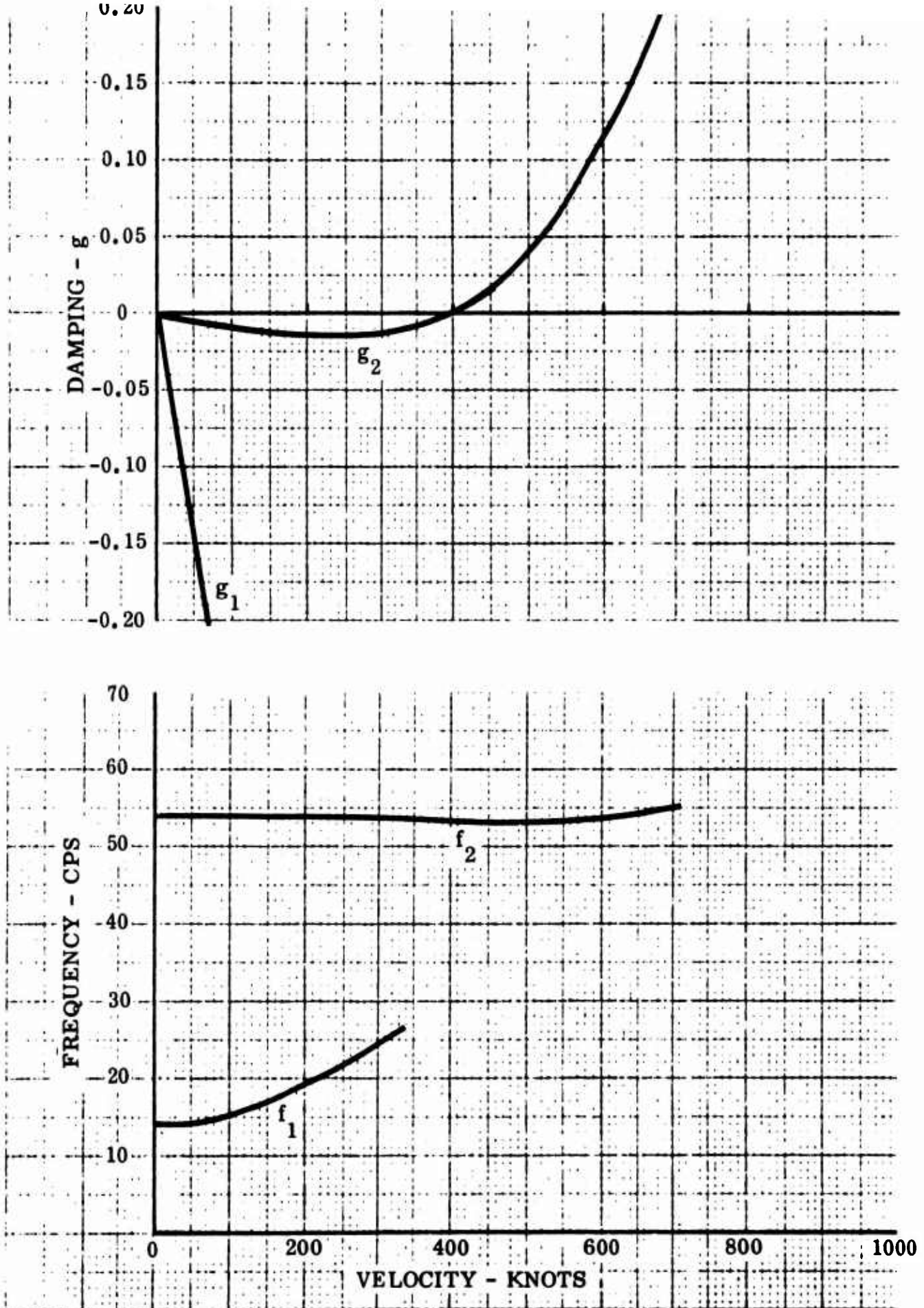
Figure 9   g-V and f-V Plots, Symmetric Aileron, f_β = 20 cps, B = 0

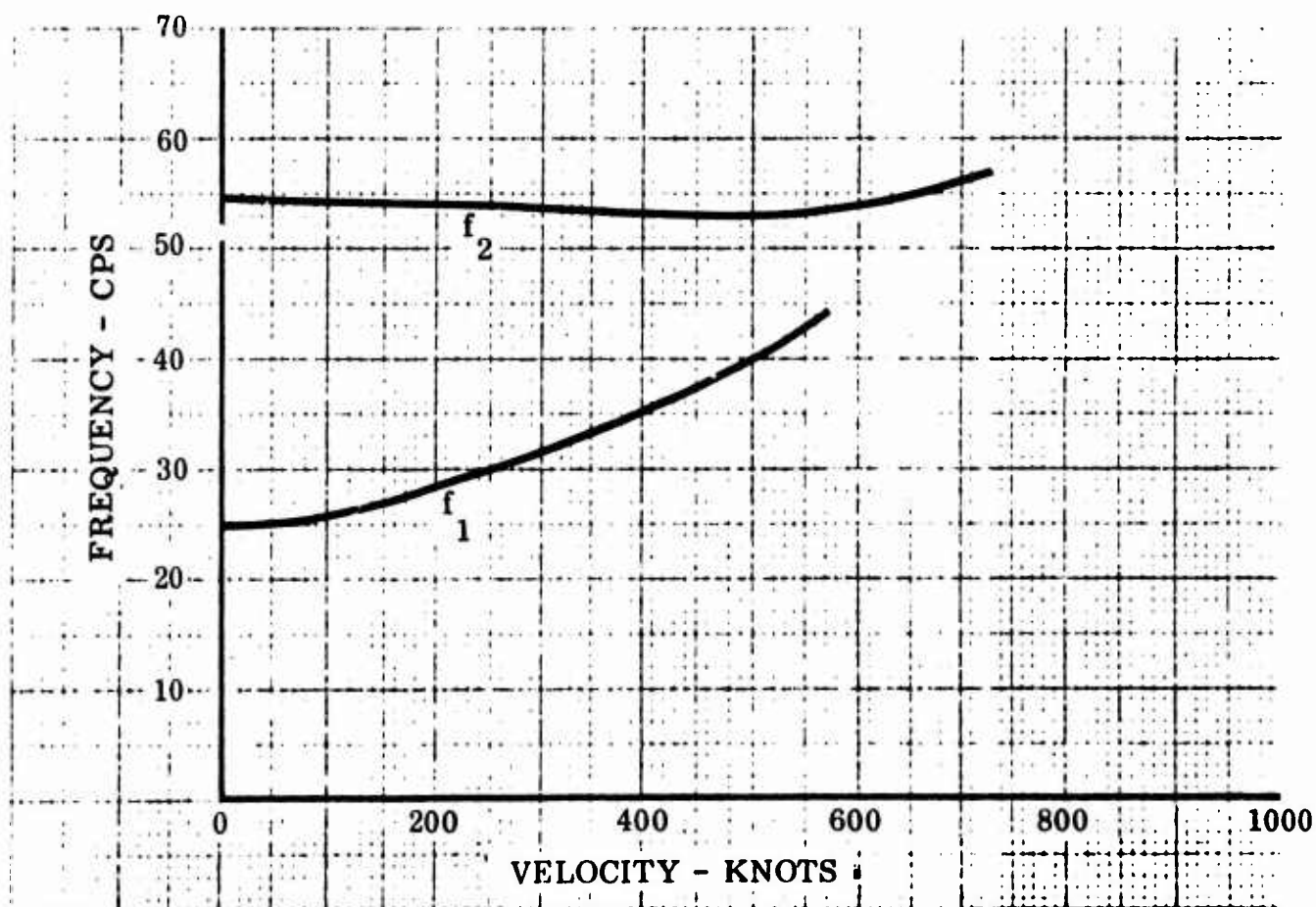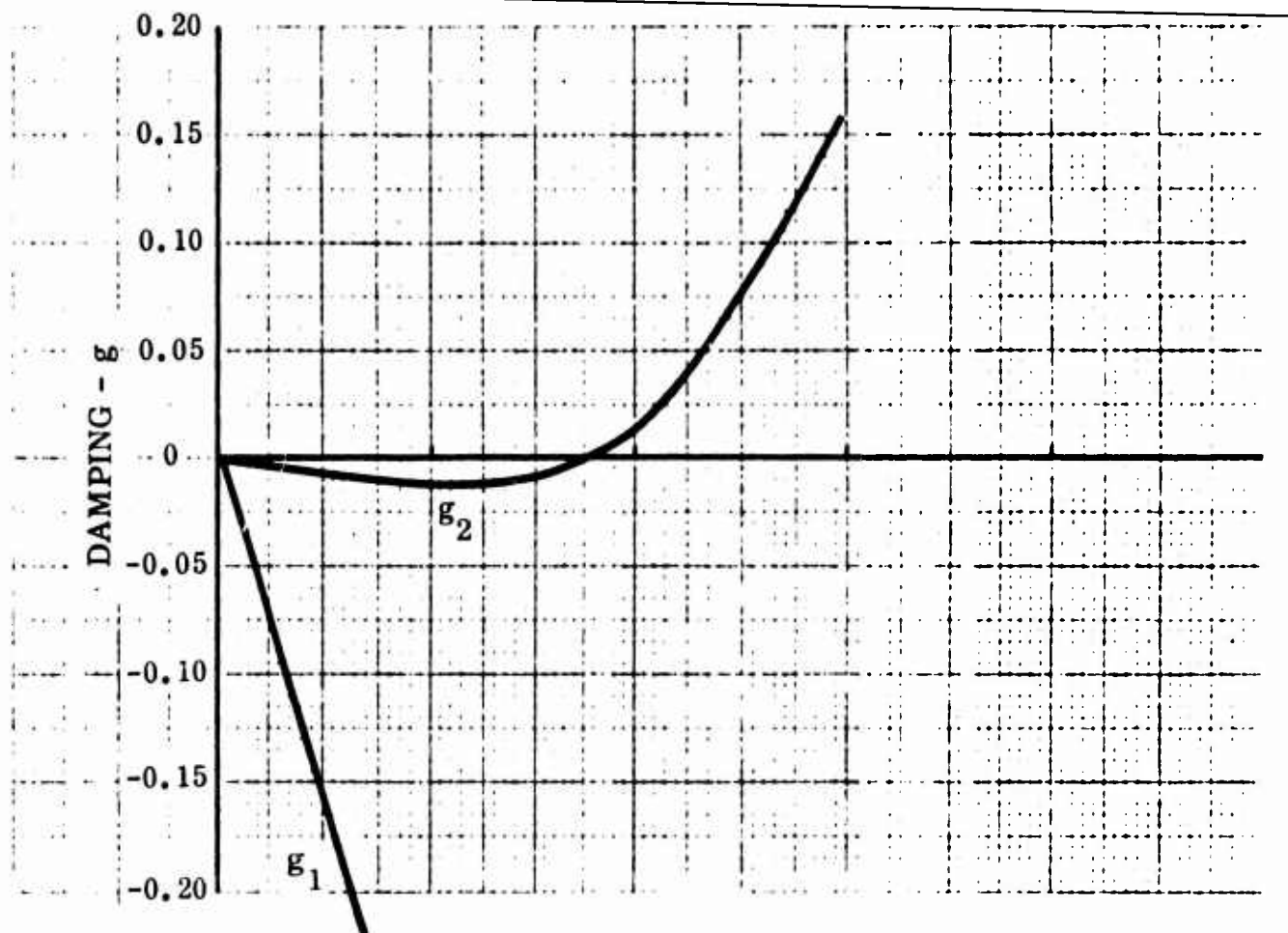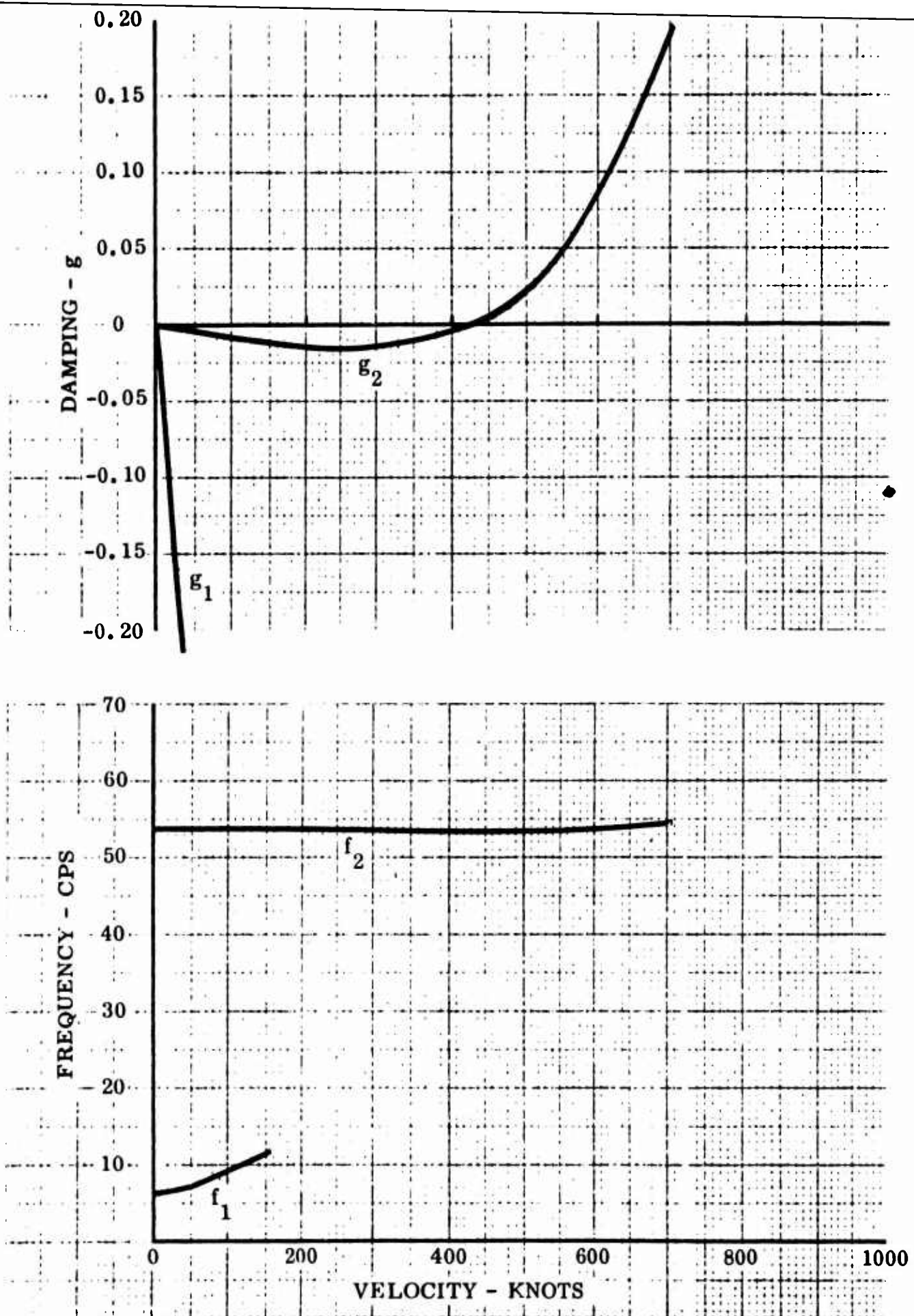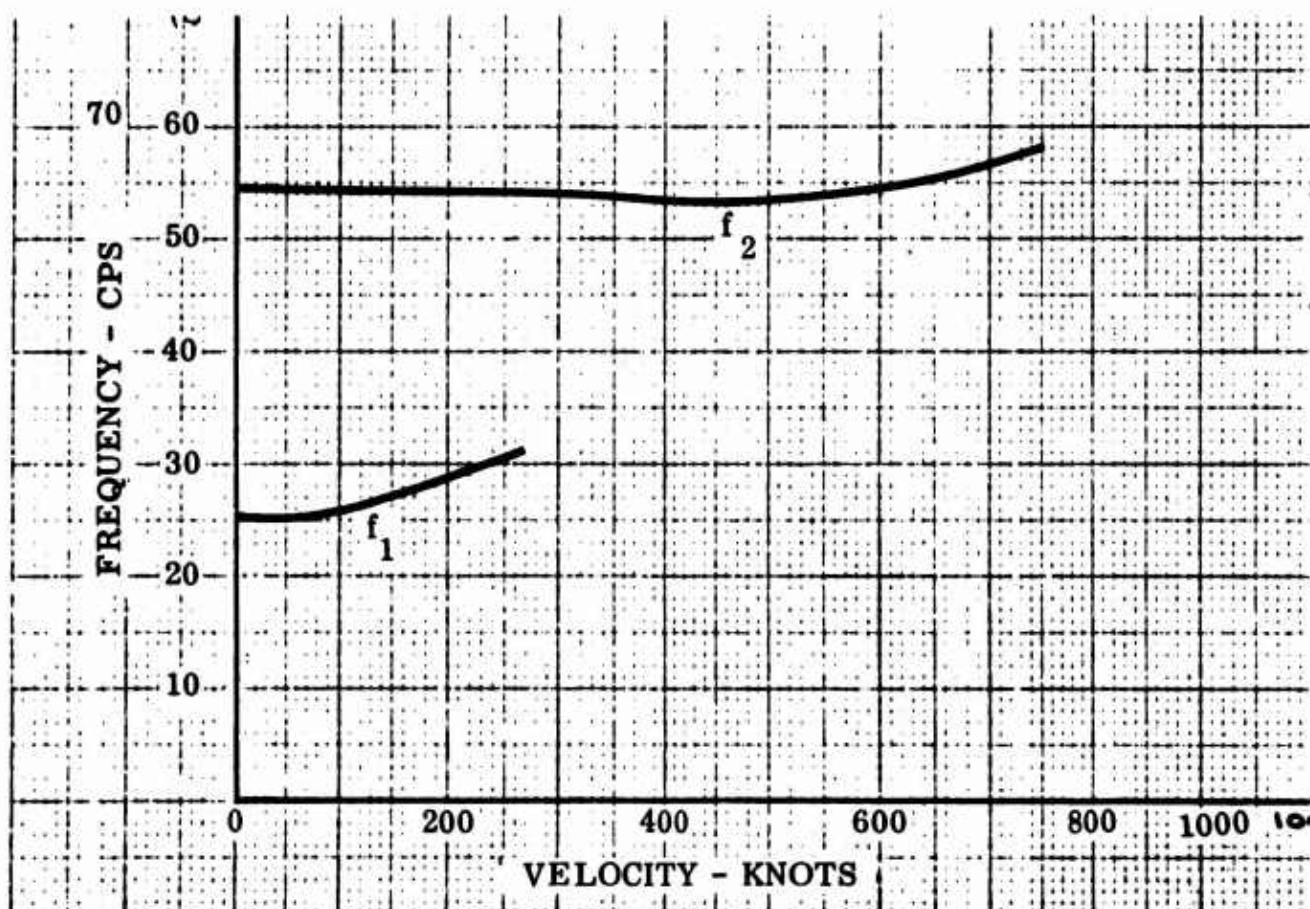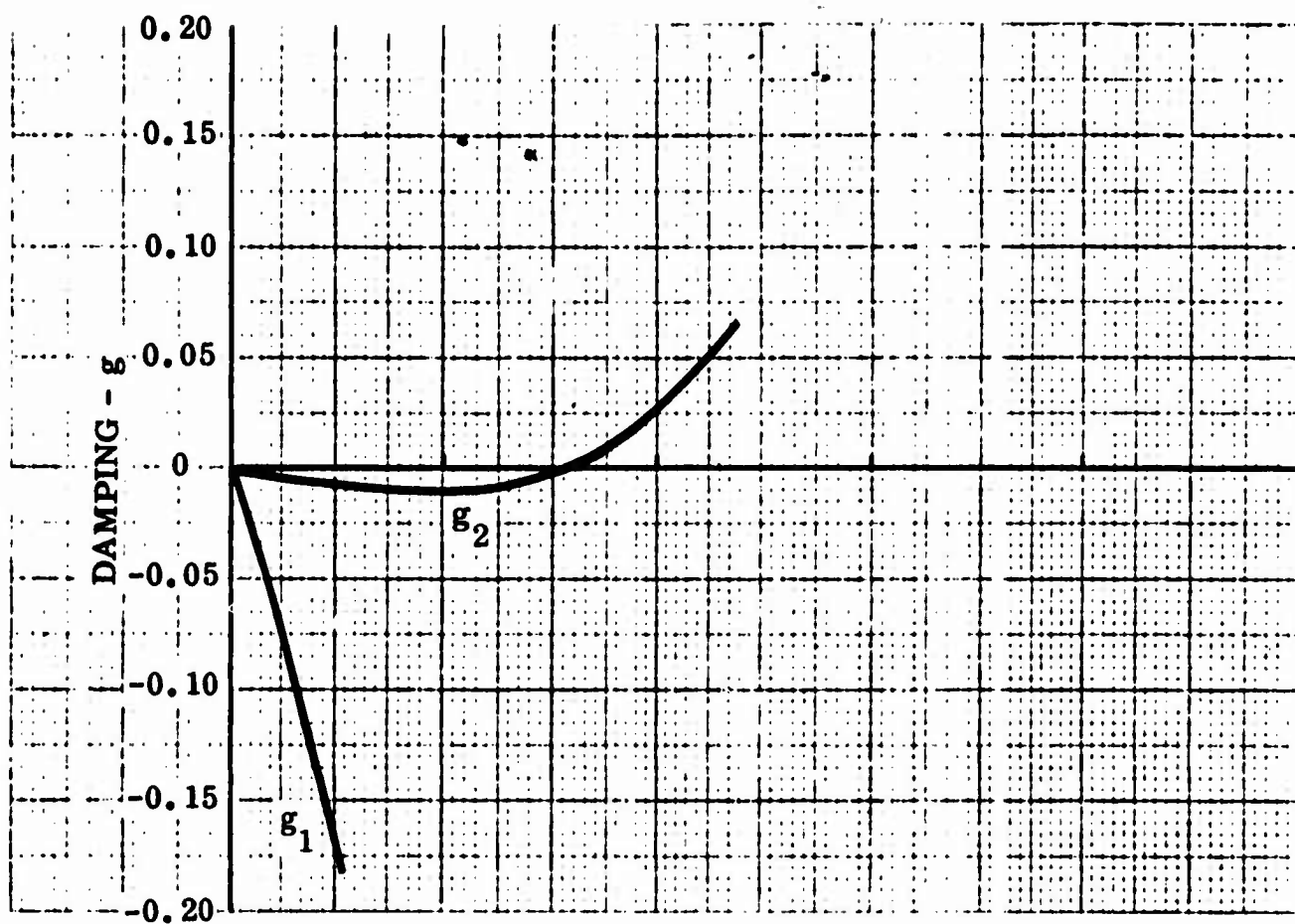Figure 10   g-V and f-V Plots, Symmetric Aileron, f_β = 30 cps, B = 0
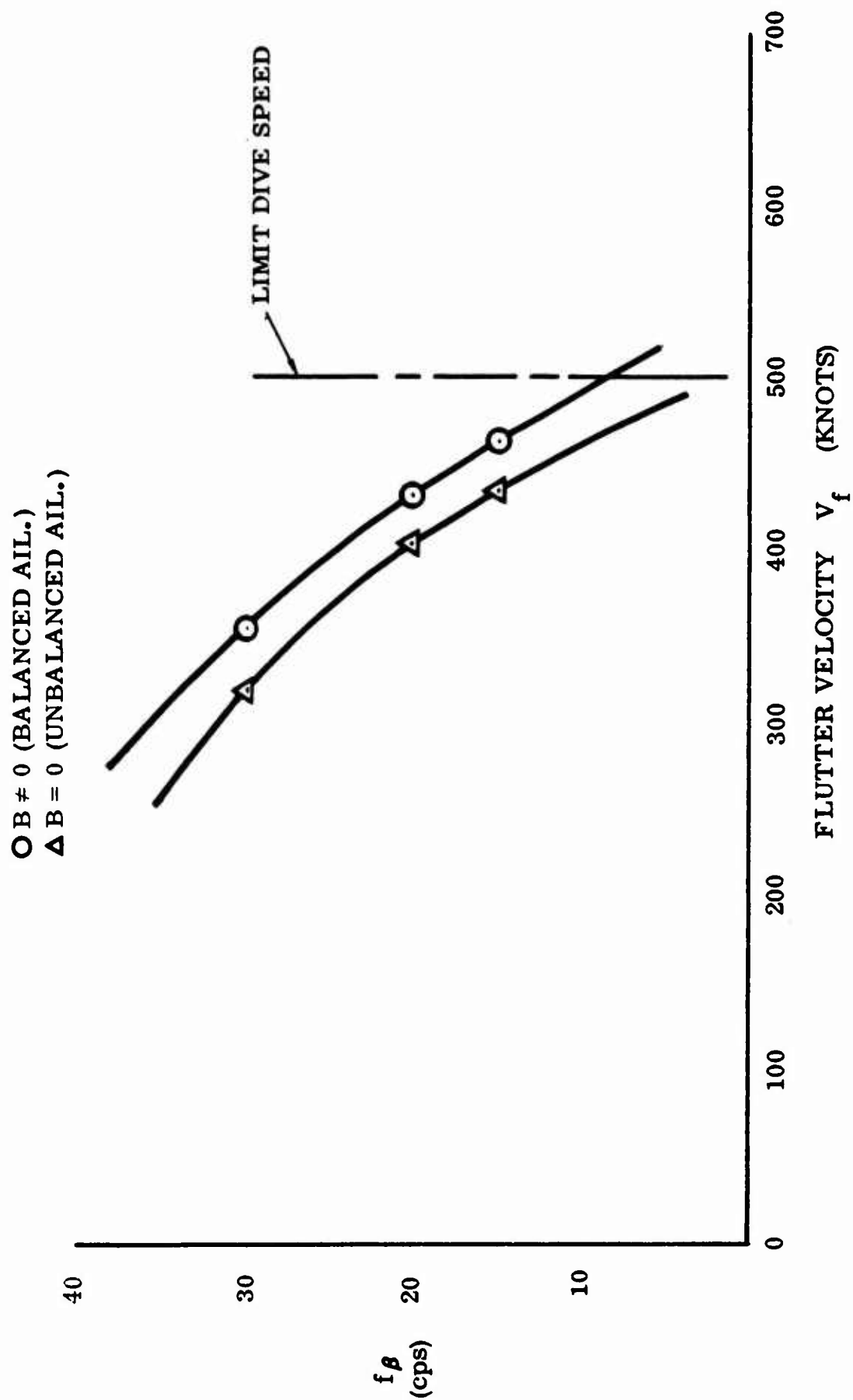
Figure 11 V_f vs f_β Cross-plot, Symmetric Aileron

○ B ≠ 0 (BALANCED AIL.)
△ B = 0 (UNBALANCED AIL.)

LIMIT DIVE SPEED

FLUTTER VELOCITY V_f (KNOTS)

f_β (cps)

Antisymmetric Analysis

For the purpose of an antisymmetric flutter analysis, the system is idealized as shown in Figure 12.
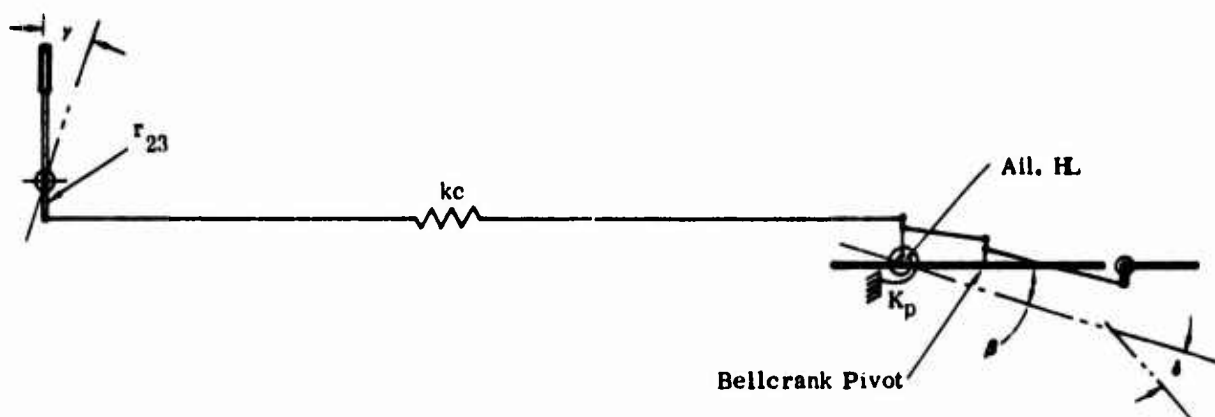
Figure 12   Idealization of Antisymmetric Aileron System

The degrees of freedom considered are as follows:

β = Aileron rotation

δ = Aileron flight tab rotation, relative to the aileron

γ = Control stick rotation

It is still assumed that there is no mechanical gearing between flight tab and aileron and that the restraint of the power boost for the control system can be represented by a simple spring.

The potential energy of the system is

$$U = \frac{1}{2} k_c \left(r_5 \beta - \frac{r_1}{r_2} \frac{r_3}{r_4} r_5 \delta + r_{23} \gamma \right)^2 + \frac{1}{2} K_p \beta^2 \qquad (55)$$

where

k_c = Linear spring restraint offered by control circuit; i.e.,
the effective spring of <u>half</u> the control circuit from control
sticks to floating link at aileron hinge line

K_p = Rotational spring restraint offered by power actuator

r_1, r_2, r_3, r_4, r_5, r_{23} = Linkage arm lengths

(See Figure 12 for a schematic representation of k_c, K_p and the r's)

Taking partial derivative of Equation (55),

$$\frac{\partial U}{\partial \beta} = k_c (a_1 \beta - a_4 \delta + a_5 \gamma) + K_p \beta$$

$$\frac{\partial U}{\partial \delta} = k_c (-a_4 \beta + a_2 \delta - a_6 \gamma)$$

$$\frac{\partial U}{\partial \gamma} = k_c (a_5 \beta - a_6 \delta + a_3 \gamma)$$

where

$$a_1 = r_5^2 \quad (= b_1 \text{ of the symmetrical case, page 33})$$

$$a_2 = \left(\frac{r_1}{r_2} \frac{r_3}{r_4} r_5 \right)^2 \quad (= b_2)$$

$$a_3 = r_{23}^2$$

$$a_4 = \frac{r_1}{r_2} \frac{r_3}{r_4} r_5^2 \quad (= b_4)$$

$$a_5 = r_5 r_{23}$$

$$a_6 = \frac{r_1}{r_2} \frac{r_3}{r_4} r_5 r_{23}$$

In matrix notation, then, the potential energy (spring) terms in Lagrange's equations of motion (Equations (1), (2), and (3)) are

$$
\begin{bmatrix}
a_1 k_c + K_p & -a_4 k_c & a_5 k_c \\
-a_4 k_c & a_2 k_c & -a_6 k_c \\
a_5 k_c & -a_6 k_c & a_3 k_c
\end{bmatrix}
\begin{bmatrix}
\beta \\
\delta \\
\gamma
\end{bmatrix}
= [s] \ \{q\}
$$

and Equation (25) is

$$
\begin{bmatrix}
I_\beta & P_{\beta\delta} & 0 \\
P_{\delta\beta} & I_\delta & 0 \\
0 & 0 & J
\end{bmatrix}
\frac{-\Omega}{\overline{K}}
\begin{bmatrix}
a_1 k_c + K_p & -a_4 k_c & a_5 k_c \\
-a_4 k_c & a_2 k_c & -a_6 k_c \\
a_5 k_c & -a_6 k_c & a_3 k_c
\end{bmatrix}
+
\begin{bmatrix}
I'_{11} & I'_{12} \\
I'_{21} & I'_{22} \\
0 & 0
\end{bmatrix}
\begin{bmatrix}
0 & \beta \\
0 & \delta \\
0 & \gamma
\end{bmatrix}
=
\begin{bmatrix}
0 \\
0 \\
0
\end{bmatrix}
$$

(56)

Upon expansion of the characteristic determinant of Equation (56), because of relationships between [S] elements in terms of the r's ([S] is singular), the following stability equation is obtained:

$$ A\Omega^2 + B\Omega + C = 0 \tag{57} $$

where A is real, and B and C are complex.

Parameters for the Antisymmetric Analysis

The linkage parameters, r_1 through r_5, are the same as given previously for the symmetric case, page 34.

$$ r_{23} = 3.20 \text{ in.} $$

The spring constants are:

$$ k_c = 911 \text{ lb./in.} $$

K_p = 39,496; 72,699; and 167,565 lb.-in./rad. corresponding to f_β = 15, 20 and 30 cps, respectively.

$$ \overline{K} = 10,000 \text{ lb.-in./rad.} $$

The value for k_c was calculated from design values for the aileron-flight tab control system. The values for K_p were determined, using Equation 27, for the various values of the uncoupled aileron frequency f_β. The scaling constant $\overline{K}$ was assigned its value arbitrarily, for computing convenience.

Results

Tables 8 through 13 and Figures 13 through 18 show the effects of varying the aileron uncoupled frequency f_β and aerodynamic balance.

Conclusions

Examination of the analysis results show that antisymmetric aileron system flutter will not occur over the range of f_β and $1/k_0$ values investigated, either with or without aerodynamic balance for the ailerons.

TABLE 8

SOLUTIONS OF STABILITY EQUATIONS

(Antisymmetric Analysis)

Plot: Figure 13

Uncoupled Natural Frequency, Aileron Rotation: f_β = 15 cps

Spring Constants:

k_c = 911 lb./in.

K_p = 39,496 lb.-in./rad.

Aerodynamics: Basic Surface with Aerodynamic Balance (B $\neq$ 0)

$\frac{1}{k_o}$	f_1 cps	V_1 Knots	g_1	f_2 cps	V_2 Knots	g_2
.00	13.9	0.0	.000	103.8	0.0	.000
.05	13.6	11.6	-.031	102.6	87.7	-.029
.10	13.6	23.3	-.061	103.4	176.9	-.060
.15	13.7	35.1	-.093	104.9	269.0	-.094
.20	13.8	47.1	-.126	107.0	365.9	-.133
.50	15.2	130.2	-.377	152.7	1305.6	-.848
.75	18.6	239.2	-.822	-	-	-
1.00	35.7	610.0	-3.822	-	-	-

Uncoupled Natural Frequency, Tab Rotation: f_δ = 102.5 cps

TABLE 9

SOLUTIONS OF STABILITY EQUATIONS

(Antisymmetric Analysis)

Plot: **Figure 14**

Uncoupled Natural Frequency, Aileron Rotation: f_β = 20 cps

Spring Constants

$$k_c = 911 \text{ lb./in.}$$

$$K_p = 72,699 \text{ lb.-in./rad.}$$

Aerodynamics: Basic Surface With Aerodynamic Balance (B $\neq$ 0)

$\frac{1}{k_0}$	f_1 cps	V_1 Knots	g_1	f_2 cps	V_2 Knots	g_2
.00	19.2	0.0	.000	103.8	0.0	.000
.05	18.7	16.0	-.031	102.6	87.7	-.029
.10	18.7	32.0	-.061	103.5	176.9	-.060
.15	18.8	48.3	-.093	104.9	269.0	-.094
.20	19.0	64.9	-.126	107.0	365.9	-.132
.50	21.0	179.6	-.377	152.5	1303.8	-.848
.75	25.8	331.0	-.818	-	-	-
1.00	52.7	901.8	-4.198	-	-	-

Uncoupled Natural Frequency, Tab Rotation: f_δ = 102.5 cps

TABLE 10

SOLUTIONS OF STABILITY EQUATIONS

(Antisymmetric Analysis)

Plot: Figure 15

Uncoupled Natural Frequency, Aileron Rotation: f_β = 30 cps

Spring Constants:

$$k_c = 911 \text{ lb./in.}$$

$$K_p = 167,565 \text{ lb.-in./rad.}$$

Aerodynamics: Basic Surface with Aerodynamic Balance (B $\neq$ 0)

$\dfrac{1}{k_o}$	f_1 cps	V_1 Knots	g_1	f_2 cps	V_2 Knots	g_2
.00	29.4	0.0	.000	103.8	0.0	.000
.05	28.6	24.5	-.031	102.7	87.7	-.029
.10	28.7	49.1	-.062	103.5	176.9	-.060
.15	28.8	74.1	-.094	104.9	269.0	-.093
.20	29.1	99.6	-.127	107.0	365.8	-.131
.50	32.3	276.5	-.377	151.9	1298.4	-.847
.75	40.1	513.7	-.799	-	-	-
1.00	103.7	1772.9	-5.281	-	-	-

Uncoupled Natural Frequency, Tab Rotation: f_δ = 102.5 cps

TABLE 11

SOLUTIONS OF STABILITY EQUATIONS

(Antisymmetric Analysis)

Plot: Figure 16

Uncoupled Natural Frequency, Aileron Rotation: $f_\beta = 15$ cps

Spring Constants:

$$k_c = 911 \text{ lb./in.}$$

$$K_p = 39,496 \text{ lb.-in/rad.}$$

Aerodynamics: Basic Surface without Aerodynamic Balance (B = 0)

$\frac{1}{k_0}$	f_1 cps	V_1 Knots	g_1	f_2 cps	V_2 Knots	g_2
.00	13.9	0.0	.000	103.8	0.0	.000
.05	13.5	11.6	-.032	102.6	87.7	-.029
.10	13.6	23.2	-.065	103.4	176.9	-.060
.15	13.7	35.1	-.098	104.9	269.0	-.094
.20	13.8	47.2	-.134	107.0	365.8	-.132
.50	15.5	132.3	-.414	151.4	1294.1	-.830
.75	19.8	254.4	-.989	-	-	-
1.00	78.4	1340.0	-19.770	-	-	-

Uncoupled Natural Frequency, Tab Rotation: f_δ 102.5 cps

TABLE 12

SOLUTIONS OF STABILITY EQUATIONS

(Antisymmetric Analysis)

Plot: Figure 17

Uncoupled Natural Frequency, Aileron Rotation: f_β = 20 cps

Spring Constants:

k_c = 911 lb./in.

K_p = 72,699 lb.-in./rad.

Aerodynamics: Basic surface without Aerodynamic Balance (B = 0)

$\dfrac{1}{k_o}$	f_1 cps	V_1 Knots	g_1	f_2 cps	V_2 Knots	g_2
.00	19.2	0.0	.000	103.8	0.0	.000
.05	18.7	15.9	-.032	102.6	87.7	-.029
.10	18.7	32.0	-.065	103.4	176.9	-.060
.15	18.8	48.3	-.099	104.9	269.0	-.094
.20	19.0	65.0	-.134	107.0	365.8	-.132
.50	21.4	182.6	-.414	151.1	1292.1	-.829
.75	27.5	352.6	-.987	-	-	-
1.00	259.6	4439.2	-110.501	-	-	-

Uncoupled Natural Frequency, Tab Rotation: f_δ = 102.5 cps

TABLE 13

SOLUTIONS OF STABILITY EQUATIONS

(Antisymmetric Analysis)

Plot: Figure 18

Uncoupled Natural Frequency, Aileron Rotation: f_β = 30 cps

Spring Constants:

k_c = 911 lb./in.

K_p = 167,565 lb.-in./rad.

Aerodynamics: Basic Surface without Aerodynamic Balance (B = 0)

$\frac{1}{k_o}$	f_1 cps	V_1 Knots	g_1	f_2 cps	V_2 Knots	g_2
.00	29.4	0.0	.000	103.8	0.0	.000
.05	28.6	24.5	-.033	102.7	87.8	-.029
.10	28.7	49.1	-.066	103.5	176.9	-.060
.15	28.9	74.1	-.100	104.9	268.9	-.093
.20	29.1	99.7	-.135	106.9	365.6	-.131
.50	32.9	281.2	-.415	150.4	1286.0	-.828
.75	42.9	550.2	-.976	-	-	-
1.00	415.5	7105.2	-34.596	-	-	-

Uncoupled Natural Frequency, Tab Rotation: f_δ = 102.5 cps

Figure 13   g-V and f-V Plots, Antisymmetric Aileron, f_β = 15 cps, B $\neq$ 0

Figure 14   g-V and f-V Plots, Antisymmetric Aileron, f_β= 20 cps, B $\neq$ 0

63

Figure 15   g-V and f-V Plots, Antisymmetric Aileron, f_β= 30 cps, B≠ 0

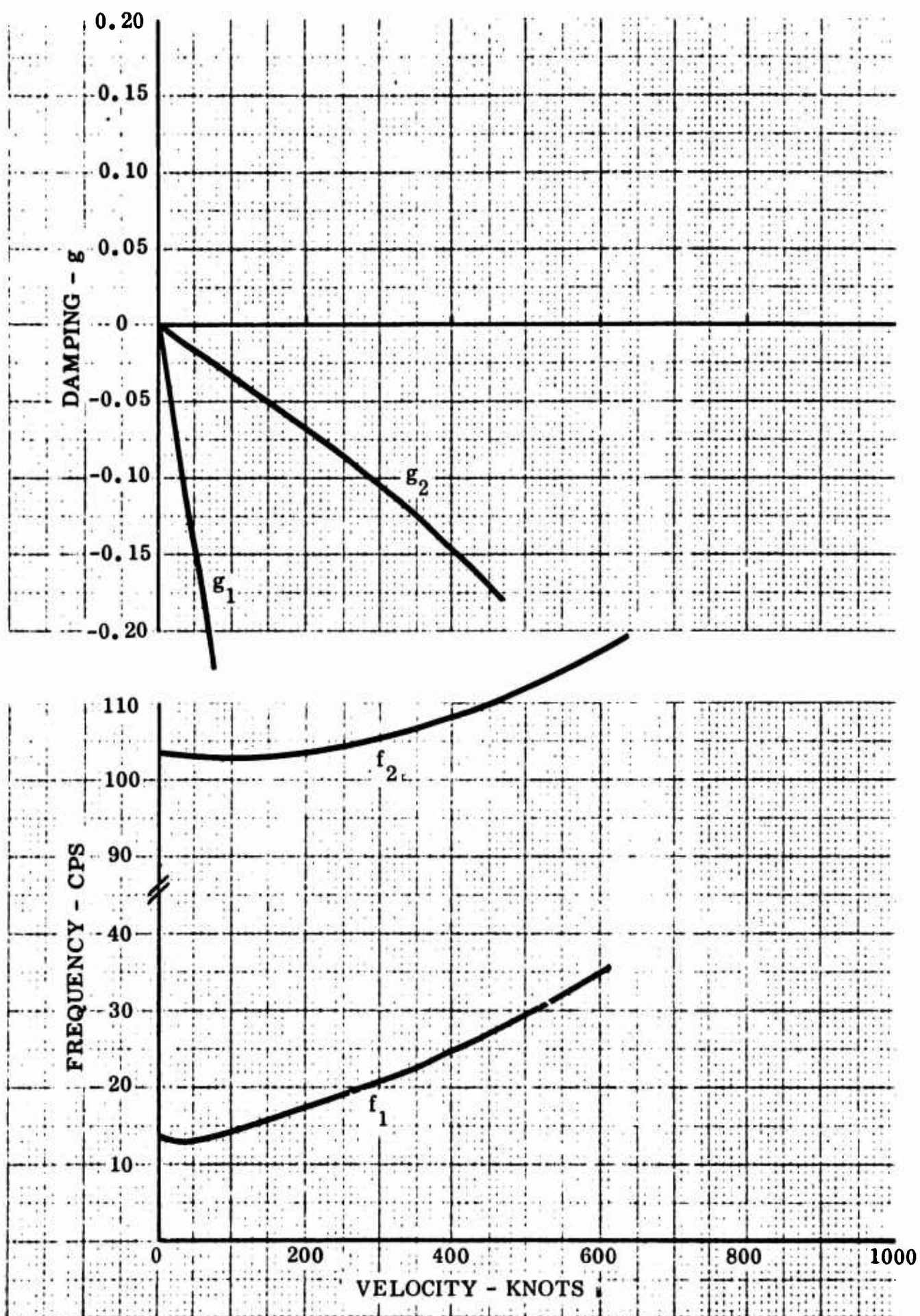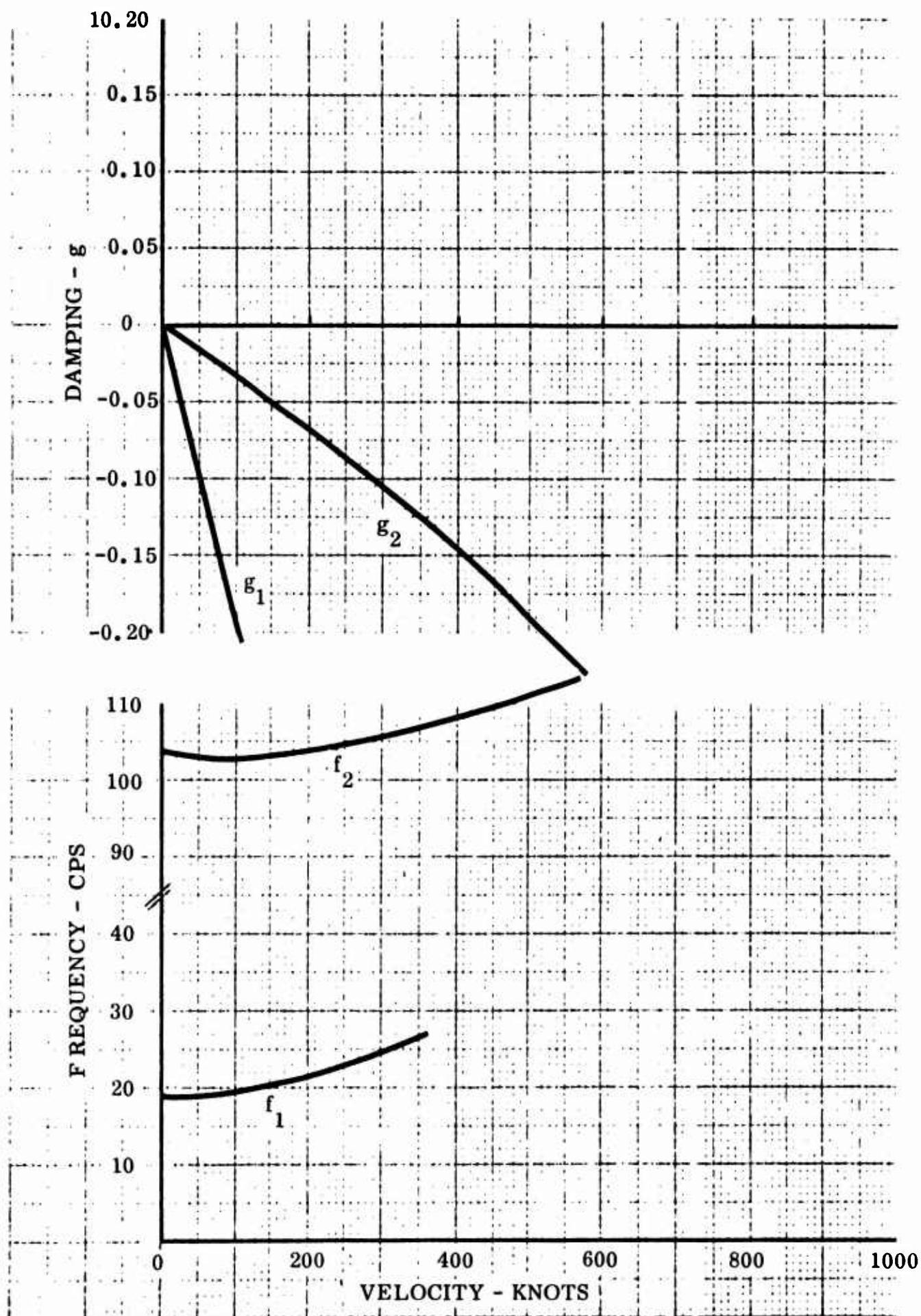Figure 16   g-V and f-V Plots, Antisymmetric Aileron, f_β = 15 cps, B = 0
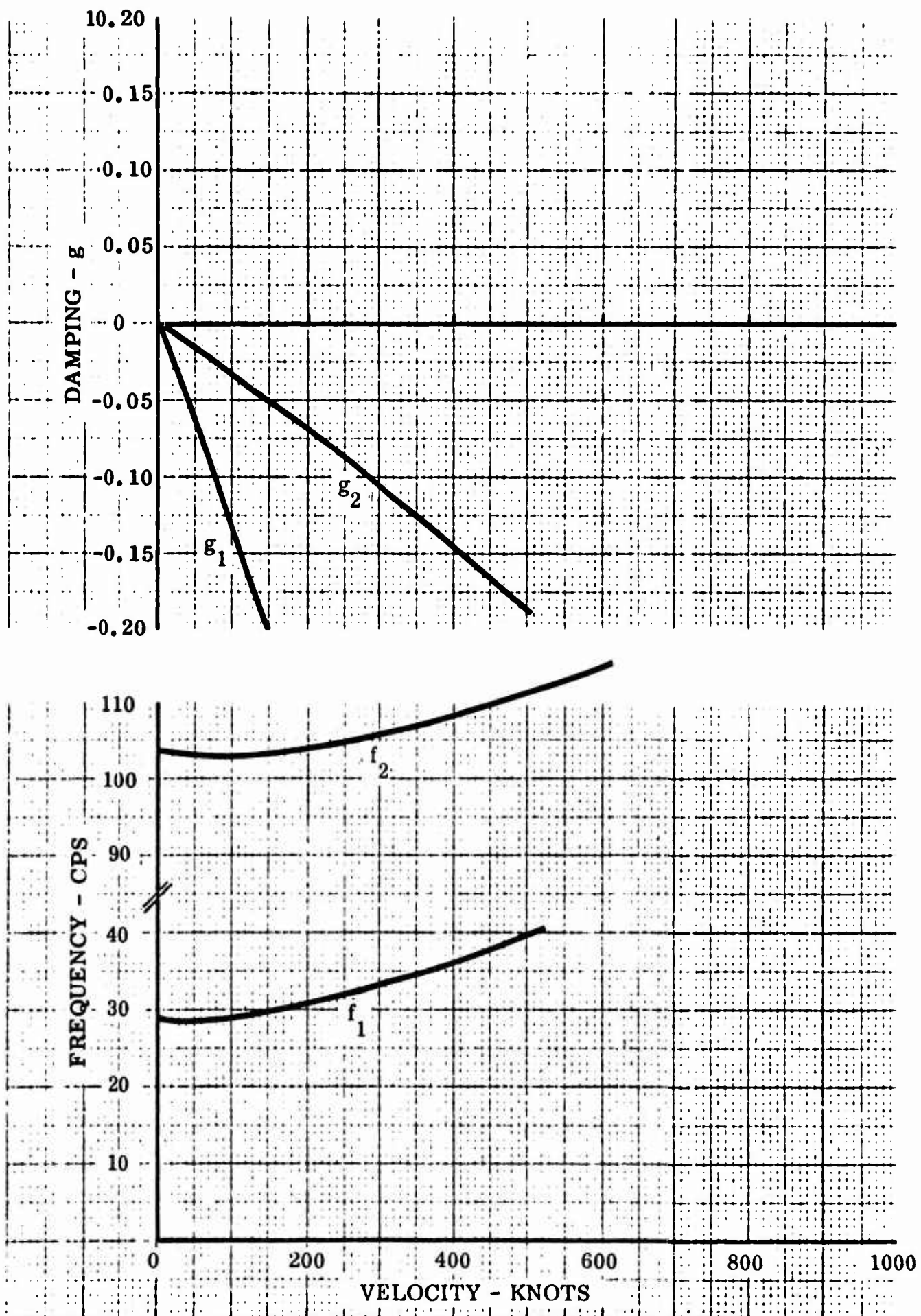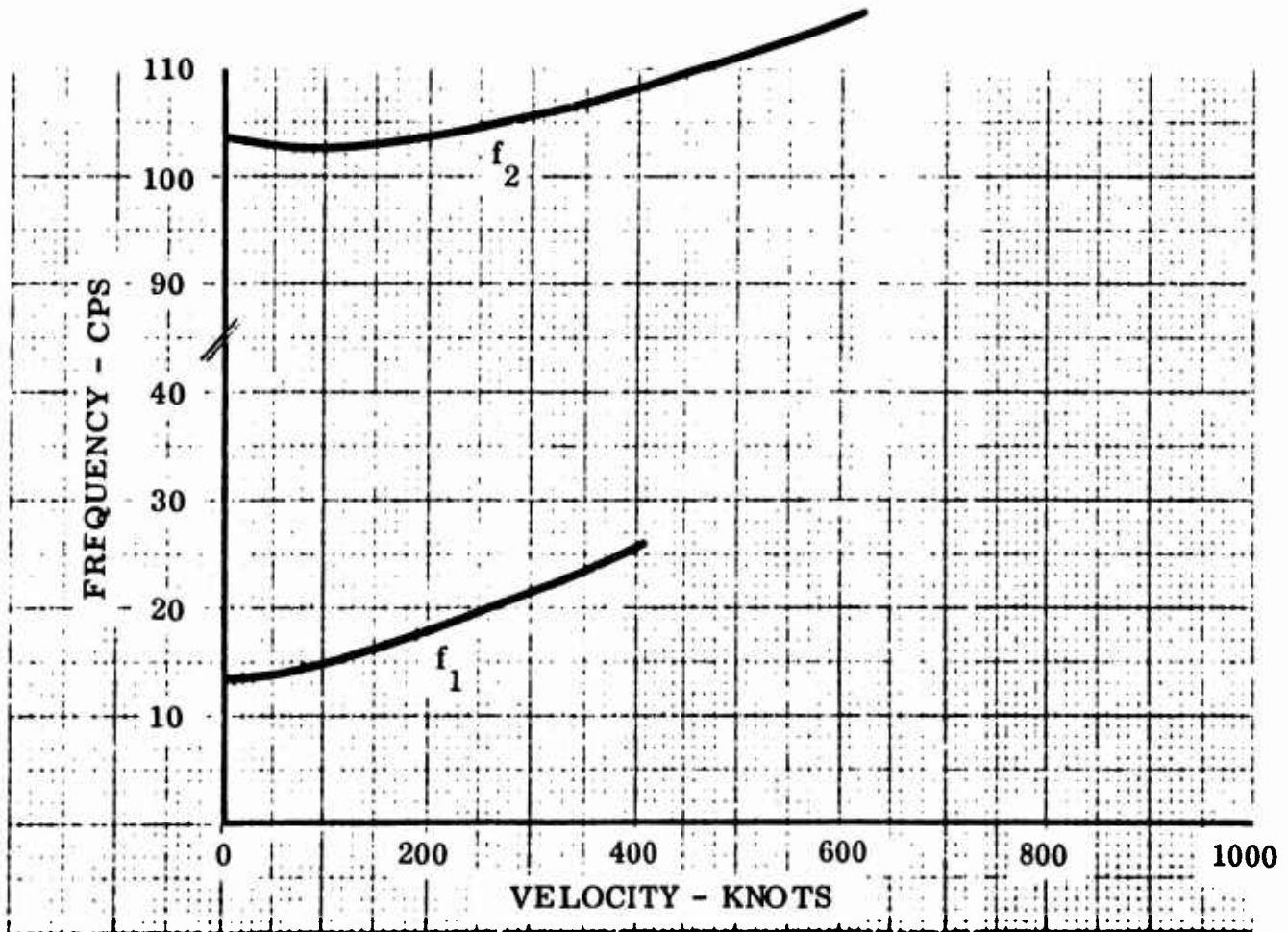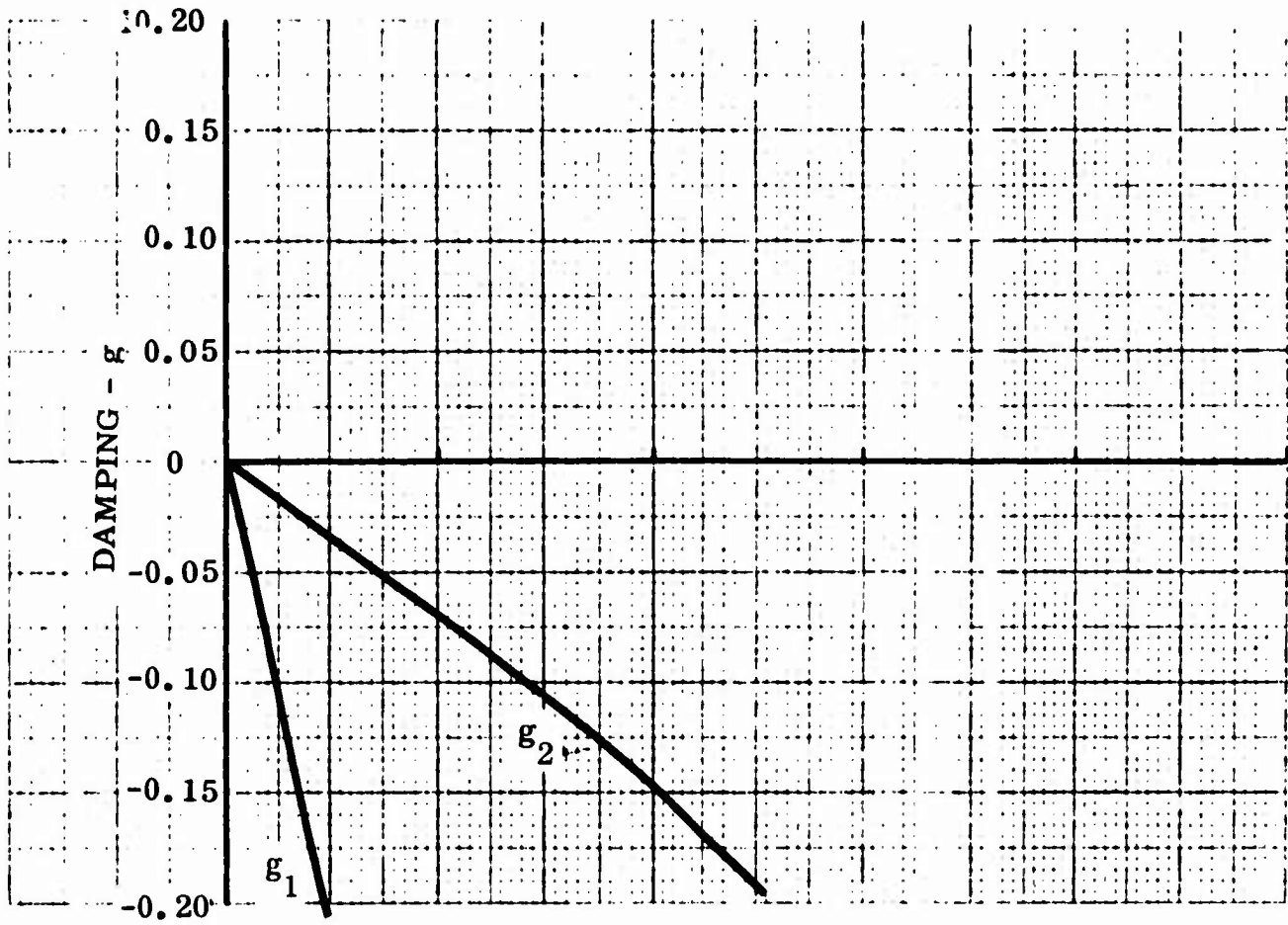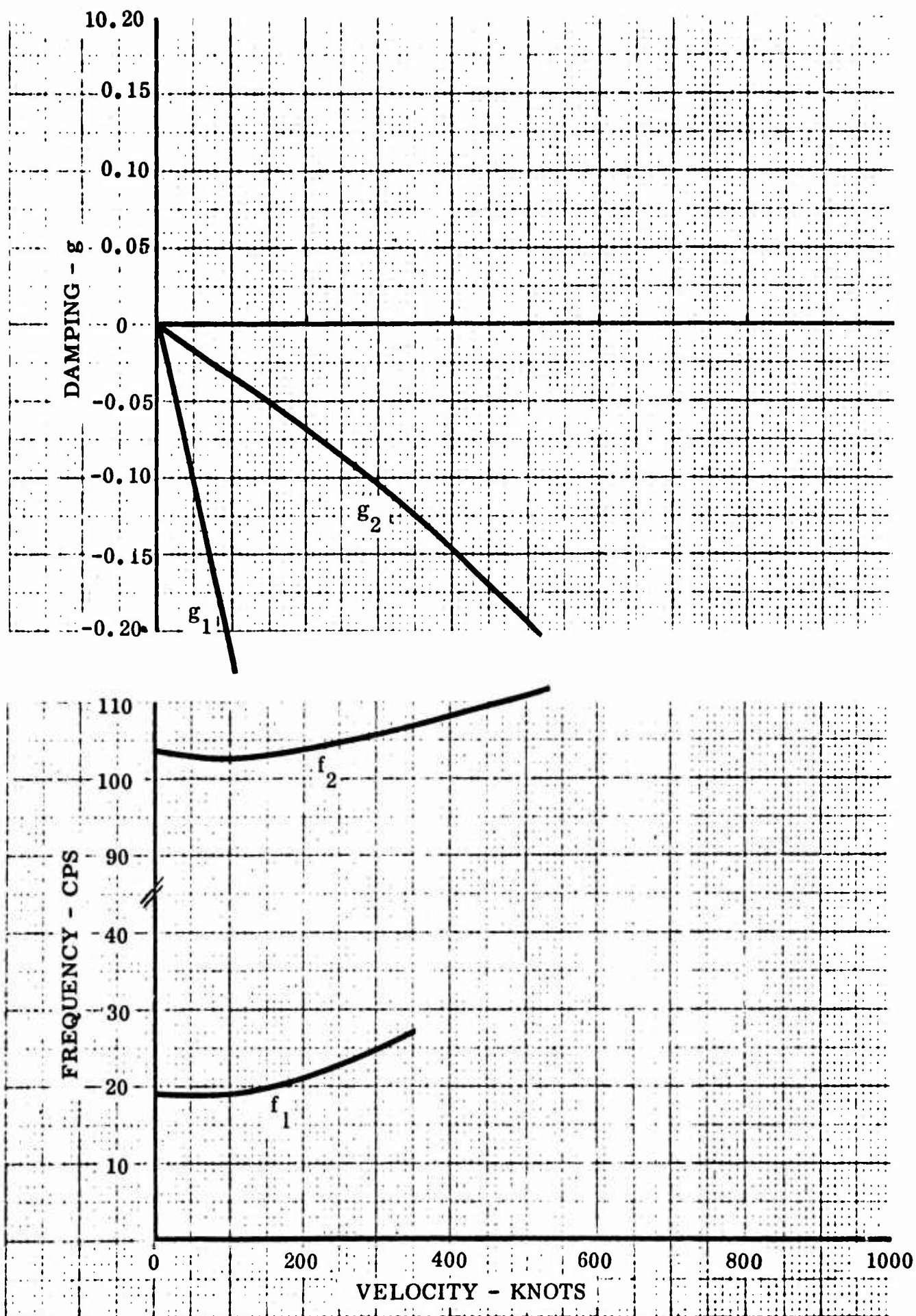
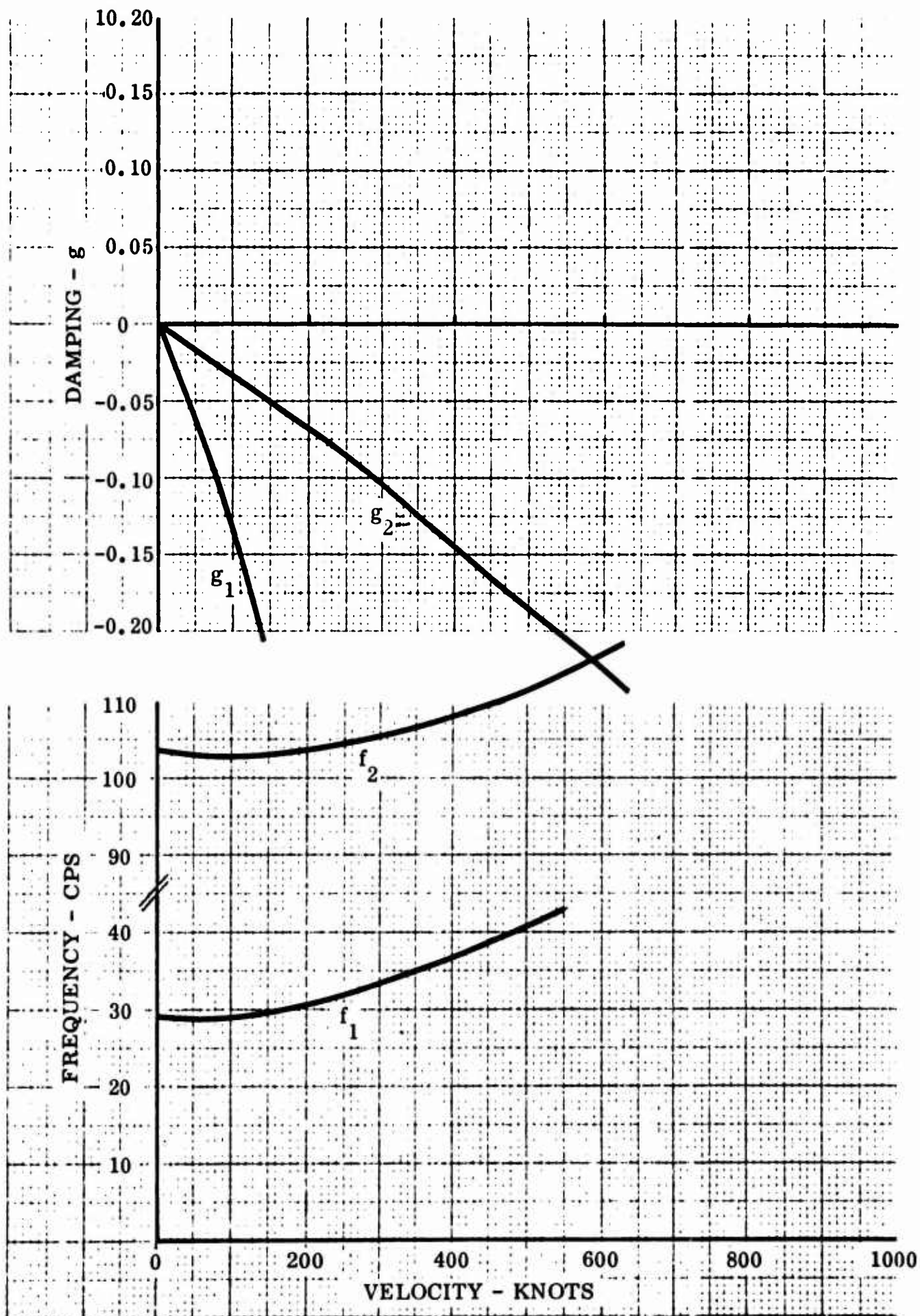Figure 17   g-V and f-V Plots, Antisymmetric Aileron, f_β = 20 cps, B = 0

Figure 18   g-V and f-V Plots, Antisymmetric Aileron, f_β = 30 cps, B = 0

4.2   RUDDER AND RUDDER TRIM TAB

A schematic of the rudder and rudder trim tab system is shown in Figure 19. A plan view of the vertical tail, rudder and trim tab is shown in Figure 20, and the aerodynamic balancing arrangement is shown in Figure 21.

Analysis

For purposes of a flutter analysis, the system is idealized as shown in Figure 22. For the trim tab system at hand, no mechanical gearing exists between the rudder and tab; i.e., $n = 0$ (n is a gear ratio, trim tab rotation to rudder rotation δ/β).

β = Rudder rotation

δ = Rudder trim tab rotation, relative to the rudder

γ = Control pedal rotation

The potential energy of the system is

$$U = \frac{1}{2} k_c (r_1 \beta - r_8 \gamma)^2 + \frac{1}{2} K_A \delta^2 \qquad (58)$$

where

k_c = Linear spring restraint offered by control circuit, i.e. the effective spring of the complete control circuit from control pedal to rudder quadrant

K_A = Rotational spring restraint offered by trim tab actuator

r_1, r_8 = Linkage arm lengths

(See Figure 22 for a schematic representation of k_c, K_A, r_1 and r_8.)

Calculating the potential energy terms that are part of Lagrange's equations of motion (Equations (1), (2) and (3)), by taking partial derivatives of Equation (58),

$$\frac{\partial U}{\partial \beta} = k_c \, (a_1 \beta - a_2 \gamma)$$

$$\frac{\partial U}{\partial \delta} = K_A \delta$$

$$\frac{\partial U}{\partial \gamma} = k_c \, (-a_2 \beta + a_3 \gamma)$$

where

$$a_1 = r_1^2$$

$$a_2 = r_1 r_8$$

$$a_3 = r_8^2$$

In matrix notation, the potential energy (spring) terms are

$$
\begin{bmatrix}
a_1 k_c & 0 & -a_2 k_c \\
0 & K_A & 0 \\
-a_2 k_c & 0 & a_3 k_c
\end{bmatrix}
\begin{bmatrix}
\beta \\
\delta \\
\gamma
\end{bmatrix}
= [S] \, \{q\}
$$

and Equation (25) is

$$
\left[
\begin{bmatrix}
I_\beta & P_{\beta\delta} & 0 \\
P_{\delta\beta} & I_\delta & 0 \\
0 & 0 & J
\end{bmatrix}
- \frac{\Omega}{\overline{K}}
\begin{bmatrix}
a_1 k_c & 0 & -a_2 k_c \\
0 & K_A & 0 \\
-a_2 k_c & 0 & a_3 k_c
\end{bmatrix}
+
\begin{bmatrix}
I'_{11} & I'_{12} & 0 \\
I'_{21} & I'_{22} & 0 \\
0 & 0 & 0
\end{bmatrix}
\right]
\begin{bmatrix}
\beta \\
\delta \\
\gamma
\end{bmatrix}
=
\begin{bmatrix}
0 \\
0 \\
0
\end{bmatrix}
$$

(59)

In the case at hand, J is the effective mass moment of inertia of the control circuit and pedal about the pedal pivot axis.

Upon expansion of the characteristic determinant of Equation (59), because of relationships between [S] elements in terms of the r's ([S] is singular), the following stability equation is obtained:

$$A\Omega^2 + B\Omega + C = 0$$

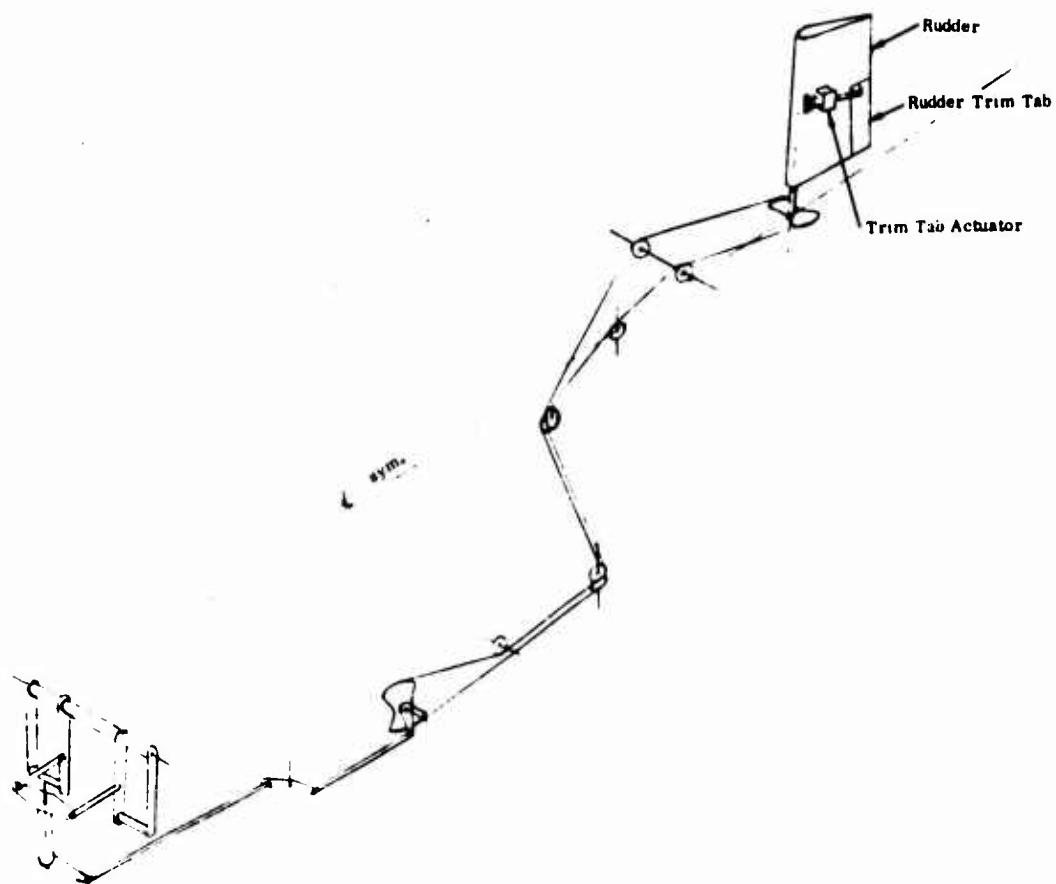where A is real, and B and C are complex.

Figure 19   Schematic of Rudder System
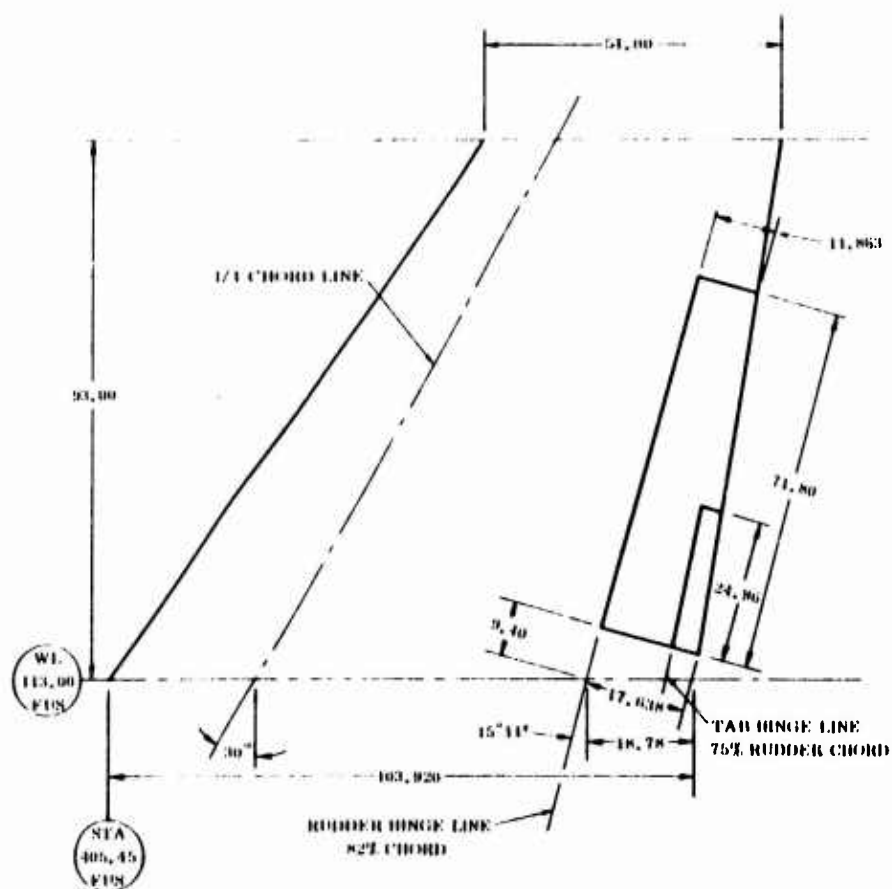

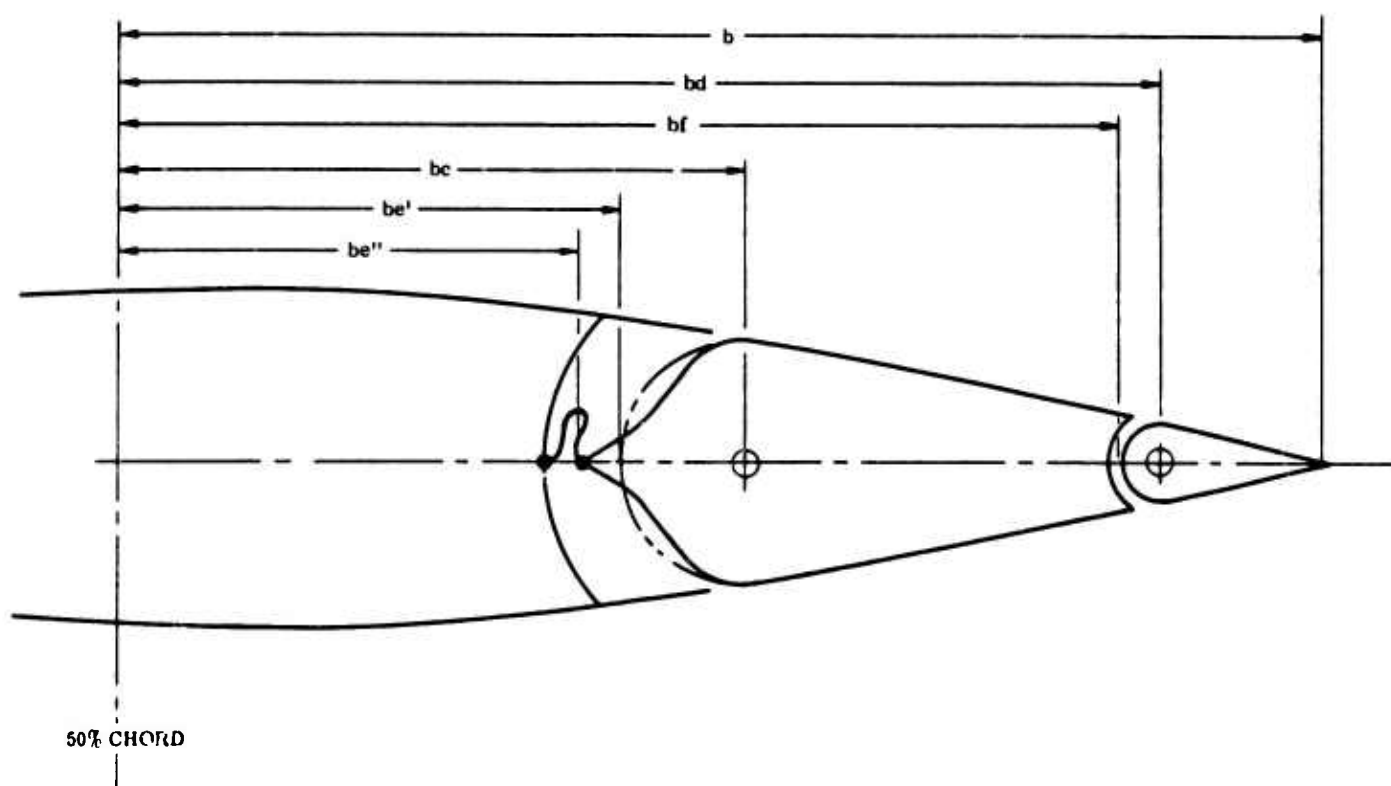Figure 20   Vertical Tail - Plan View

Figure 21   Rudder Aerodynamic Balancing Arrangement
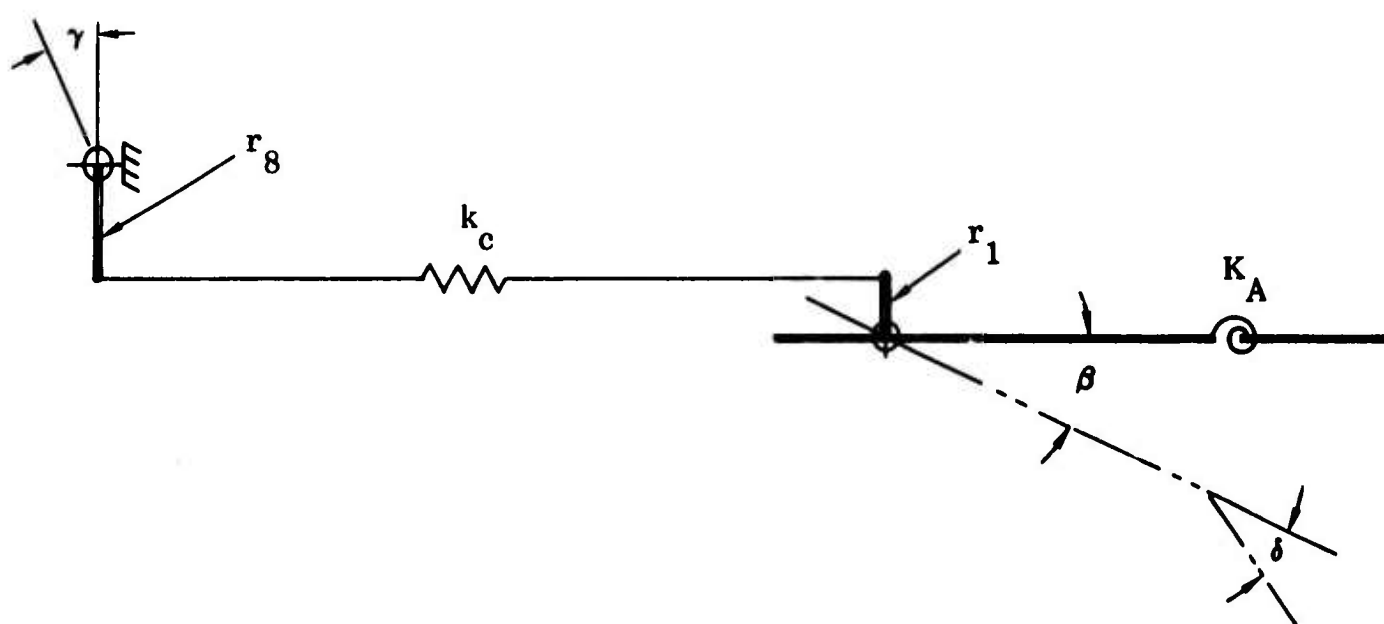
Figure 22   Idealization of Rudder System

Parameters

Table 14 lists the aerodynamic parameters required to evaluate the oscil-
latory forces as defined in References 2, 3 and 4 and in Equation (22).

The inertia parameters are

$$I_{\beta} = 2.31997 \text{ lb.-in.-sec.}^2$$

$$I_{\delta} = 0.02604 \text{ lb.-in.-sec.}^2$$

$$S_{\delta} = 0.00596 \text{ lb.-sec.}^2 \text{ (Tail heavy)}$$

$$\ell_t = 11.902 \text{ in.}$$

$$J = 0.95234 \text{ lb.-in.-sec.}^2$$

The uncoupled rudder trim tab rotation natural frequencies, a basic
parameter for this preliminary analysis, are f_{δ} = 20, 40 and 60 cps.

The linkage parameters are:

$$r_1 = 5.5 \text{ in.}$$

$$r_8 = 9.6 \text{ in.}$$

The spring constants are:

$$k_c = 357 \text{ lb./in.}$$

$$K_A = 411, 1645, \text{ and } 3702 \text{ lb.-in./rad. corresponding to}$$
$$f_{\delta} = 20, 40 \text{ and } 60 \text{ cps, respectively.}$$

$$\overline{K} = 10,000 \text{ lb.-in./rad.}$$

The value for k_c was calculated from design values for the rudder-trim
tab system. The values for K_A were determined using Equation 28, for
the various values of uncoupled trim tab frequency f_{δ}. The scaling con-
stant $\overline{K}$ was assigned its value arbitrarily, for computing convenience.

Results

Tables 15 to 20 and Figures 23 to 28 show the effects of varying the rudder trim tab uncoupled frequency f_δ and aerodynamic balance. Figure 29 shows a cross-plot of sea-level flutter velocity V_f versus f_δ.

Conclusions

In order to clear the flight envelope to 500 knots + 15% (575 knots) at sea level, as required, examination of the tables and curves shows that the uncoupled trim tab frequency f_δ must be at least 59 cps for the aerodynamically unbalanced rudder ($\beta = 0$) and at least 50 cps for the aerodynamically balanced rudder ($\beta \neq 0$). Thus an increased K_A value, trim tab actuator stiffness, is indicated. The coupled, predominantly rudder mode (the lower-frequency branch) is stable for all f_δ values investigated. The flutter condition occurs in the coupled, predominantly trim tab mode (the higher-frequency branch). f_δ, and particularly the value of K_A, as expected, strongly influences both the flutter velocity and frequency. They both increase with increasing f_δ. Further analysis should be made on calculated refinements to the circuit stiffness as the design develops and on the basis of tested values of uncoupled rudder and trim tab natural frequencies.

Aerodynamic balance of the rudder has considerable effect on the flutter velocity. Flutter velocities are substantially greater for the aerodynamically balanced rudder ($\beta \neq 0$) than for the unbalanced one ($\beta = 0$), for the same f_δ value. Figure 29 shows a quantitative comparison.

TABLE 14

RUDDER - RUDDER TRIM TAB AERODYNAMIC PARAMETERS

Rudder - Rudder Trim Tab Geometry:

Sta. No.	W.L. in.	b in.	c	e'	e''	g	F_{BB}	d	f	
1	118.63	50.449	0.640	0.579	0.511	0.690	0.00649	0.910	0.910	⎫
2	126.66	48.294	0.640	0.579	0.511	0.690	0.00652	0.910	0.910	⎬ Rudder
3	134.69	46.139	0.640	0.580	0.510	0.690	0.00658	0.910	0.910	⎬ &
4_I	142.72	43.984	0.640	0.580	0.510	0.690	0.00662	0.910	0.910	Tab
4_o	142.72	43.984	0.640	0.580	0.510	0.690	0.00662	-	-	⎫
5	152.61	41.329	0.640	0.581	0.510	0.690	0.00670	-	-	⎬
6	162.50	38.675	0.640	0.582	0.510	0.690	0.00679	-	-	⎬ Rudder
7	172.39	36.021	0.640	0.582	0.509	0.690	0.00687	-	-	
8	182.28	33.361	0.640	0.583	0.509	0.690	0.00698	-	-	⎭

Aerodynamic Balance Arrangement:

    Rudder, internal - simple nose overhang (curtain seal)
    Trim Tab, none - radius nose

Hinge Moment Corrections:

$$\frac{\left(C_{H_{c_{\delta_c}}}\right)_{Exp.}}{\left(C_{H_{c_{\delta_c}}}\right)_3} = 1.0 \quad ; \quad \frac{\left(C_{H_{c_{\delta_t}}}\right)_{Exp.}}{\left(C_{H_{c_{\delta_t}}}\right)_3} = 1.0$$

$$\frac{\left(C_{H_{t_{\delta_c}}}\right)_{Exp.}}{\left(C_{H_{t_{\delta_c}}}\right)_3} = 1.0 \quad ; \quad \frac{\left(C_{H_{t_{\delta_t}}}\right)_{Exp.}}{\left(C_{H_{t_{\delta_t}}}\right)_3} = 1.0$$

TABLE 14 (Continued)

$$\frac{\left(\dfrac{\Delta C_{H_{c_{\delta_c}}}}{}\right)_{\text{Exp.}}}{\left(\Delta C_{H_{c_{\delta_c}}}\right)_3} = 1.0 \qquad ; \qquad \frac{\left(\dfrac{\Delta C_{H_{c_{\delta_t}}}}{}\right)_{\text{Exp.}}}{\left(\Delta C_{H_{c_{\delta_t}}}\right)_3} = 1.0$$

Pressure Recovery Factor:

$K = 1.0$

General:

Reference half chord (b_o) = 51.960 in.

$\cos \psi_{c/4} = 0.865999$

$\cos \psi_{\text{⊕}_c} = 0.965086$

$\cos \psi_{\text{⊕}_t} = 0.980775$

Altitude - sea level ($\rho = 0.114626 \times 10^{-6}$ lb-sec.^{2}-in.$^{-4}$)

TABLE 15

SOLUTIONS OF STABILITY EQUATIONS

Plot: Figure 23

Uncoupled Natural Frequency, Trim Tab Rotation: f_δ = 20 cps

Spring Constants:

k_c = 357 lb./in.

K_A = 411 lb.-in./rad

Aerodynamics: Basic Surface with Aerodynamic Balance (B ≠ 0)

$\frac{1}{k_o}$	f_1 cps	V_1 Knots	g_1	f_2 cps	V_2 Knots	g_2
.00	21.3	0.0	.000	32.1	0.0	.000
.20	20.6	34.1	-.100	22.2	71.4	-.039
.40	11.3	72.6	-.238	21.6	139.4	-.028
.60	12.8	123.4	-.521	20.9	202.5	.140
.80	15.3	197.8	-1.166	22.9	295.2	.603
1.00	20.7	334.4	-2.827	33.0	532.3	2.039
1.20	97.5	1885.6	-75.178	--	--	--

V_f = 170 knots

Uncoupled Natural Frequency, Rudder Rotation: f_β = 10.86 cps

TABLE 16

SOLUTIONS OF STABILITY EQUATIONS

Plot: Figure 24

Uncoupled Natural Frequency, Trim Tab Rotation: f_δ = 40 cps

Spring Constants:

k_c = 357 lb./in.

K_A = 1645 lb.-in/rad.

Aerodynamics: Basic Surface with Aerodynamic Balance (B $\neq$ 0)

$\dfrac{1}{k_o}$	f_1 cps	V_1 Knots	g_1	f_2 cps	V_2 Knots	g_2
.00	31.1	0.0	.000	44.0	0.0	.000
.20	10.7	34.5	-.092	43.7	140.9	-.047
.40	11.5	71.4	-.197	43.8	282.6	-.067
.60	11.8	113.8	-.336	43.7	423.0	-.017
.80	13.0	167.8	-.563	43.6	562.1	.196
1.00	15.3	246.6	-1.018	46.5	749.3	.806
1.20	20.1	388.6	-2.211	75.8	1467.2	4.394
1.40	42.9	967.3	-11.996	-	-	-

V_f = 446 knots

Uncoupled Natural Frequency, Rudder Rotation: f_β = 10.86 cps

TABLE 17

SOLUTIONS OF STABILITY EQUATIONS

Plot: Figure 25

Uncoupled Natural Frequency, Trim Tab Rotation: f_δ = 60 cps

Spring Constants:

$$k_c = 357 \text{ lb./in.}$$

$$K_A = 3702 \text{ lb.-in./rad.}$$

Aerodynamics: Basic Surface with Aerodynamic Balance ($B \neq 0$)

$\dfrac{1}{k_o}$	f_1 cps	V_1 Knots	g_1	f_2 cps	V_2 Knots	g_2
.00	31.4	0.0	.000	65.5	0.0	.000
.20	10.7	34.6	-.090	65.4	210.9	-.048
.40	11.0	71.2	-.191	65.9	424.8	-.073
.60	11.6	112.5	-.318	66.2	640.4	-.034
.80	12.6	163.0	-.503	66.2	853.7	.148
1.00	14.4	232.7	-.831	68.0	1095.7	.652
1.20	18.0	348.7	-1.591	88.5	1712.6	2.655
1.40	29.2	659.4	-4.955	-	-	-

$$V_f = 700 \text{ knots}$$

Uncoupled Natural Frequency, Rudder Rotation: f_β = 10.86 cps

TABLE 18

SOLUTIONS OF STABILITY EQUATIONS

Plot: Figure 26

Uncoupled Natural Frequency, Trim Tab Rotation: f_δ = 20 cps

Spring Constants:

$$k_c = 357 \text{ lb./in.}$$

$$K_A = 411 \text{ lb.-in./rad.}$$

Aerodynamics: Basic Surface without Aerodynamic Balance (B = 0)

$\dfrac{1}{k_o}$	f_1 cps	V_1 Knots	g_1	f_2 cps	V_2 Knots	g_2
.00	21.3	0.0	.000	32.1	0.0	.000
.20	10.6	34.2	-.112	22.1	71.3	-.037
.40	11.5	74.1	-.280	21.4	138.0	-.003
.60	13.5	130.6	-.693	20.9	202.1	.277
.80	17.2	221.4	-1.721	25.1	323.3	1.046
1.00	30.0	483.8	-6.857	60.2	969.7	9.019
1.20	-	-	-	-	--	-

$$V_f = 138 \text{ knots}$$

Uncoupled Natural Frequency, Rudder Rotation: f_β = 10.86 cps

TABLE 19

SOLUTIONS OF STABILITY EQUATIONS

Plot: Figure 27

Uncoupled Natural Frequency, Trim Tab Rotation: f_δ = 40 cps

Spring Constants:

$$k_c = 357 \text{ lb./in.}$$

$$K_A = 1645 \text{ lb.-in./rad.}$$

Aerodynamics: Basic Surface without Aerodynamic Balance (B = 0)

$\dfrac{1}{k_o}$	f_1 cps	V_1 Knots	g_1	f_2 cps	V_2 Knots	g_2
.00	31.1	0.0	.000	44.0	0.0	.000
.20	10.7	34.6	-.104	43.6	140.7	-.045
.40	11.3	72.7	-.229	43.4	279.9	-.051
.60	12.4	119.6	-.422	42.4	409.9	.064
.80	14.6	188.4	-.827	41.7	538.1	.489
1.00	19.8	319.8	-2.046	54.1	871.9	2.234
1.20	64.8	1252.9	-27.060	-	-	-

V_f = 379 knots

Uncoupled Natural Frequency, Rudder Rotation: f_β = 10.86 cps

TABLE 20

SOLUTIONS OF STABILITY EQUATIONS

Plot: Figure 28

Uncoupled Natural Frequency, Trim Tab Rotation: f_δ = 60 cps

Spring Constants:

k_c = 357 lb./in.

K_A = 3702 lb.-in./rad.

Aerodynamics: Basic Surface without Aerodynamic Balance (B = 0)

$\dfrac{1}{k_o}$	f_1 cps	V_1 Knots	g_1	f_2 cps	V_2 Knots	g_2
.00	31.4	0.0	.000	65.5	0.0	.000
.20	10.8	34.7	-.102	65.3	210.6	-.047
.40	11.2	72.5	-.223	65.3	421.0	-.057
.60	12.2	117.9	-.394	64.1	620.4	.040
.80	14.1	181.4	-.711	62.2	801.9	.401
1.00	18.4	296.2	-1.567	70.9	1142.5	1.690
1.20	40.4	781.8	-9.309	-	-	-

V_f = 587 knots

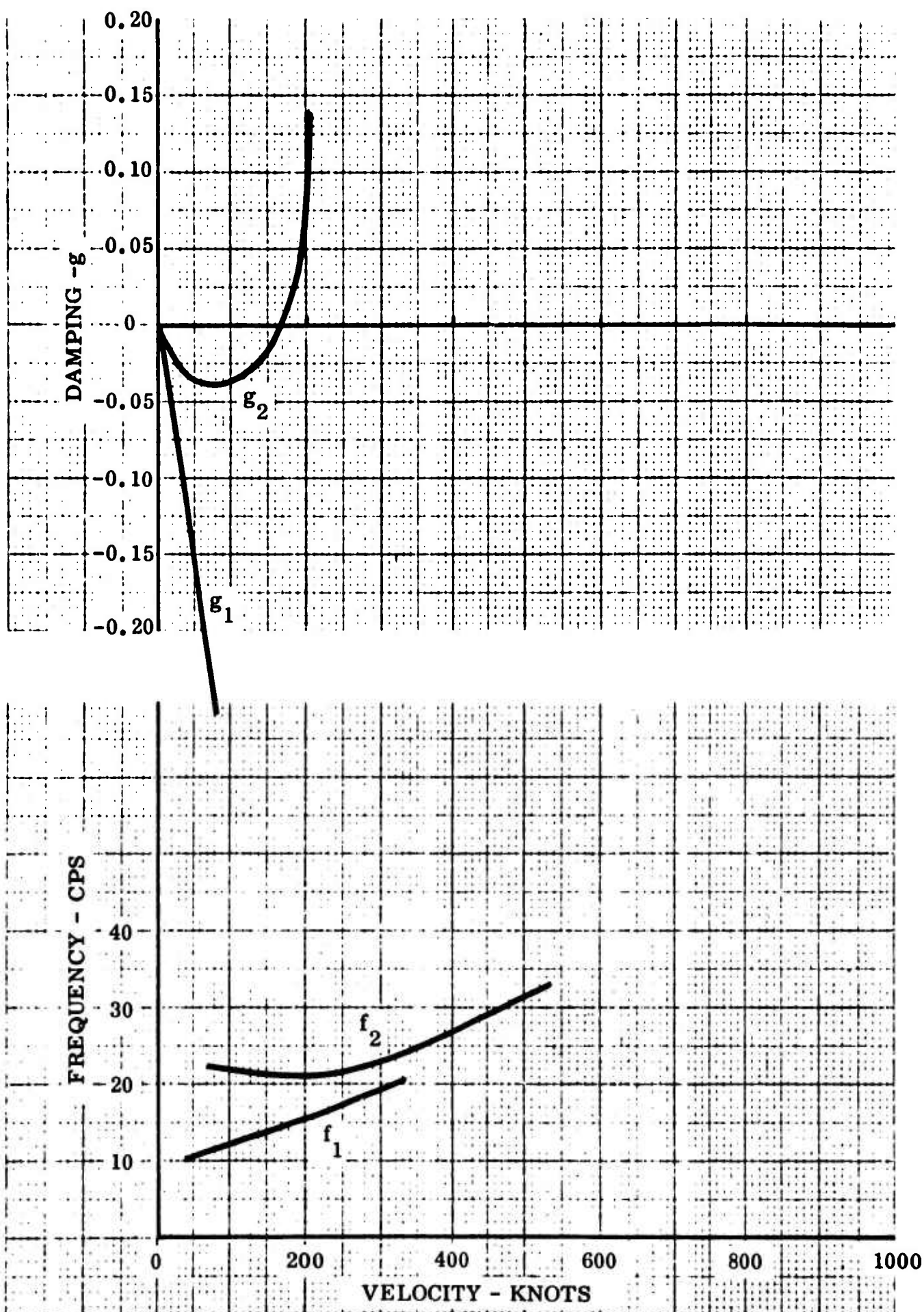Uncoupled Natural Frequency, Rudder Rotation: f_β = 10.86 cps

Figure 23   g-V and f-V Plots, Rudder, f_δ = 20 cps, B $\neq$ 0

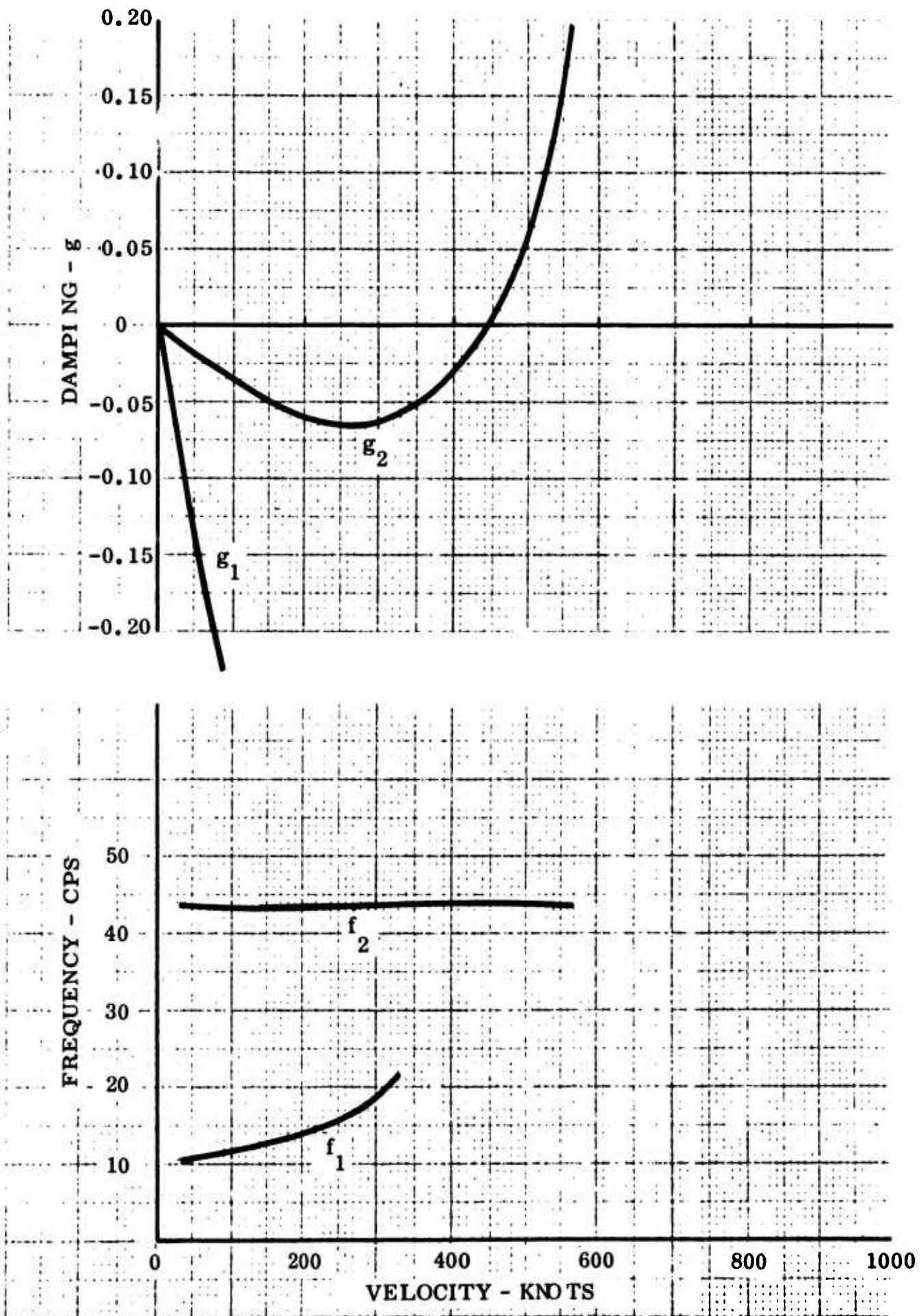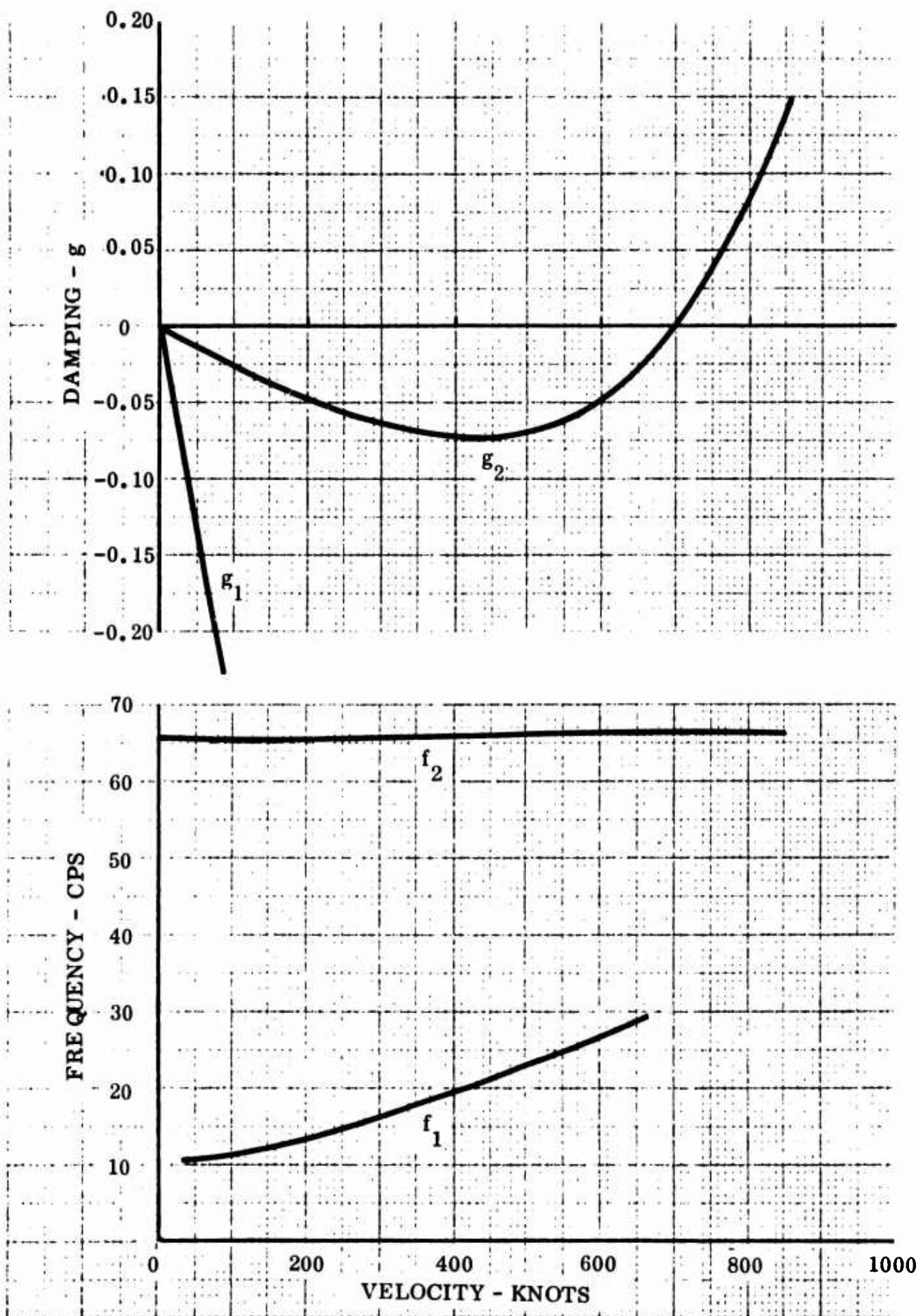Figure 24   g-V and f-V Plots, Rudder, f_{δ} = 40 cps, B $\neq$ 0

Figure 25   g-V and f-V Plots, Rudder, f_δ = 60 cps, B $\neq$ 0
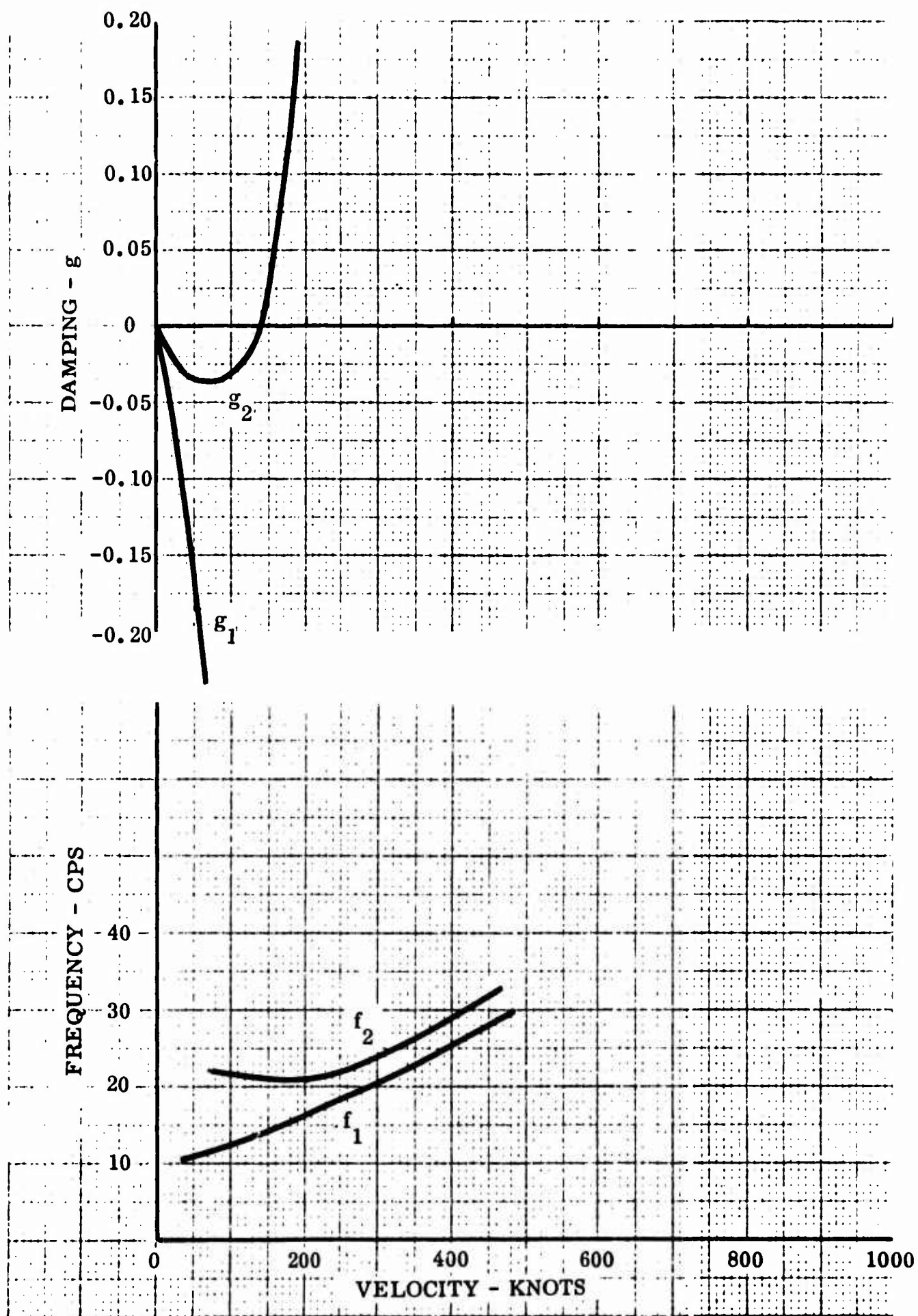
Figure 26   g-V and f-V Plots, Rudder, f_δ = 20 cps, B = 0
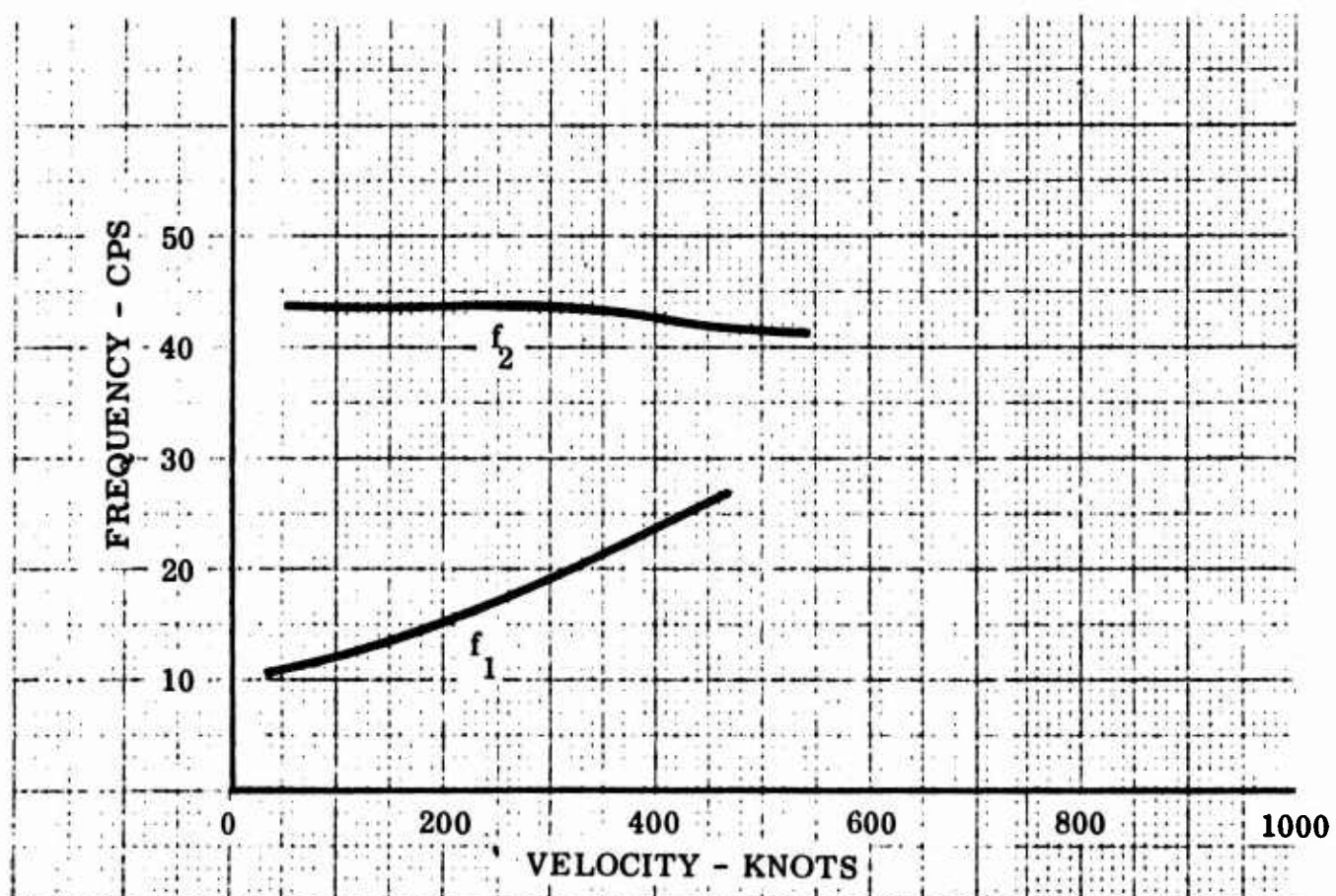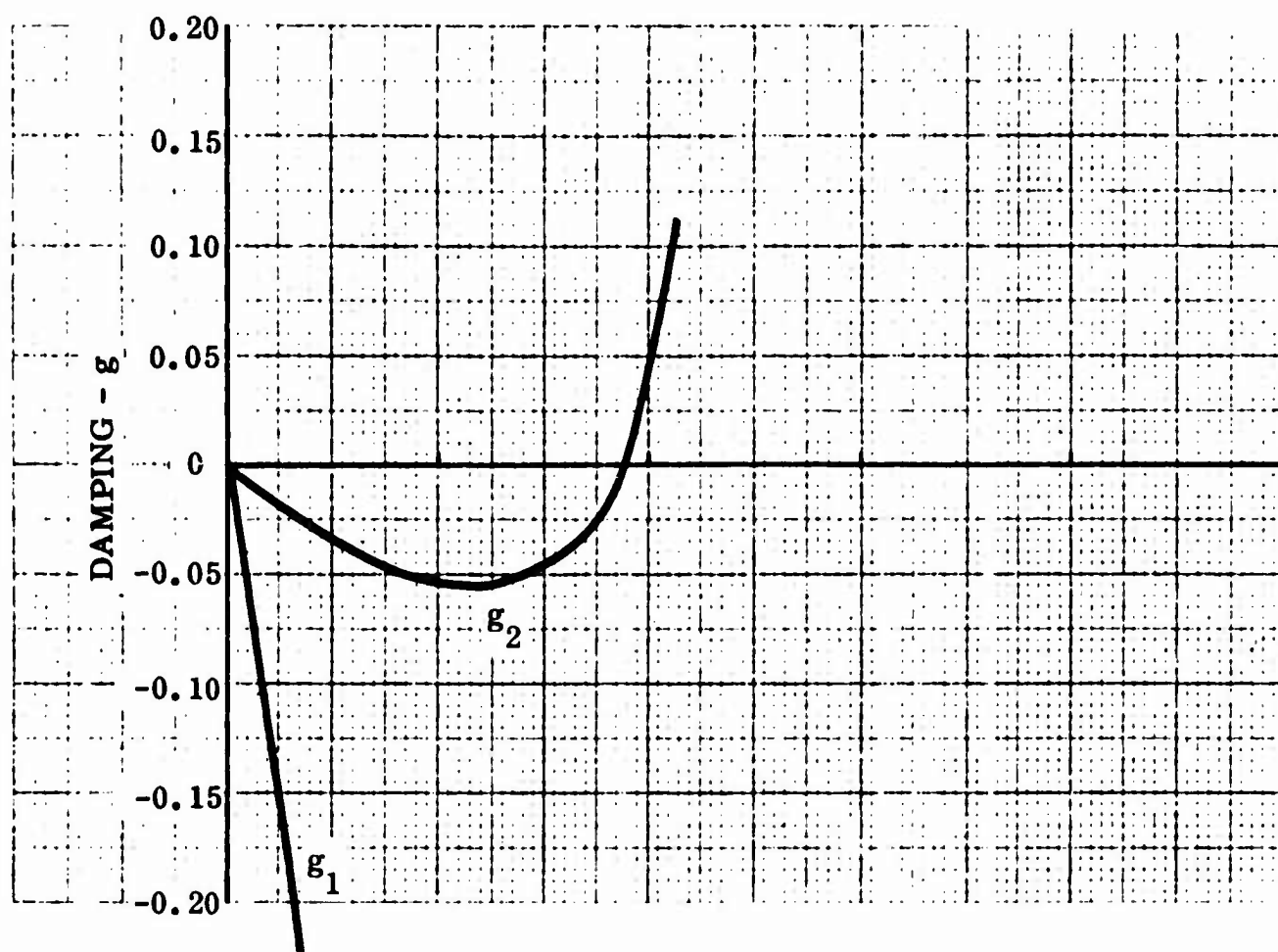
Figure 27   g-V and f-V Plots, Rudder, f_δ = 40 cps, B = 0

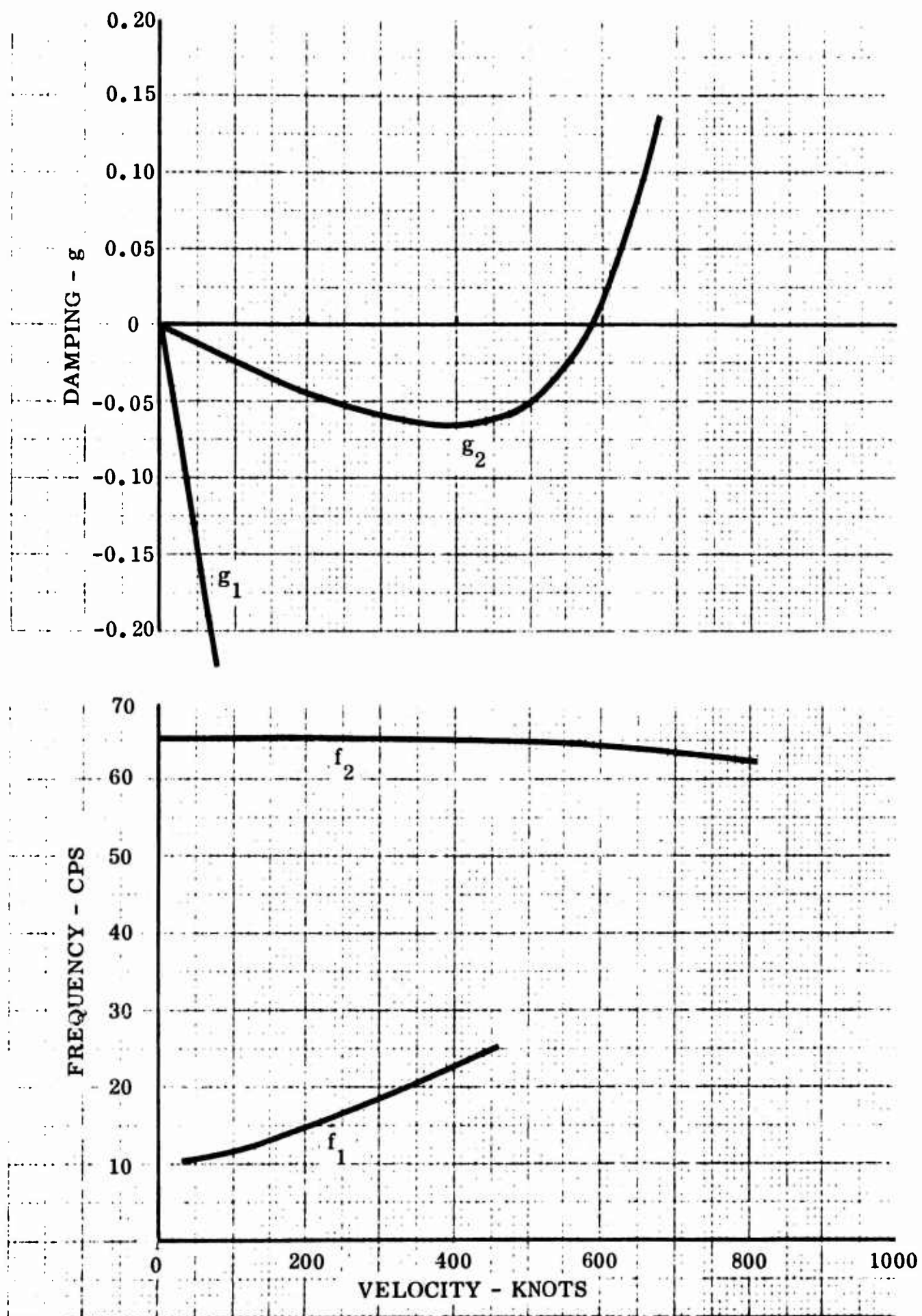Figure 28   g-V and f-V Plots, Rudder, f_δ = 60 cps, B = 0

Figure 29 V_f vs. f_δ Cross-plot, Rudder

O B ≠ 0 (BALANCED RUDDER)
Δ B = 0 (UNBALANCED RUDDER)

Limit Dive Speed

FLUTTER VELOCITY V_f (KNOTS)

f_δ (CPS)
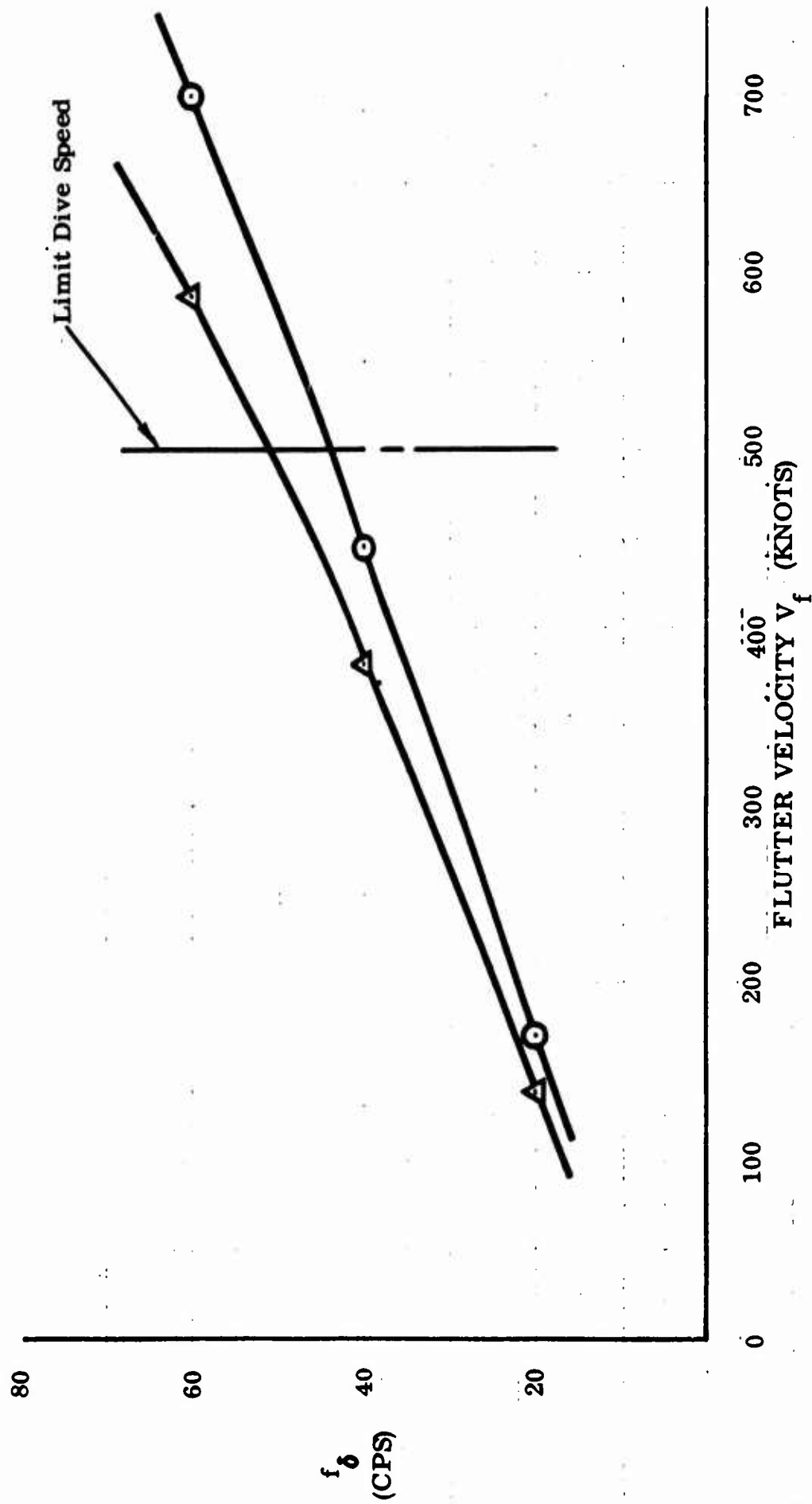
4.3   HORIZONTAL STABILIZER AND ELEVATOR

A schematic of the horizontal stabilizer and elevator system is shown in Figure 30. A plan view of the horizontal stabilizer and elevator is shown in Figure 31, and the aerodynamic balancing arrangement is shown in Figure 32.

Analysis

For purposes of a flutter analysis, the system is idealized as shown in Figure 33. Only the symmetric condition is treated here. Examination of the system shows that for the antisymmetric condition, a node exists at the centerline of symmetry. Thus, antisymmetric rotational motion of a representative station of the elevator and horizontal stabilizer are those of torsional cantilevers. The spring restraint is that of the elevator interconnect torque tube and the torque box material for these two inertial elements. There is no motion of the elevator control system since the elevator horn is located on the node (physically it is very near the aircraft centerline of symmetry at the vertical tail tip). Thus, the antisymmetric elevator system is extremely stiff relative to the symmetric one, while the inertias of the surfaces remain the same. For an antisymmetric analysis, the generalized coordinate γ, control stick rotation, would cease to be a consideration, and control circuit stiffness as well as horizontal stabilizer trim actuator stiffness (the actuator is also located at the node) would cease to be elements of the analysis; there would be no coupling to the control system. On the basis of these observations, the antisymmetric elevator flutter condition is clearly not critical in comparison to the far softer symmetric case.

The degrees of freedom considered for the symmetric analysis are:

α = Horizontal stabilizer rotation

β = Elevator rotation, relative to horizontal stabilizer

γ = Control stick rotation

The potential energy of the system is

$$U = \frac{1}{2} k_c \left(-r_1 \beta - r_8 \gamma\right)^2 + \frac{1}{2} K_H \alpha^2 \tag{61}$$

where k_c = Linear spring restraint offered by control circuit, i.e., the effective spring of <u>half</u> the control circuit from control stick to elevator horn

K_H = Rotational spring restraint offered by horizontal stabilizer trim actuator, half of the actual spring, due to symmetry

r_1, r_8 = Linkage arm lengths

(See Figure 33 for a schematic representation of k_c, K_H, r_1 and r_8.)

Calculating the potential energy terms that are part of Lagrange's equations of motion (Equations (43), (44) and (45)) by taking partial derivatives of Equation (61),

$$\frac{\partial U}{\partial \alpha} = K_H \alpha$$

$$\frac{\partial U}{\partial \beta} = k_c (a_1 \beta + a_3 \gamma)$$

$$\frac{\partial U}{\partial \gamma} = k_c (a_3 \beta + a_2 \gamma)$$

where $a_1 = r_1^2$

$a_2 = r_8^2$

$a_3 = r_1 r_8$

In matrix notation, the potential energy (spring) terms, then, are

$$\begin{bmatrix} K_H & 0 & 0 \\ 0 & a_1 k_c & a_3 k_c \\ 0 & a_3 k_c & a_2 k_c \end{bmatrix} \begin{bmatrix} \alpha \\ \beta \\ \gamma \end{bmatrix} = [S] \{q\}$$

and Equation (25), with the changes in generalized coordinates discussed on page 18, becomes

$$
\left[
\begin{bmatrix}
I_\alpha & P_{\alpha\beta} & 0 \\
P_{\alpha\beta} & I_\beta & 0 \\
0 & 0 & J_0
\end{bmatrix}
\frac{-\Omega}{\overline{K}}
\begin{bmatrix}
K_H & 0 & 0 \\
0 & a_1 k_c & a_3 k_c \\
0 & a_3 k_c & a_2 k_c
\end{bmatrix}
+
\begin{bmatrix}
I'_{11} & I'_{12} & 0 \\
I'_{21} & I'_{22} & 0 \\
0 & 0 & 0
\end{bmatrix}
\right]
\begin{bmatrix}
\alpha \\
\beta \\
\gamma
\end{bmatrix}
=
\begin{bmatrix}
0 \\
0 \\
0
\end{bmatrix}
$$

(62)

In the case at hand, because of symmetry, J_0 is the effective mass moment of inertia of <u>half</u> the control circuit and control stick about the control stick axis of rotation.

Upon expansion of the characteristic determinant of Equation (62), because of relationships between [S] elements in terms of the r's ([S] is singular), the following stability equation is obtained:

$$
A\Omega^2 + B\Omega + C = 0
$$

(63)

where A is real, and B and C are complex.

Parameters

Table 21 lists the aerodynamic parameters required to evaluate the oscillatory forces as defined in References 2 and 4 and in Equations (50) and (51).

The inertia parameters are:

$I_\alpha = 42.1394$ lb.-in.-sec.^{2} (half horizontal stabilizer)

$I_\beta = 0.8906$ lb.-in.-sec.^{2} (half elevator)

$S_\beta = -0.0153$ lb.-sec.^{2} (half elevator) - (nose heavy)

$l = 21.09$ in.

$J_0 = 1.4404$ lb.-in.-sec.^{2}

The uncoupled horizontal stabilizer rotation natural frequencies, basic parameters for this preliminary analysis, are $f_\alpha = 20, 40$ and 60 cps.

The linkage parameters are:

$$r_1 = 4.0 \text{ in.}$$

$$r_8 = 5.125 \text{ in.}$$

The spring constants are:

$$k_c = 1145 \text{ lb./in. (half system)}$$

$K_H = 665,400;\ 2,661,800 \text{ and } 5,988,900 \text{ lb.-in./rad. corresponding to } f_\alpha = 20,\ 40 \text{ and } 60 \text{ cps, respectively.}$

$$\overline{K} = 10,000 \text{ lb.-in./rad.}$$

The value for k_c was calculated from design values for the elevator system. The values of K_H were determined for the various values of uncoupled horizontal tail frequency f_α. The scaling constant $\overline{K}$ was assigned its value aribitrarily, for computing convenience.

Results

Tables 22 through 27 and Figures 34 through 39 show the effects of varying the horizontal stabilizer uncoupled frequency f_α and aerodynamic balance.

Conclusions

Examination of the analysis results shows that elevator system flutter will not occur over the range of f_β and $1/k_0$ values investigated, either with or without aerodynamic balance for the elevator.
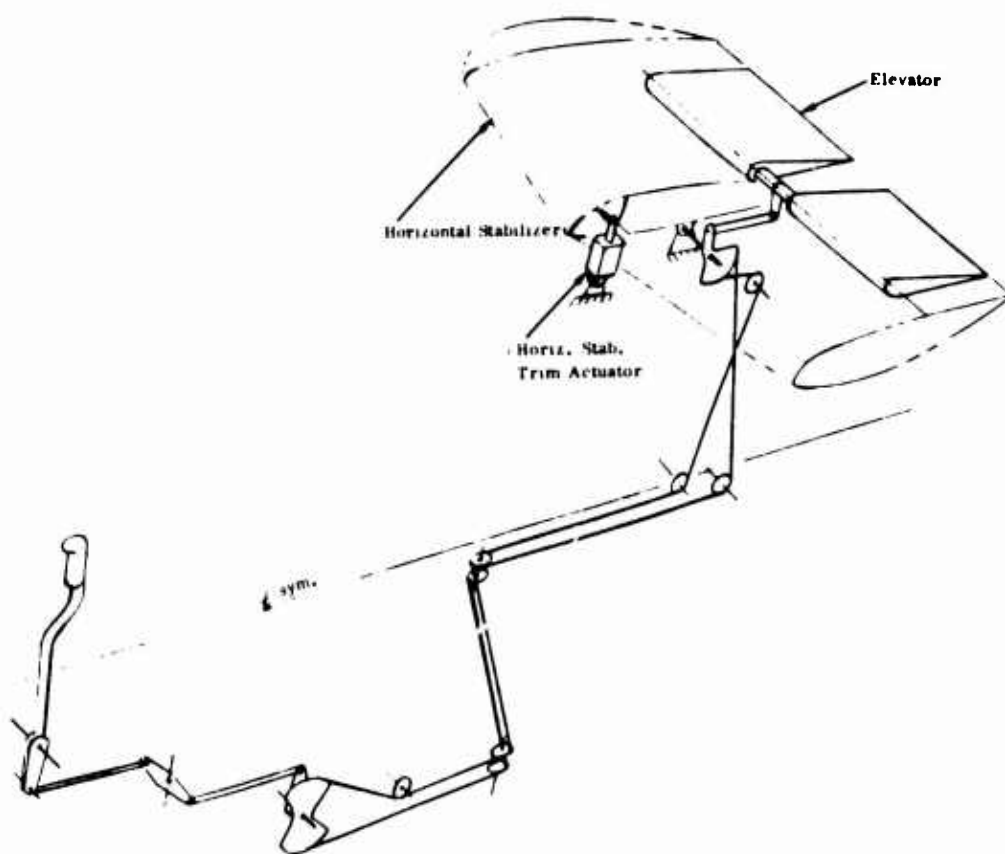
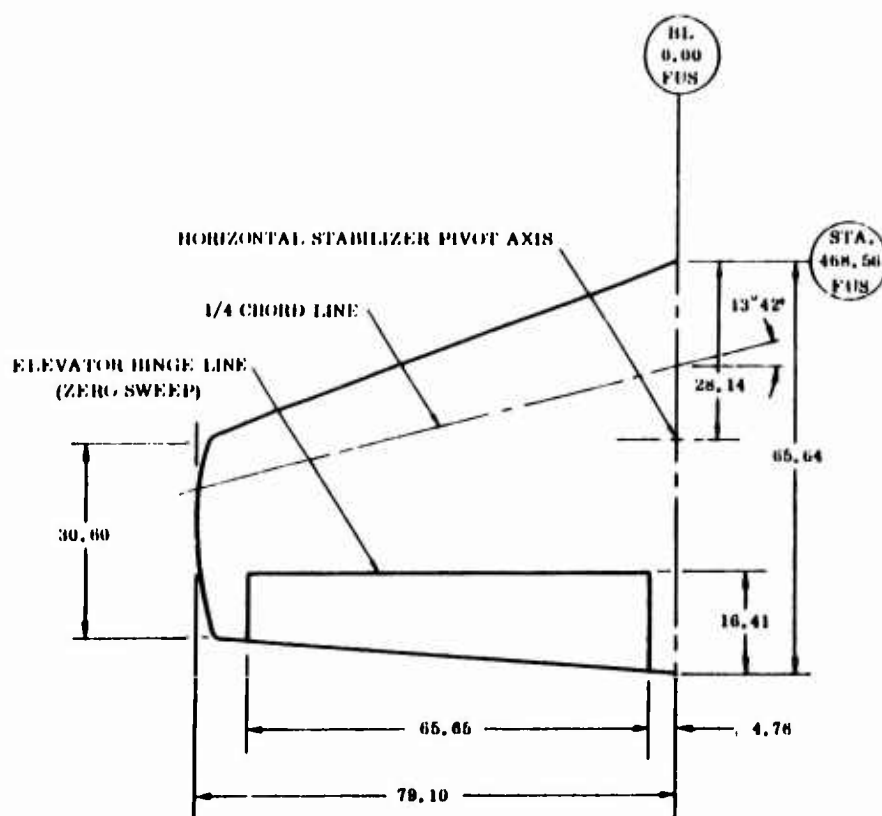Figure 30   Schematic of Elevator System

Figure 31   Horizontal Tail -   Plan View

Figure 32   Elevator Aerodynamic Balancing Arrangement

Figure 33   Idealization of Elevator System

TABLE 21

HORIZONTAL STABILIZER - ELEVATOR
AERODYNAMIC PARAMETERS

Horizontal Stabilizer - Elevator Geometry:

Sta. No.	B.L. in.	b in.	c	e'	e"	g	F_{BB}	g in.	a in.	
1	0.00	32.820	-	-	-	-	-	-2.500	9.230	} Stab
2_I	4.26	31.876	-	-	-	-	-	-1.773	8.919	
2_O	4.26	31.876	0.497	0.443	0.377	0.557	0.00578	-1.773	8.919	
3	17.39	28.968	0.487	0.431	0.364	0.547	0.00595	0.468	7.959	Stab
4	30.52	26.060	0.474	0.415	0.349	0.534	0.00610	2.709	7.000	+
5	43.65	23.152	0.458	0.396	0.330	0.518	0.00630	4.950	6.040	Elev
6	56.78	20.244	0.438	0.371	0.305	0.498	0.00661	7.191	5.081	
7_I	69.91	17.335	0.410	0.338	0.272	0.470	0.00692	9.432	4.122	
7_O	69.91	17.335	-	-	-	-	-	9.432	4.122	} Stab
8	79.10	15.300	-	-	-	-	-	11.000	3.450	

Aerodynamic Balance Arrangement:

Elevator, internal - simple nose overhang (curtain seal)

Hinge Moment Corrections:

$$\frac{\left(C_{H_{c_\alpha}}\right)_{Exp.}}{\left(C_{H_{c_\alpha}}\right)_3} = 1.0 \quad ; \quad \frac{\left(C_{H_{c_{\delta_c}}}\right)_{Exp.}}{\left(C_{H_{c_{\delta_c}}}\right)_3} = 1.0$$

$$\frac{\left(\Delta C_{H_{c_\alpha}}\right)_{Exp.}}{\left(\Delta C_{H_{c_\alpha}}\right)_3} = 1.0 \quad ; \quad \frac{\left(\Delta C_{H_{c_{\delta_c}}}\right)_{Exp.}}{\left(\Delta C_{H_{c_{\delta_c}}}\right)_3} = 1.0$$

95

TABLE 21   (Continued)

Pressure Recovery Factor:

$$K = 1.0$$

General:

Reference half chord (b_o) = 32.820 in.

$\cos \psi_{c/4}$ = 0.971554

$\cos \psi_{H_c}$ = 1.00

Altitude - sea level ($\rho = 0.114626 \times 10^{-6}$ lb.-sec.^{2}-in.$^{-4}$)

TABLE 22

SOLUTIONS OF STABILITY EQUATIONS

Plot: Figure 34

Uncoupled Natural Frequency, Horizontal Stabilizer Rotation: $f_\alpha = 20$ cps

Spring Constants:

$$k_c = 1145 \text{ lb./in.}$$

$$K_H = 665,400 \text{ lb.-in./rad.}$$

Aerodynamics: Basic Surface with Aerodynamic Balance $(B \neq 0)$

$\dfrac{1}{k_o}$	f_1 cps	V_1 Knots	g_1	f_2 cps	V_2 Knots	g_2
.00	32.5	0.0	.000	20.0	0.0	.000
.15	22.7	34.7	-.060	19.1	29.2	-.054
.25	22.7	57.8	-.103	19.2	49.0	-.088
.45	22.7	103.9	-.218	19.7	90.3	-.141
.65	23.3	154.2	-.416	20.1	132.9	-.147
1.00	27.9	284.1	-1.045	20.0	203.2	-.151
2.00	-	-	-	18.4	374.8	-.229
4.00	-	-	-	14.0	570.7	-.316
6.00	-	-	-	10.6	645.0	-.310
8.00	-	-	-	8.3	673.6	-.280
11.00	-	-	-	6.1	688.7	-.237

Uncoupled Natural Frequency, Elevator Rotation: $f_\beta = 22.83$ cps

TABLE 23

SOLUTIONS OF STABILITY EQUATIONS

Plot: Figure 35

Uncoupled Natural Frequency, Horizontal Stabilizer Rotation: f_α =40 cps

Spring Constants:

$$k_c = 1145 \text{ lb./in.}$$

$$K_H = 2,661,800 \text{ lb.-in./rad.}$$

Aerodynamics: Basic Surface with Aerodynamic Balance (B $\neq$ 0)

$\dfrac{1}{k_o}$	f_1 cps	V_1 Knots	g_1	f_2 cps	V_2 Knots	g_2
.00	32.3	0.0	.000	40.3	0.0	.000
.15	22.1	33.8	-.095	39.3	60.0	-.019
.25	22.3	56.9	-.162	39.2	99.7	-.031
.45	23.2	106.2	-.313	38.8	177.9	-.052
.65	24.8	164.1	-.515	38.3	253.5	-.065
1.00	31.2	317.6	-1.255	37.4	381.2	-.060
2.00	-	-	-	35.8	728.9	-.147
4.00	-	-	-	27.4	1116.7	-.283

Uncoupled Natural Frequency, Elevator Rotation: f_β = 22.83 cps

TABLE 24

SOLUTIONS OF STABILITY EQUATIONS

Plot: Figure 36

Uncoupled Natural Frequency, Horizontal Stabilizer Rotation: $f_\alpha = 60$ cps

Spring Constants:

$$k_c = 1145 \text{ lb./in.}$$

$$K_H = 5,988,900 \text{ lb.-in./rad.}$$

Aerodynamics: Basic Surface with Aerodynamic Balance (B $\neq$ 0)

$\dfrac{1}{k_o}$	f_1 cps	V_1 Knots	g_1	f_2 cps	V_2 Knots	g_2
.00	32.3	0.0	.000	60.3	0.0	.000
.15	22.2	33.8	-.093	58.8	89.8	-.020
.25	22.4	57.0	-.159	58.6	149.3	-.034
.45	23.2	106.3	-.305	58.2	266.4	-.059
.65	24.8	163.8	-.498	57.4	379.7	-.079
1.00	31.1	316.2	-1.188	55.5	565.5	-.087
2.00	-	-	-	53.1	1080.8	-.130

Uncoupled Natural Frequency, Elevator Rotation: $f_\beta = 22.83$ cps

TABLE 25

SOLUTIONS OF STABILITY EQUATIONS

Plot: Figure 37

Uncoupled Natural Frequency, Horizontal Stabilizer Rotation: f_α = 20 cps

Spring Constants:

k_c = 1145 lb./in.

K_H = 665,400 lb.-in./rad.

Aerodynamics: Basic Surface without Aerodynamic Balance (B = 0)

$\dfrac{1}{k_o}$	f_1 cps	V_1 Knots	g_1	f_2 cps	V_2 Knots	g_2
.00	32.5	0.0	.000	20.0	0.0	.000
.15	22.7	34.6	-.064	19.1	29.2	-.054
.25	22.7	57.7	-.113	19.3	49.1	-.088
.45	22.9	104.7	-.247	19.7	90.4	-.133
.65	24.0	158.5	-.475	20.0	132.3	-.137
1.00	30.7	312.2	-1.318	19.8	201.9	-.149
2.00	-	-	-	18.3	372.7	-.230
4.00	-	-	-	14.0	569.7	-.319
6.00	-	-	-	10.6	645.3	-.314
8.00	-	-	-	8.3	674.6	-.285
11.00	-	-	-	6.2	690.1	-.241

Uncoupled Natural Frequency, Elevator Rotation: f_β = 22.83 cps

TABLE 26

SOLUTIONS OF STABILITY EQUATIONS

Plot: Figure 38

Uncoupled Natural Frequency, Horizontal Stabilizer Rotation: f_α = 40 cps

Spring Constants:

$$k_c = 1145 \text{ lb./in.}$$

$$K_H = 2,661,800 \text{ lb.-in./rad.}$$

Aerodynamics: Basic Surface without Aerodynamic Balance (B = 0)

$\dfrac{1}{k_o}$	f_1 cps	V_1 Knots	g_1	f_2 cps	V_2 Knots	g_2
.00	32.3	0.0	.000	40.3	0.0	.000
.15	22.1	33.8	-.100	39.2	59.9	-.019
.25	22.4	57.0	-.170	39.2	99.7	-.031
.45	23.4	107.3	-.334	38.8	178.0	-.052
.65	25.4	168.1	-.567	38.3	253.4	-.064
1.00	34.4	350.5	-1.601	37.6	382.5	-.057
2.00	-	-	-	35.8	729.1	-.162
4.00	-	-	-	27.5	1118.6	-.290

Uncoupled Natural Frequency, Elevator Rotation: f_β = 22.83 cps

TABLE 27

SOLUTIONS OF STABILITY EQUATIONS

Plot: Figure 39

Uncoupled Natural Frequency, Horizontal Stabilizer Rotation: f_α = 60 cps

Spring Constants:

k_c = 1145 lb./in.

K_H = 5,988,900 lb.-in/rad.

Aerodynamics: Basic Surface without Aerodynamic Balance (B = 0)

$\dfrac{1}{k_o}$	f_1 cps	V_1 Knots	g_1	f_2 cps	V_2 Knots	g_2
.00	32.4	0.0	.000	60.3	0.0	.000
.15	22.2	33.8	-.098	58.7	89.7	-.021
.25	22.4	57.1	-.167	58.6	149.2	-.034
.45	23.4	107.4	-.327	58.1	266.3	-.059
.65	25.4	167.8	-.548	57.3	379.4	-.079
1.00	34.3	349.6	-1.525	55.6	565.8	-.080
2.00	-	-	-	53.3	1084.5	-.147

Uncoupled Natural Frequency, Elevator Rotation: f_β = 22.83 cps
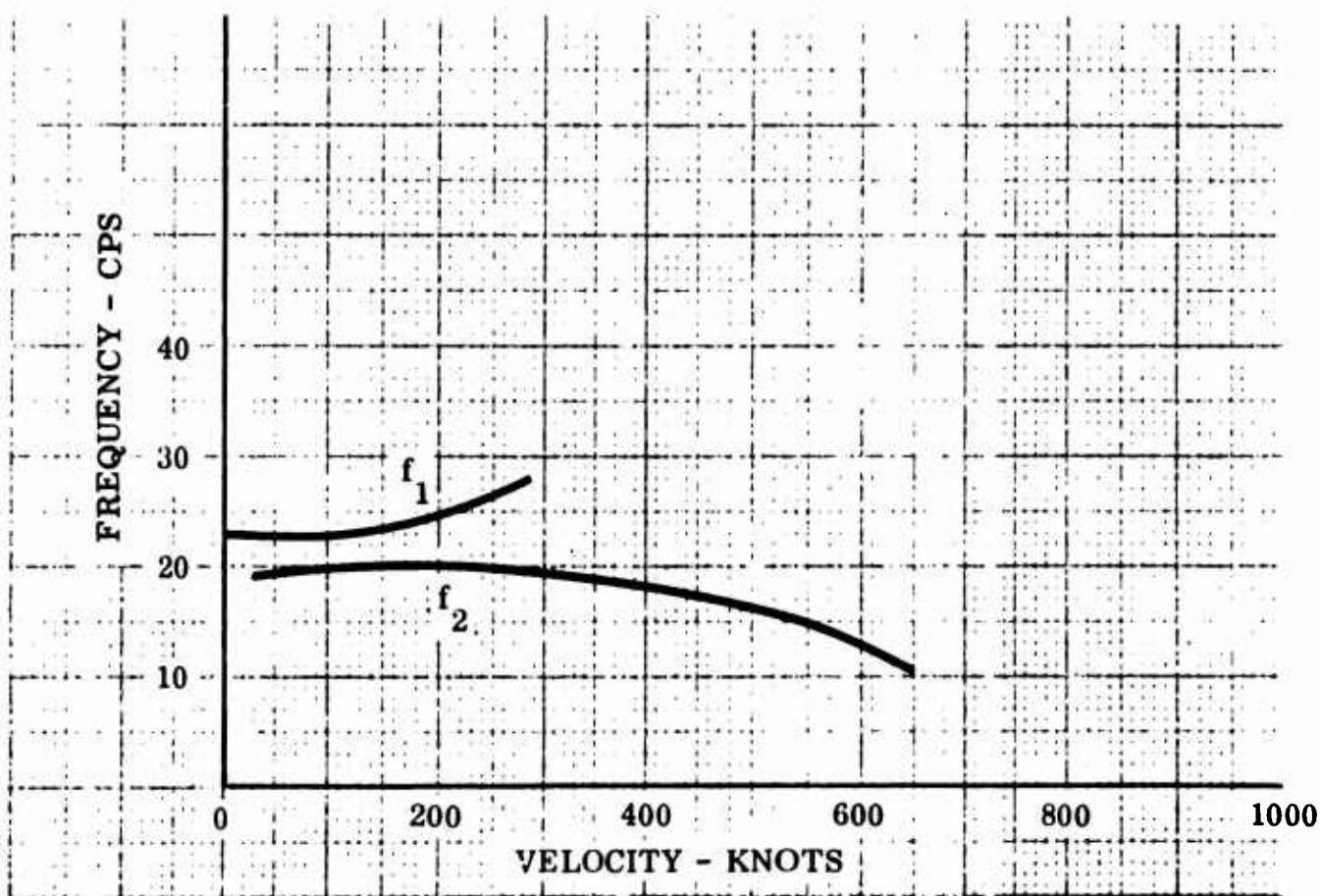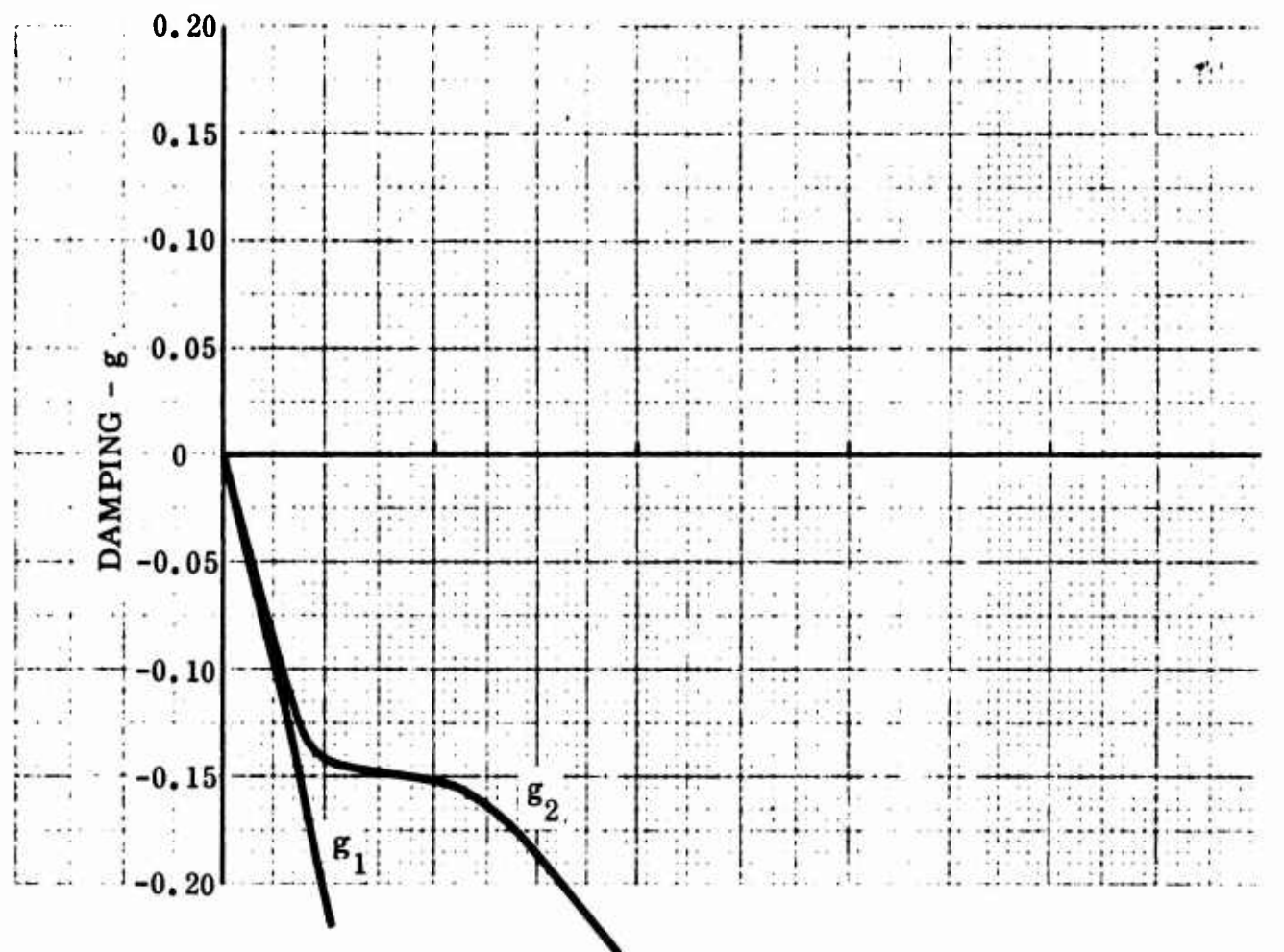
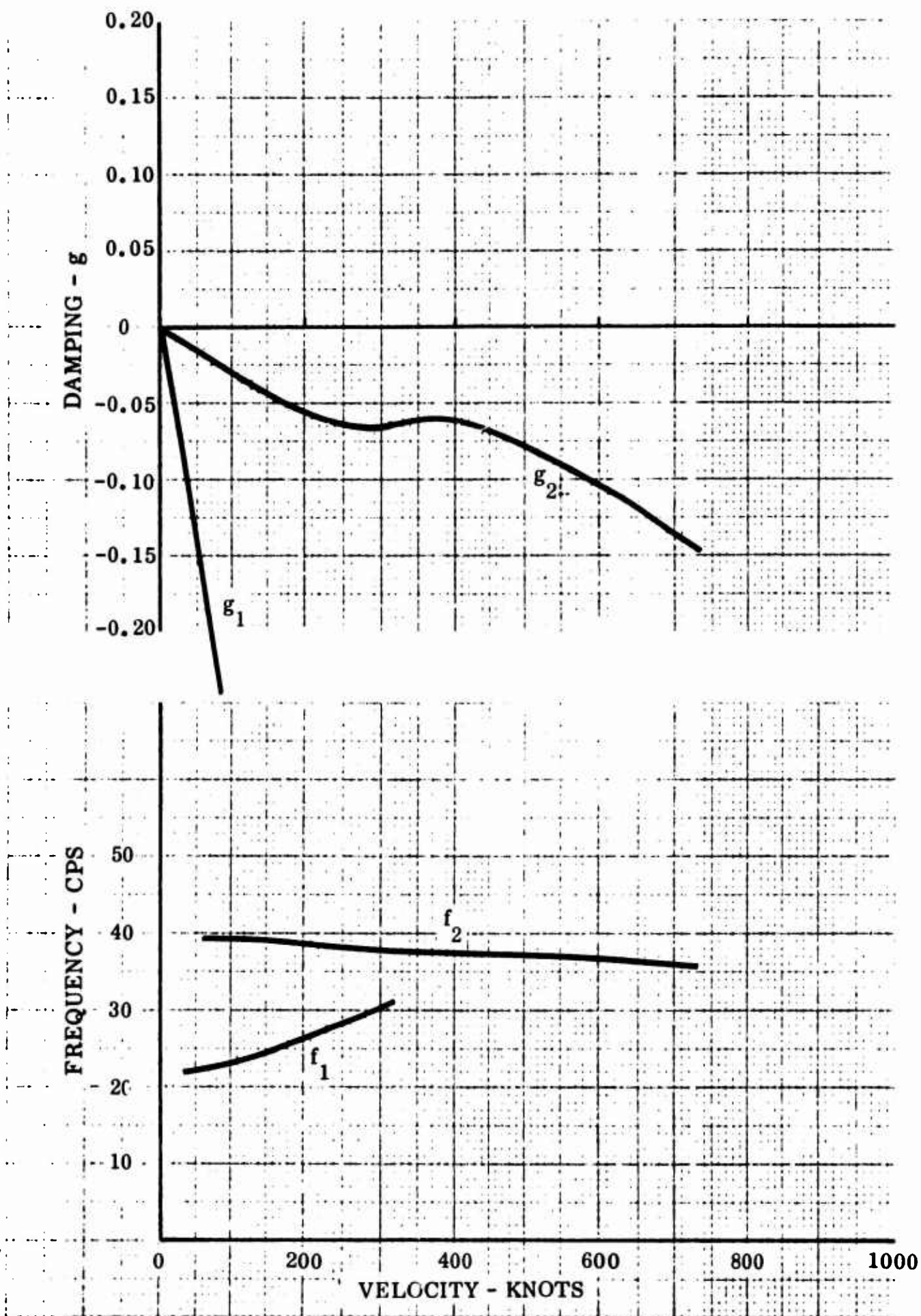Figure   34   g-V and f-V Plots, Elevator, f_α = 20 cps,   B $\neq$ 0

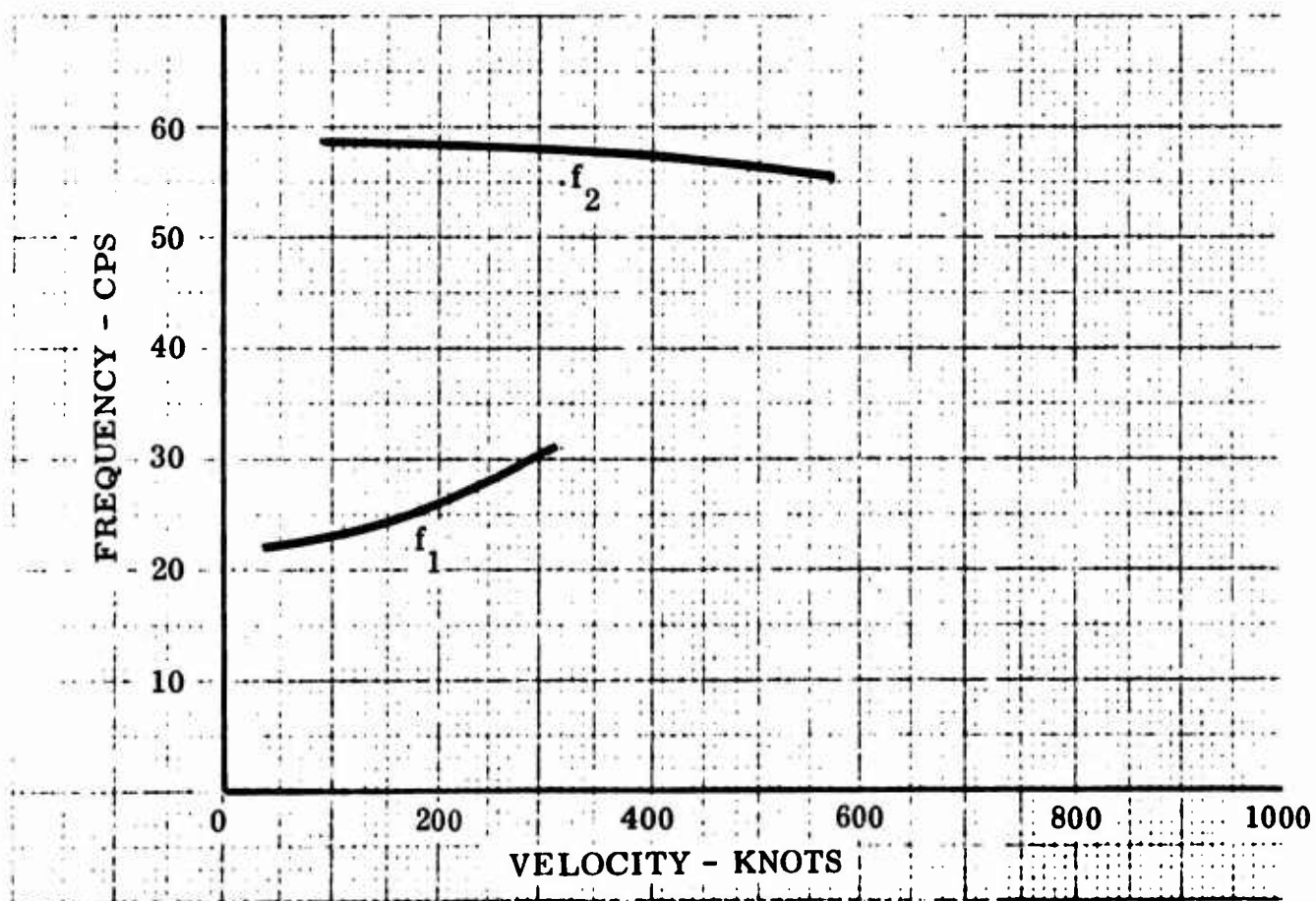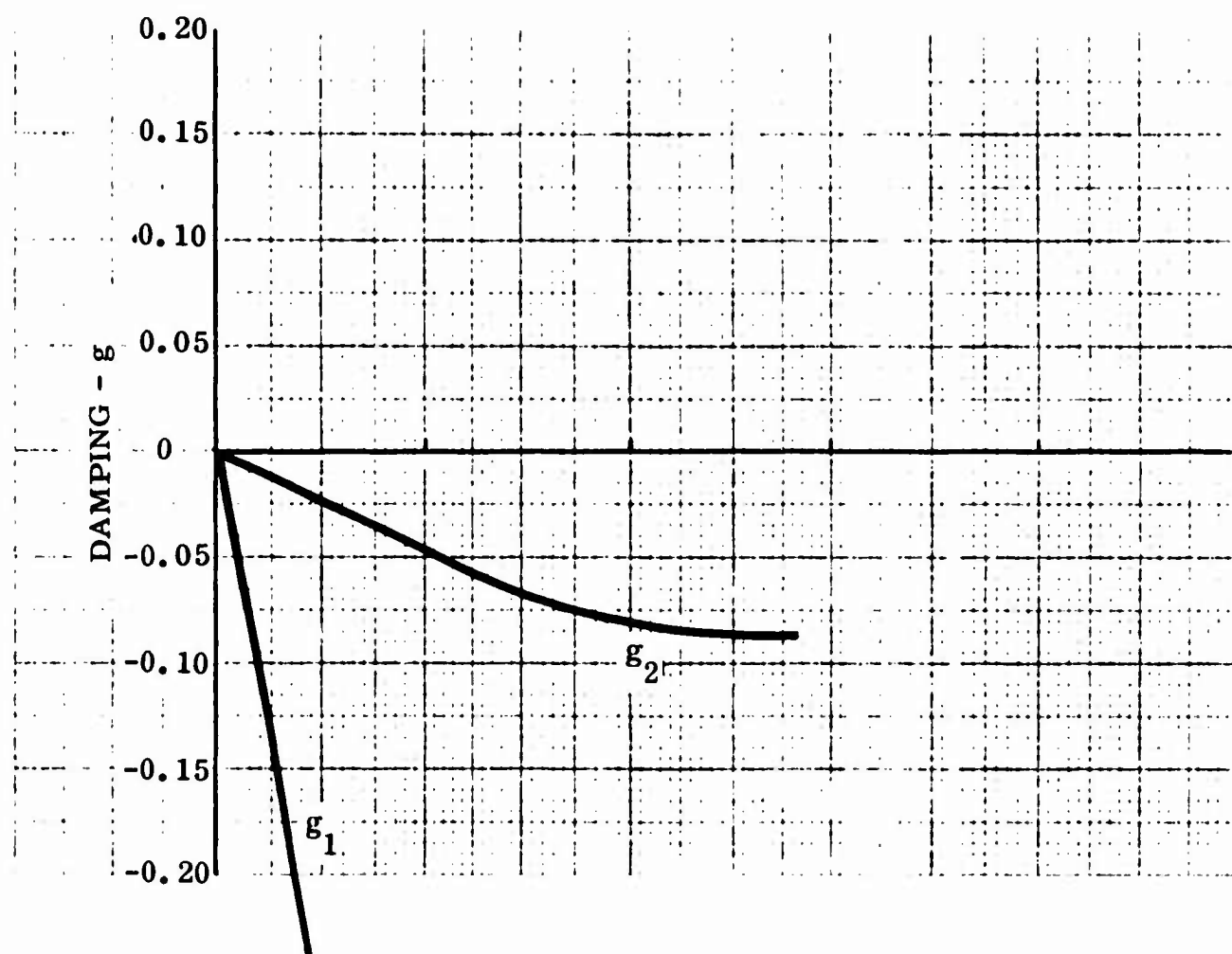Figure 35   g-V and f-V Plots, Elevator, f_α = 40 cps, B $\neq$ 0

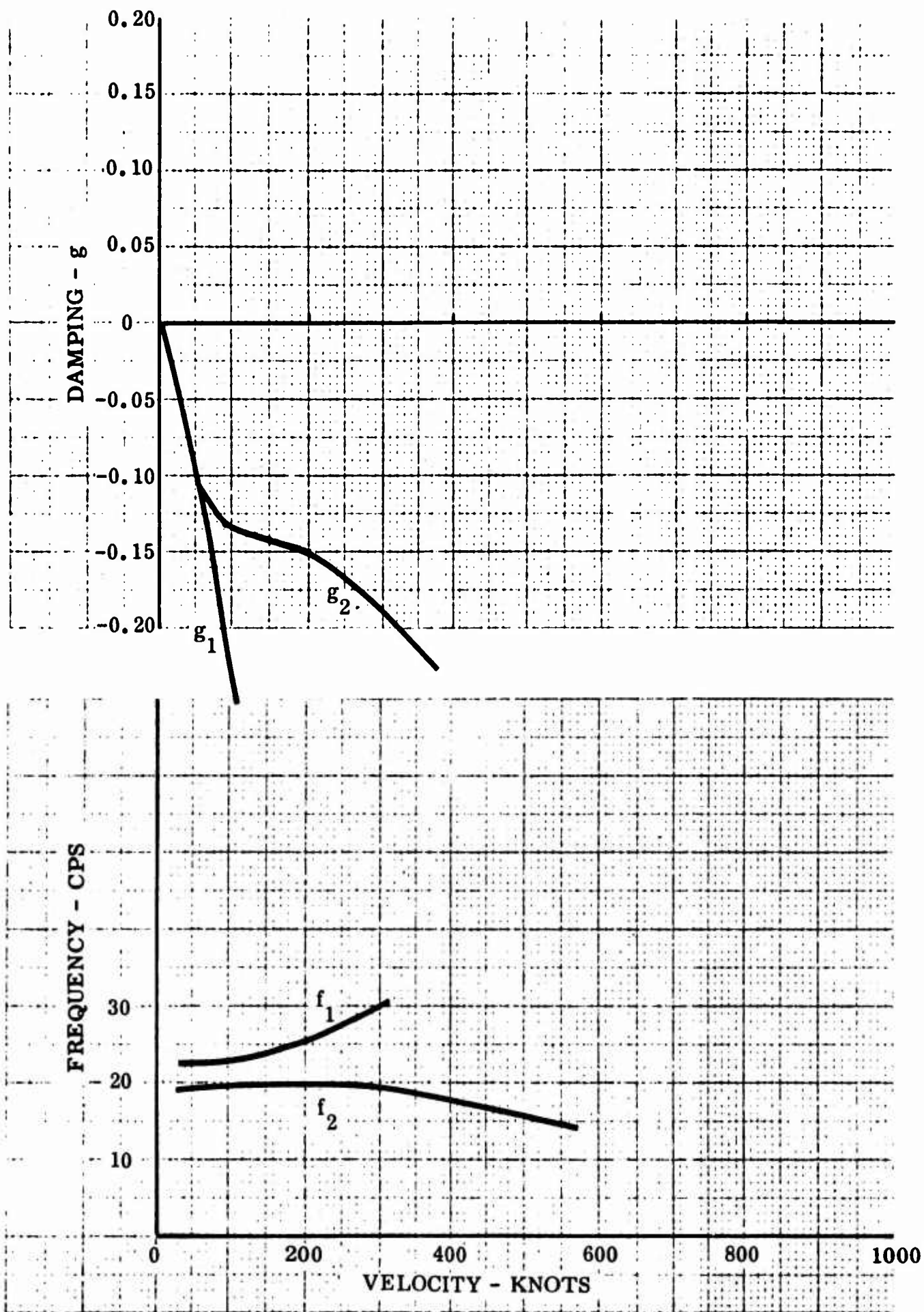Figure 36   g-V and f-V Plots, Elevator, $f_\alpha = 60$ cps, $B \neq 0$

105

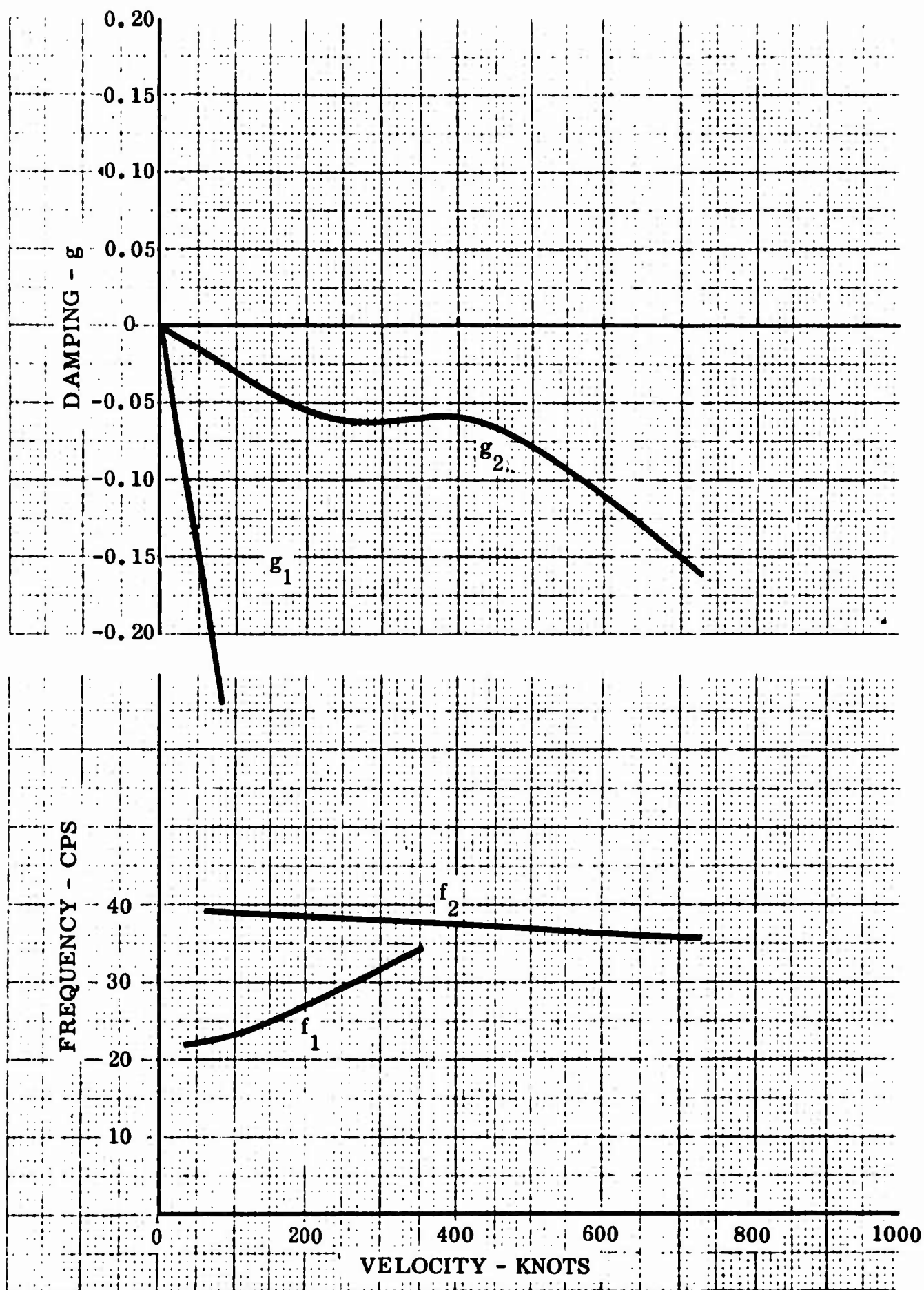Figure 37   g-V and f-V Plots, Elevator, f_α = 20 cps, B = 0

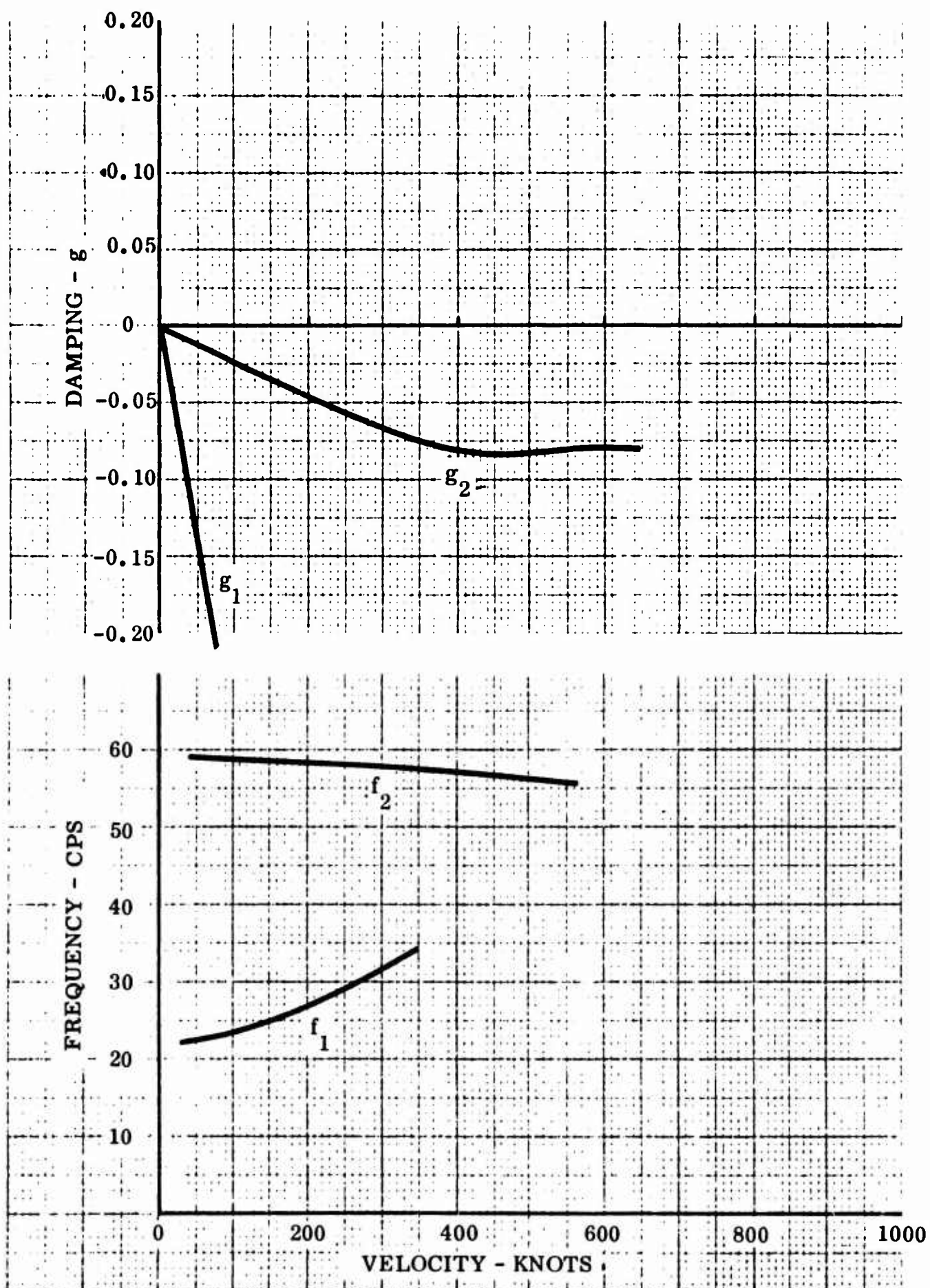Figure 38   g-V and f-V Plots, Elevator, f_α = 40 cps, B = 0

Figure 39   g-V and f-V Plots, Elevator, $f_\alpha = 60$ cps, B = 0

5.0 CONCLUSIONS AND RECOMMENDATIONS

Flutter analyses of all XV-5A control surfaces have been made, based
on preliminary input information. Increased stiffness of the aileron
control circuit (the symmetric aileron condition is critical) is re-
quired, and the stiffness of the rudder trim tab actuator should be
such that the uncoupled rigid body tab rotational frequency is at least
50 cps in order to ensure a flutter-free airplane within the estab-
lished flight envelope. The antisymmetric aileron condition and
elevator are flutter-free.

It is recommended that further flutter analysis of all control surfaces
be made on the basis of refinements to stiffness and inertia proper-
ties as the design develops, incorporating experimentally determined
properties as they become available. It is recommended that the report
herein be used as intended: for interpretive purposes as an aid to
design development and not as a definitive prediction of control system
flutter performance. Further, this report can and should be used in con-
junction with the formulation of main surface flutter analyses (wing, and
empennage, for example) to determine important control surface degrees
of freedom that should be considered in the main surface analyses.

6.0 APPENDIX

6.1 <u>REFERENCES</u>

1. Krupnick, M. - Model 30 (CV-600) Airplane Tab Flutter Analysis, General Dynamics/Convair Report ZU-30-004, 15 September 1960.

2. Smilg, B., and Wasserman, L. S. - Application of Three-Dimensional Flutter Theory to Aircraft Structures, Air Force Technical Report 4798, 1942.

3. Wasserman, L. S., Mykytow, W. J., and Spielberg, I. N. - Tab Flutter Theory and Applications, Air Force Technical Report 5153, 1944.

4. Ashley, H. - Subsonic Flutter of a Control Surface with a Balance Board, General Dynamics/Convair Memo DG-G-177, 30 July 1957.